GEOMETRY OF LATE PALEOZOIC THRUSTING BETWEEN WILBURTON-HARTSHORNE AREA, ARKOMA BASIN, SOUTHEAST OKLAHOMA

By

ATA SAGNAK

Bachelor of Science

Middle East Technical University

Ankara, Turkey

1992

Submitted to the Faculty of the
Graduate College of the
Oklahoma State University
in partial fulfillment of
the requirements for
the Degree of
MASTER OF SCIENCE
May, 1996

OKLAHOMA STATE UNIVERSITY

GEOMETRY OF LATE PALEOZOIC THRUSTING

BETWEEN WILBURTON-HARTSHORNE AREA,

ARKOMA BASIN, SOUTHEAST OKLAHOMA

Thesis Approved:

Sidney Green
Thesis Adviser

Ruth A. Shaw

Darwin L. Boardman

Thomas C. Collins
Dean of the Graduate College

ACKNOWLEDGEMENTS

I would like to express my sincere appreciation to my committee chair, Dr. Ibrahim Cemen. His advice, insight, and friendship throughout this work were invaluable and greatly appreciated. His understanding and kindness will never be forgotten. I wish to thank my other committee members, Dr. Zuhair Al-Shaieb for his help throughout every stage of my work and also for including me in the Oklahoma Center for the Advancement in Science and Technology (OCAST) project, and Dr. Darwin Boardman II, for his suggestions and valuable advice. I must also acknowledge OCAST for funding this thesis.

My sincere thanks to Jim Puckette for his vast knowledge of geology and his willingness to share that knowledge no matter how many other things he has to do (like a doctoral dissertation!) Thank you, Jim. I would also like to thank Catherine Price and Syed Y. Mehdi for their great friendship and endless help. Justin Evans and Michael Sykes deserve credit for helping me with the computers.

I greatly appreciate Neil H. Suneson and LeRoy Hemish who shared their knowledge about the study area with me and allowed their unpublished mapping efforts to be used in this study. I must also thank them for welcoming me on their fieldtrip to the Ouachita Mountains.

My fellow graduate students and project-mates deserve credit for their geological and technical expertise.

My sincerest appreciation goes to Dr. Hikmet Pekcan, who offered me the Rotary International Ambassadorial Scholarship, and to the members of Ankara Bahcelievler Rotary Club for nominating me for this scholarship, and to The Rotary Foundation of Rotary International for awarding me the 1993-1994 Ambassadorial Scholarship. My journey to OSU began with this award. It will never be forgotten and will always be carried as an honor.

Finally, to my parents: Thank you for your endless support, encouragement and patience. Without your understanding and guidance, this study would not have been successfully completed.

TABLE OF CONTENTS

Chapter		Page
I.	INTRODUCTION	1
	Statement of Purpose	3
	Methods of Investigation	5
	Previous Investigations	10
	Tectonics of Ouachita Mountains	10
	Arkoma Basin	17
	Wilburton Gas Field and Surrounding Areas	18
II.	STRATIGRAPHY OF THE ARKOMA BASIN	20
III.	PETROLOGY, DIAGENESIS AND DEPOSITIONAL ENVIRONMENT OF THE SPIRO SANDSTONE	28
	Petrology and Diagenesis	28
	Detrital Constituents	28
	Diagenetic Constituents and Features	31
	Cement	31
	Diagenetic Clays	35
	Porosity	35
	Diagenesis	37
	Depositional Environment	39
IV.	GEOMETRY OF FOLD AND THRUST ASSEMBLAGES	42
	Thrust Systems	42
	Imbricate Fans	43
	Duplexes	46
	Sequence of Development of Duplexes	52
	Triangle Zones	54
V.	PROPOSED STRUCTURAL GEOMETRY OF FRONTAL THRUST BELT OF OUACHITA MOUNTAINS	58

Chapter Page

VI. STRUCTURAL GEOLOGY 66

Major Thrust Faults 76
Ti Valley Fault 77
Pine Mountain Fault 81
Choctaw Fault and Associated Structural Features 81
Basal Detachment Surfaces 83
Duplex Structures and the Lower Atokan Detachment 84
Carbon Fault 87
Triangle Zone 89
Normal Faults and Strike Slip Faults 89
Folds 90
Restored Cross-Sections and Amount of Shortening 91

VII. CONCLUSIONS 103

REFERENCES 104

APPENDICES 113

APPENDIX I 114

APPENDIX II 119

LIST OF FIGURES

Figure		Page
1.	Major geologic provinces of eastern Oklahoma and western Arkansas.....	2
2.	Location map of the study area.....	4
3.	Representative well log for the Spiro sandstone.....	7
4.	Representative well log for the Red Oak sandstone.....	8
5.	Representative well log for Marker X.....	9
6.	Method of correction for deviated wells.....	11
7.	Diagrammatic evolution of the southern margin of North America.....	13
8.	Generalized cross-sections showing the sedimentation in the Arkoma Basin - Ouachita Mountain area from Late Cambrian through Atokan time.....	16
9.	Stratigraphic chart for the Arkoma Basin and the Ouachita Mountains....	21
10.	Stratigraphic chart illustrating the Atokan Series in the Arkoma Basin....	25
11.	Stratigraphy of the Desmoinesian in the Arkoma Basin.....	27
12.	Subrounded quartz grains and calcite cement.....	29
13.	Skeletal fragments replaced by calcite.....	32
14.	Chamosite coated quartz grains and minor zircon.....	33
15.	Heavily carbonate cemented (calcite and dolomite) area.....	34
16.	Chamosite coating surrounding quartz grains preserves the primary porosity.....	36
17.	Secondary porosity formed from dissolution of echinoderm spines.....	38

Figure Page

18. Preservation and/or development of porosity as related to diagenetic evolution 41

19. Classification of thrust systems 44

20. Imbricate systems 45

21. Duplex classification 48

22. Breached duplex 50

23. Corrugated duplex 50

24. Link thrusts 51

25. Sequential development of duplexes 53

26. Triangle Zone 55

27. Intercutaneous thrust wedge 55

28. Three end member geometries for triangle zones 56

29. Sketch cross-section showing styles of deformation in the subsurface at the transition zone between the Arkoma Basin and Ouachita Mountains as proposed by Arbenz 59

30. Sketch cross-section showing styles of deformation in the subsurface at the transition zone between the Arkoma Basin and Ouachita Mountains as proposed by Hardie 61

31. Sketch cross-section showing styles of deformation in the subsurface at the transition zone between the Arkoma Basin and Ouachita Mountains as proposed by Milliken 61

32. Sketch cross-section showing styles of deformation in the subsurface at the transition zone between the Arkoma Basin and Ouachita Mountains as proposed by Camp and Ratliff 62

33. Sketch cross-section showing styles of deformation in the subsurface at the transition zone between the Arkoma Basin and Ouachita Mountains as proposed by Reeves and others 62

Figure Page

34. Sketch cross-section showing styles of deformation in the subsurface at the transition zone between the Arkoma Basin and Ouachita Mountains as proposed by Perry and others 64

35. Sketch cross-section showing styles of deformation in the subsurface at the transition zone between the Arkoma Basin and Ouachita Mountains as proposed by Roberts 64

36. Sketch cross-section showing the geometry to the west of the Wilburton gas field 65

37. Structural cross-section A-A' 68

38. Structural cross-section B-B' 69

39. Structural cross-section C-C' 70

40. Structural cross-section D-D' 71

41. Structural cross-section E-E' 72

42. Structural cross-section F-F' 73

43. Structural cross-section G-G' 74

44. Structural cross-section H-H' 75

45. Interpreted seismic profile along cross-section C-C' 78

46. Interpreted seismic profile along cross-section E-E' 79

47. Major thrust fault and a splay 80

48. Restored cross-section A-A' 92

49. Restored cross-section B-B' 93

50. Restored cross-section C-C' 94

51. Restored cross-section D-D' 95

52. Restored cross-section E-E' 96

Figure Page

53. Restored cross-section F-F' 97

54. Restored cross-section G-G' 98

55. Restored cross-section H-H' 99

LIST OF PLATES

I.	Simplified Geological Map of the Wilburton Gas Field Area.....	In Pocket
II	Simplified Geological Map of the Study Area Showing the Lines of Cross-Sections.....	In Pocket
III.	Balanced and Restored Cross-Section A-A'.....	In Pocket
IV.	Balanced and Restored Cross-Section B-B'.....	In Pocket
V.	Balanced and Restored Cross-Section C-C'.....	In Pocket
VI.	Balanced and Restored Cross-Section D-D'.....	In Pocket
VII.	Balanced and Restored Cross-Section E-E'.....	In Pocket
VIII.	Balanced and Restored Cross-Section F-F'.....	In Pocket
IX.	Balanced and Restored Cross-Section G-G'.....	In Pocket
X.	Balanced and Restored Cross-Section H-H'.....	In Pocket
XI.	Simplified Structural Contour Map on the Top of Spiro in the Footwall Block of Choctaw Fault.....	In Pocket

CHAPTER 1

INTRODUCTION

The Arkoma Basin and Ouachita Mountains are elongate tectonic features extending in an east-west direction in eastern Oklahoma and west-central Arkansas (Figure 1). The Arkoma Basin is considered to be a foreland basin formed during the Ouachita Orogeny. The Ouachita Mountains lie to the south of the Ozark Plateau and extend from west-central to southeastern Oklahoma. The main rock types in the Oklahoma area are sandstone and shale. Based on the structurai style and stratigraphy, the Ouachita Mountains in the Oklahoma area are divided into three distinct assemblages, namely the frontal belt, central belt, and Broken Bow Uplift.

The frontal belt is bounded by the Choctaw fault to the north and the Windingstair fault to the south. The belt consists of imbricately thrusted, tilted, and tightly folded shallow water Morrowan strata to the north and basinal rocks to the south. The Atokan turbidites overlie the Morrowan strata throughout the frontal belt.

The Central Belt is characterized by broad synclines separated by tight thrust cored anticlines. Mississippian and early Pennsylvanian turbidites crop out in this belt with the exception of pre-Mississippian rocks in the Potato Hills area (Suneson and others 1990).

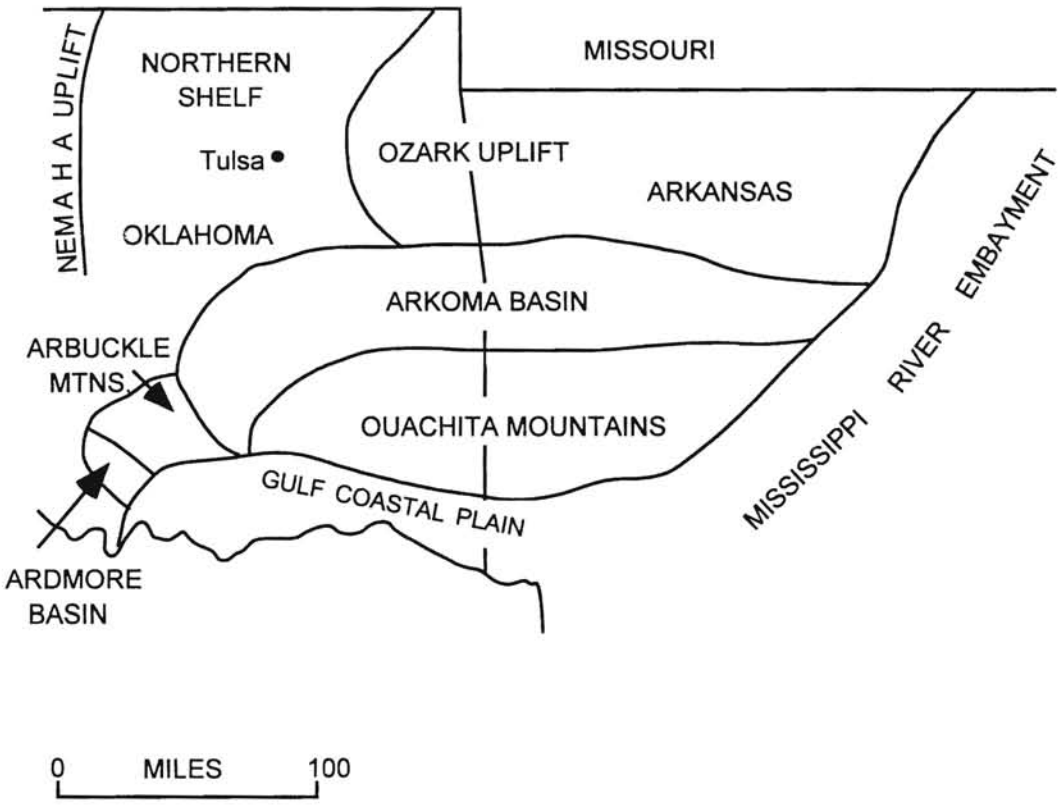

Figure 1: Major geologic provinces of eastern Oklahoma and western Arkansas (From Johnson, 1988)

The Broken Bow Uplift is composed of early Ordovician to early Mississippian deep water strata. The units in this part of the Ouachita Mountains are isoclinally folded and thrusted (Suneson and others 1990).

The Arkoma Basin is a mixed assemblage of structural styles characterized by both compressional and extensional features (Arbenz, 1989). In Oklahoma, the Mulberry fault; a down to-the-south normal fault is considered the northern boundary. The southern boundary is well defined by the surface trace of the Choctaw fault. Both the Mulberry fault and the Choctaw fault die to the east in Arkansas. The boundaries of the basin in Arkansas are drawn according to the termination of the folds in the north and the next major thrust fault in the south. The southern part of the basin is dominated by a thin-skinned compressional fold belt. Shortened synclines and anticlines overlie the block faulted Atokan and older rocks separated by a detachment surface (Arbenz, 1989).

Statement of Purpose

The study area includes parts of Latimer and Pittsburg Counties (T3N-6N, R16E-19E) which comprise a total of thirteen townships in Oklahoma (Figure 2). This area coincides with the Wilburton gas field and areas adjacent to it. The study was part of an Oklahoma Center for Advancement in Science and Technology (OCAST) project examining overthrusted natural gas reservoirs in the Arkoma Basin.

The main purpose of this study is to delineate the subsurface structural geometry of the Wilburton-Hartshorne area in southeast Oklahoma. The long debated, complex geometry of the area with the questions about presence of duplex structures, a roof thrust

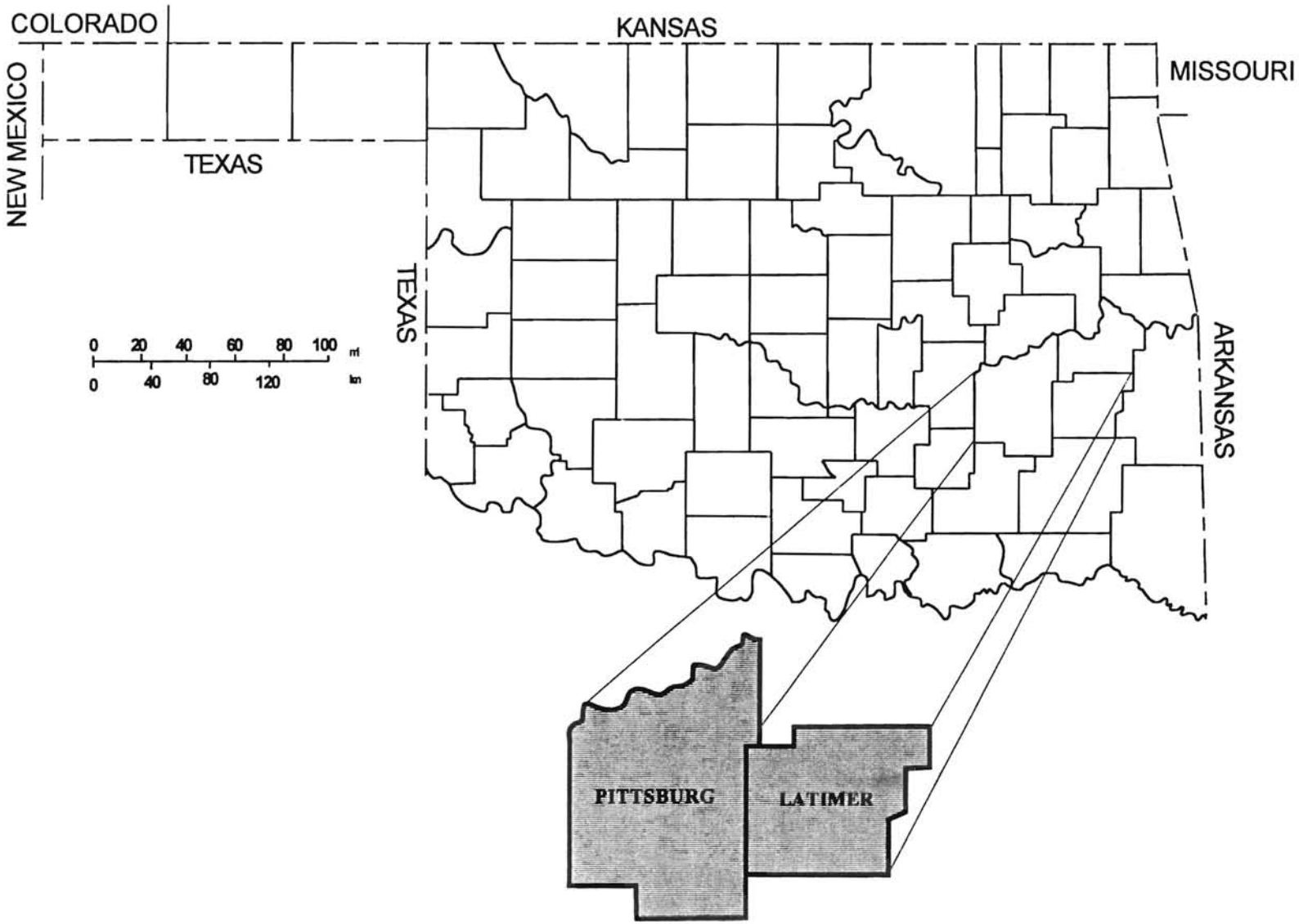

Figure 2: Location map of the study area

and geometry of thrust faults in the area are the sole problems that are studied in this research.

The main objectives of this study are three fold:

(1) to determine the geometry of the thrusting in the area between Wilburton and Hartshorne;

(2) to determine the presence and position of the detachment surfaces and duplex structures; and

(3) to examine petrologic characteristics of the Spiro sandstone in the study area through the use of thin-sections made from an available core in Pan American Petroleum Company Reusch #1 well.

Methods of Investigation

Necessary to the stated objectives, this study utilized the following informations and accomplished the followings:

1) Surface geological information is gathered from various published Oklahoma Geological Survey (OGS) geological maps and unpublished recent maps by Neil H. Suneson and LeRoy Hemish of OGS.

2) A simplified geological map of the study area is prepared from the surface geology mapped by Neil H. Suneson, C.A. Ferguson, and LeRoy Hemish.

3) Wire line well logs are obtained from the Oklahoma City Log Library. Spontaneous potential (SP), induction, gamma ray, and resistivity/conductivity logs are examined to locate the Spiro sandstone, the Red Oak sandstone, and a marker named as Marker X in

this study. These units are chosen because they were most widely recognizable and are important to delineate the thrust geometry in the area.

4) Available scout tickets are examined to corroborate the interpretations from the wire-line well logs.

5) Seismic profiles donated by EXXON Corporation are examined and interpreted.

6) Eight balanced structural cross-sections are constructed to delineate the geometry of thrusting in the area between Wilburton and Hartshorne (Plates III through X).

7) The balanced structural cross-sections are restored using the key-bed restoration method in order to determine the amount of shortening in the study area.

8) A structural contour map on top of the Spiro Sandstone is constructed using the information obtained from wire-line well logs and interpreted seismic lines (Plate XI).

9) Thirteen thin-sections prepared from the Pan-American Petroleum Company Reusch # 1 core are examined as well as visual examination of the core (Appendix I).

All of the structural cross-sections are constructed perpendicular to the major structures (parallel to the tectonic transport direction) to yield the most accurate geometry in the study area. The seismic profiles are also selected for interpretation in the same way. In the construction of the structural cross-sections, the Spiro sandstone, the Red Oak sandstone, and a sand unit termed "Marker X" in this study as well as the Hartshorne Formation, the McAlester Formation, the Savanna Formation, and the Boggy Formation are used with their interpretive wirel-ine well-log signatures. Figures 3, 4, and 5 illustrate representative wire-line well log signatures for the Spiro sandstone, the Red Oak sandstone, and the "Marker X" respectively.

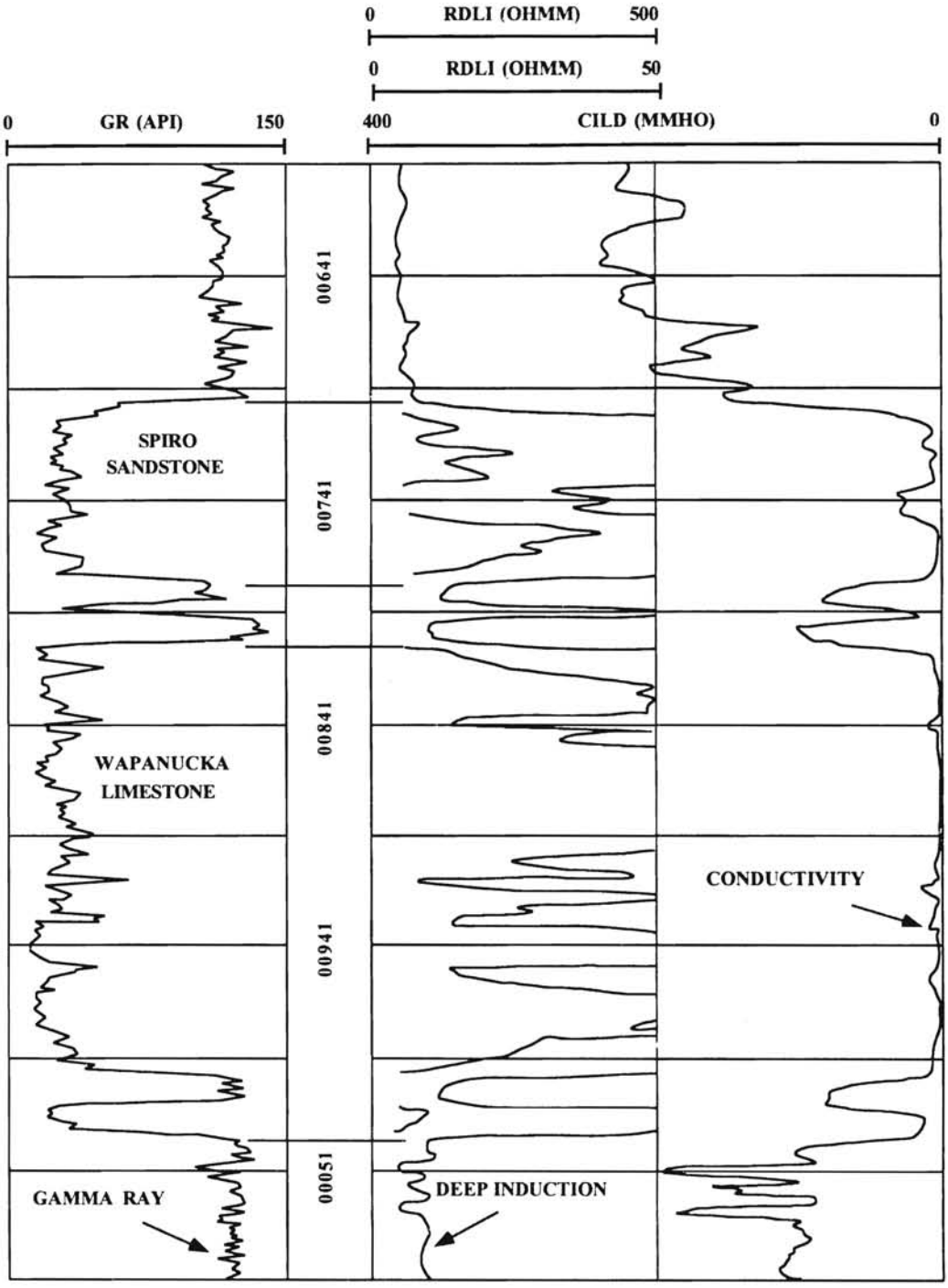

Figure 3: Representative well log for the Spiro sandstone
(TEXACO Inc., Dominic Silva No. 36-1,
Sec 36, T.4.N., R.16.E.)

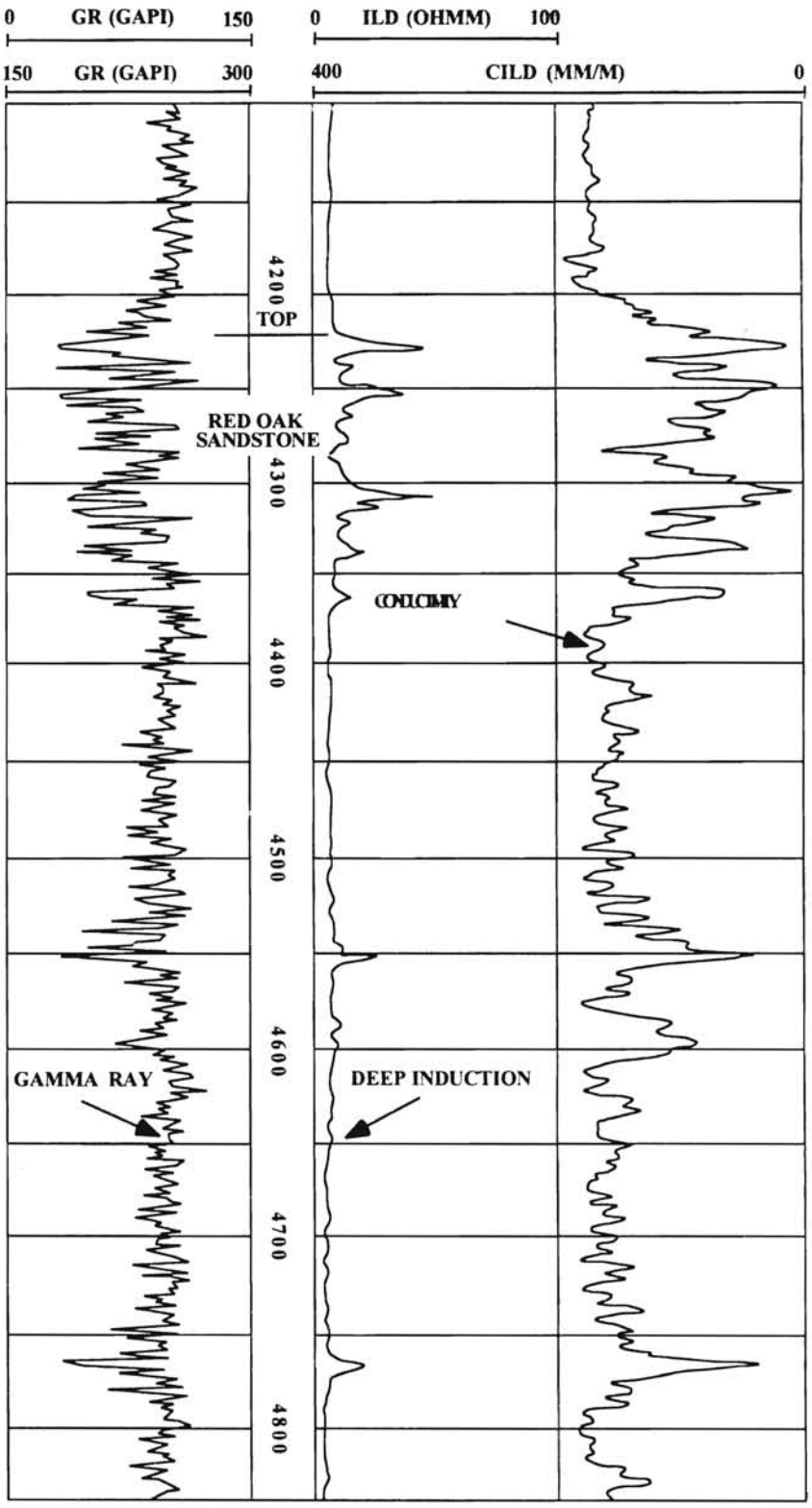

Figure 4: Representative well log for the Red Oak sandstone (ARCO Oil & Gas Co., Paschall #3, Sec 21, T.5.N., R.18.E.)

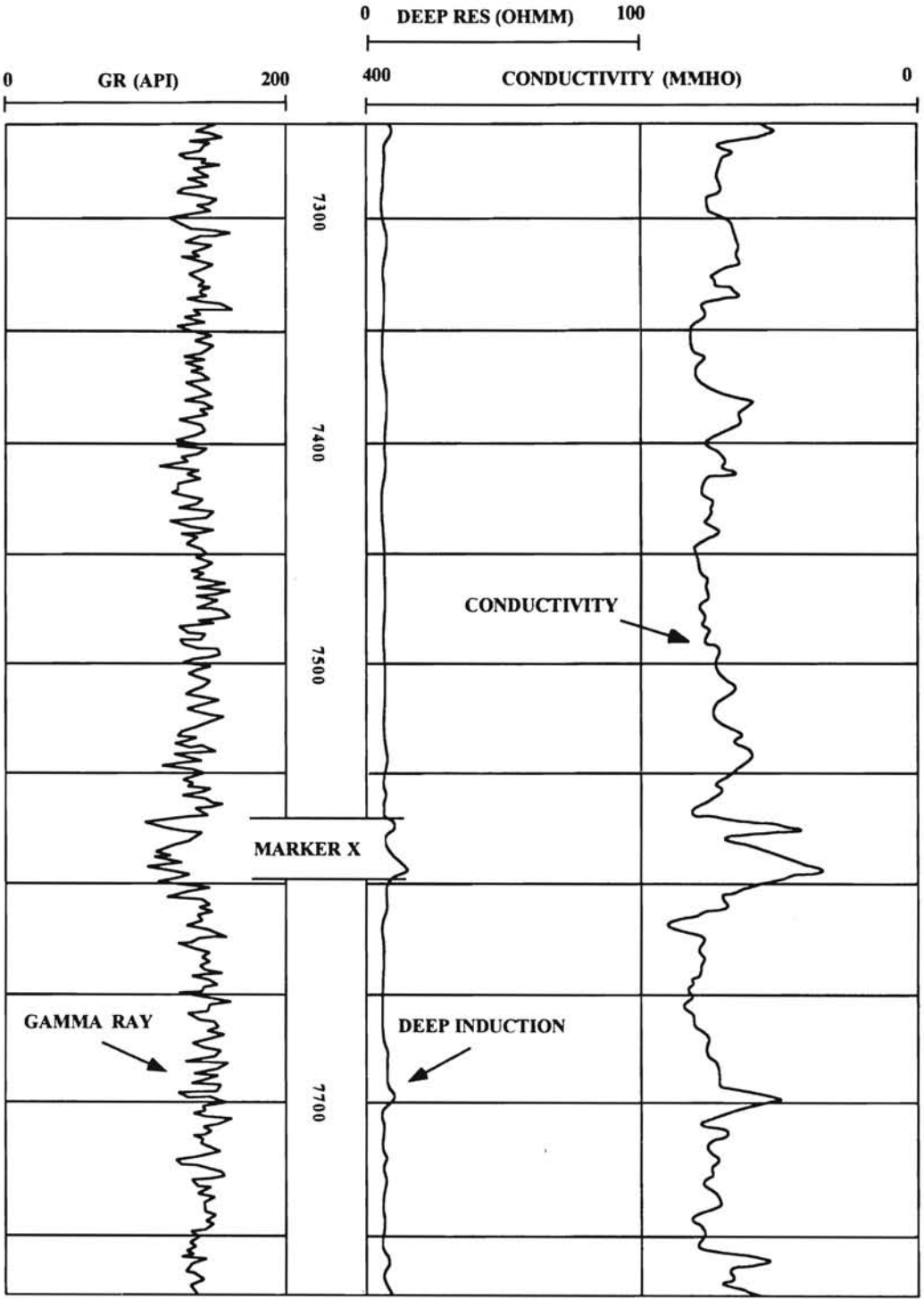

Figure 5: Representative well log for the Marker X
(JMC Exp. Co. Caudron #5, Sec 26, T.5.N., R.17.E.)

Structural cross-sections are first constructed in 1:24000 horizontal scale from the geological maps. Together with their reduced restorations, they are included as plates. These plates are also digitized and computer drafted with the aide of the drafting program Canvas. The computer generated cross-sections are slightly simplified and are included in the text as figures.

During the study, some problems in gathering and interpreting the data were encountered. Several existing wire-line well logs were unavailable. The wells are assumed to be vertical unless their completion cards and Herndon base map indicate otherwise. For the deviated wells, the surface and borehole locations are found from the completion cards and Herndon Base map. The vertical depths of the rock units in the cross-sections in deviated wells are approximated using simple geometric methods (Figure 6). Only the top of the units is considered in constructing the structural cross-sections. The unit termed "Spiro" on the cross-sections represents the Spiro sandstone-Wapanucka limestone package with a uniform thickness and does not represent the true thickness. These two units are not differentiated individually.

Previous Investigations

Tectonics of the Ouachita Mountains

The Ouachita orogenic belt and the Arkoma Basin are closely related tectonic features that were formed during the Early and Middle Pennsylvanian. (Johnson 1988). The Arkoma Basin is an arcuate structural depression that extends from south-central Oklahoma to east-central Arkansas (Figure 1). It is bounded by the Ouachita

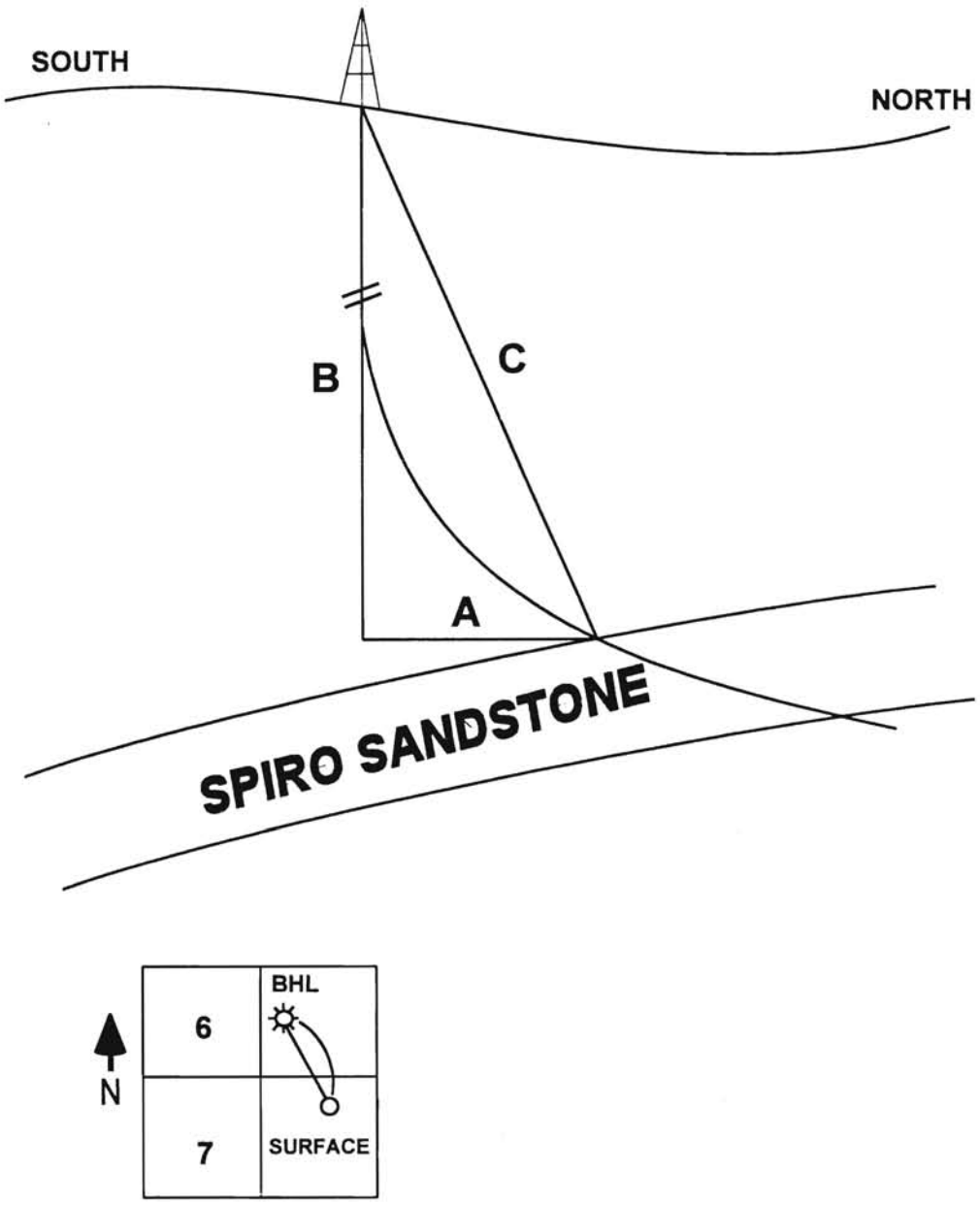

Figure 6: Method of correction for deviated wells (Modified from Hess, 1995)

Mountains to the south, the Arbuckle Mountains to the southwest, the Northern Oklahoma Platform to the west and northwest, and the Ozark uplift to the north. To the east, the basin exists beneath the Mesozoic cover of the Mississippi River Embayment. (Houseknecht and Kacena, 1983).

There have been several studies dealing with tectonic evolution of the Arkoma Basin and the Ouachita Mountains. Buchanan and Johnson (1968), Keller and Cebull (1973), and Walper (1977) all proposed a south-dipping subduction zone. Houseknecht and Kacena (1983) and Houseknecht (1986) integrated various previous works and presented a model for the formation of the Arkoma Basin and Ouachita Fold and Thrust Belt. Recently, many of these models have agreed on a scenario that involves southward dipping subduction of an Atlantic-type continental margin beneath either an island-arc system, a micro continent or a larger continental mass referred to as Llanoria (Houseknecht and Kacena, 1983).

During the Late Precambrian-Early Cambrian, a major episode of rifting resulted in the opening of a proto-Atlantic (Iapetus) ocean (Figure 7a). This type of rifting resulted in the development of rift basins along the southern margin of the northern continental mass (North America). Following the initial opening of the proto-Atlantic ocean, the southern margin of North America evolved into a passive Atlantic type margin that persisted throughout the early and middle Paleozoic (Figure 7b) with a classic shelf-slope-rise geometry (Houseknecht and Kacena, 1983). On the shelf, carbonates and sandstones of shallow marine to non-marine environments were deposited with numerous regional unconformities. Southward towards the slope, shales, sandstones, and limestones

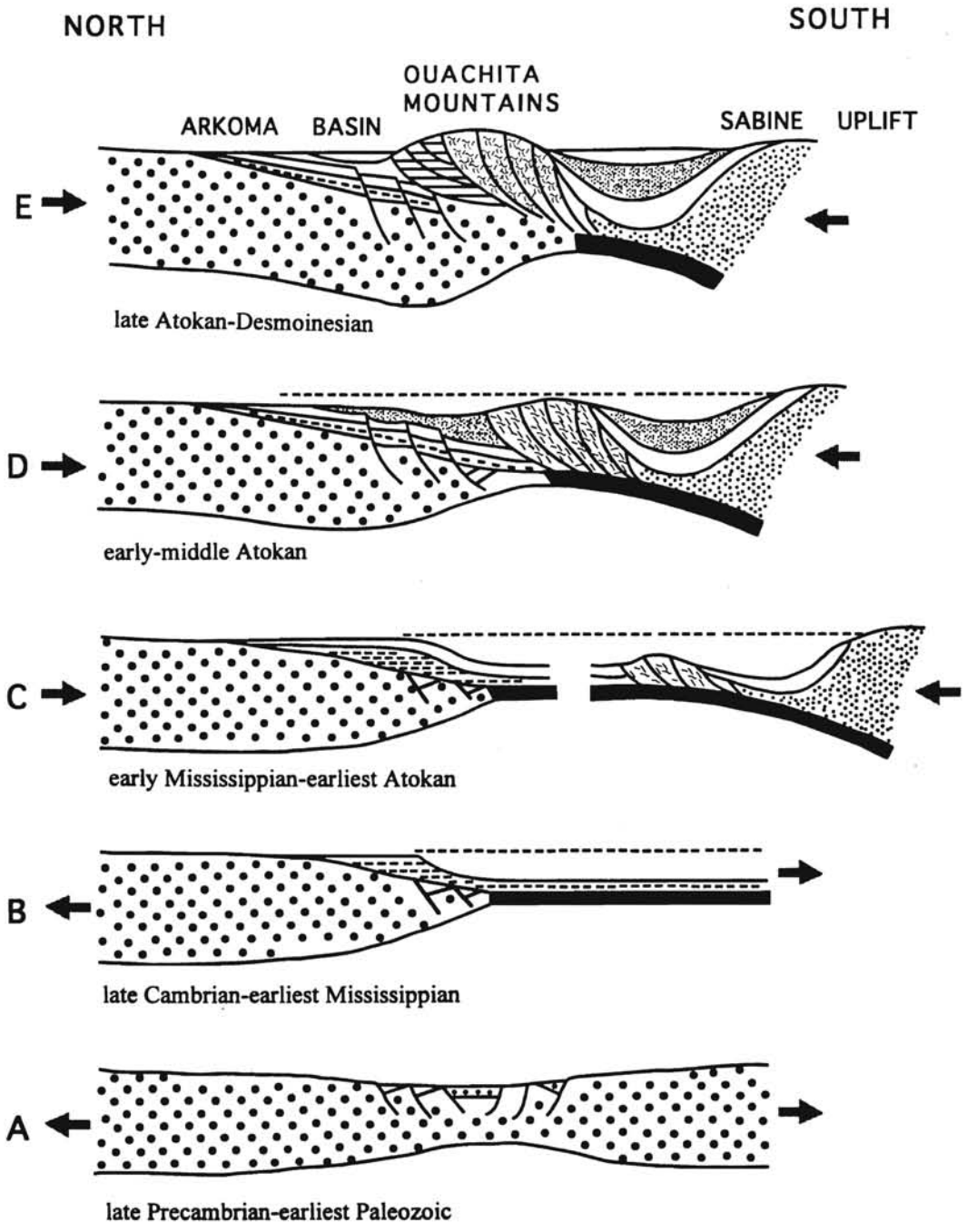

Figure 7: Diagrammatic evolution of southern margin of North America (From Houseknecht and Kacena, 1983)

characteristic of deeper water originated. Today, these deeper facies rocks crop out as northerly thrusted units in the core of the Ouachita Mountains. This basin is referred to as Iapetus Ocean (Ouachita Ocean) by Houseknecht and Kacena (1983).

During the Devonian or Mississippian, the ocean began to close. The closure led to subduction of the oceanic lithosphere beneath the southern continental mass of Llanoria (Figure 7c). It is unknown when the convergence began, but the widespread metamorphic event during the Devonian strongly suggests subduction. The presence of detrital material indicative of an orogenic provenance (Morris 1974) and locally abundant volcanic debris including tuffs and volcaniclastic sandstones in the Stanley Shale strongly suggest that subduction was occuring during the Mississippian. To the south of the Ouachita Mountains, along the flanks of the Sabine Uplift, Mississippian volcanic rocks occur in the subsurface suggesting the presence of a magmatic arc which developed along the northern margin of Llanoria during closure. A subduction complex may have evolved along the southern margin of the subduction zone which limited the amount of volcaniclastic detritus reaching the remnant ocean basin and trench (Houseknecht and Kacena 1983).

During the interval from late Mississipian to early Atokan, convergence continued and the remnant ocean gradually closed. The shelf units that were deposited earlier remained undisturbed except for an increase in the detrital material from north. In this time interval, the basin persisted and limestones, shales and sandstones were deposited in environments ranging from shallow marine to non-marine. The basal Atokan Spiro sandstone deposited in the Early Atokan in such environmental diversity.

During this time the remnant ocean basin became a site of rapid flysch deposition. The sediments were mostly derived from east where the collision resulted in uplift along the Ouachita trend. Sediments poured into the deep basin where they were dispersed longitudinally westward and ultimately deposited on submarine fans and in associated abyssal environments resulting in more than 5 km of flysch deposition during Mississippian and Morrowan time. The Stanley, Jackfork and Johns Valley formations are the units formed from flysch deposits in the deep basin.

With the continuing subduction of the remnant ocean basin, the northward advancing subduction complex overrode the rifted continental margin of North America by early Atokan time (Figure 7d). Due to increased vertical load and flexural bending caused by the subducting plate, the southern margin of the North American continental crust experienced widespread normal faulting in the foreland. The normal faults generally strike parallel to the Ouachita trend and are mostly downthrown to the south, offsetting both the crystalline basement and overlying Cambrian prism. Due to this normal faulting, the rates of both subsidence and sedimentation increased. Contemporaneous fault movement with the deposition of lower to middle Atokan shales and sandstones resulted in abrupt thickening of sediments across the normal faults (Figure 8). This thickened Atoka strata represents a transition between passive margin sedimentation and foreland basin sedimentation (Houseknecht and Kacena 1983).

In the late Atokan time, foreland style thrusting dominated the area as the subduction complex pushed northward (Figure 7d). As a result of the uplift along the frontal belt of Ouachitas, a foreland basin developed. Shallow marine, deltaic, and fluvial sedimentation occurred in this newly evolved basin. Upper Atokan and Desmoinesian

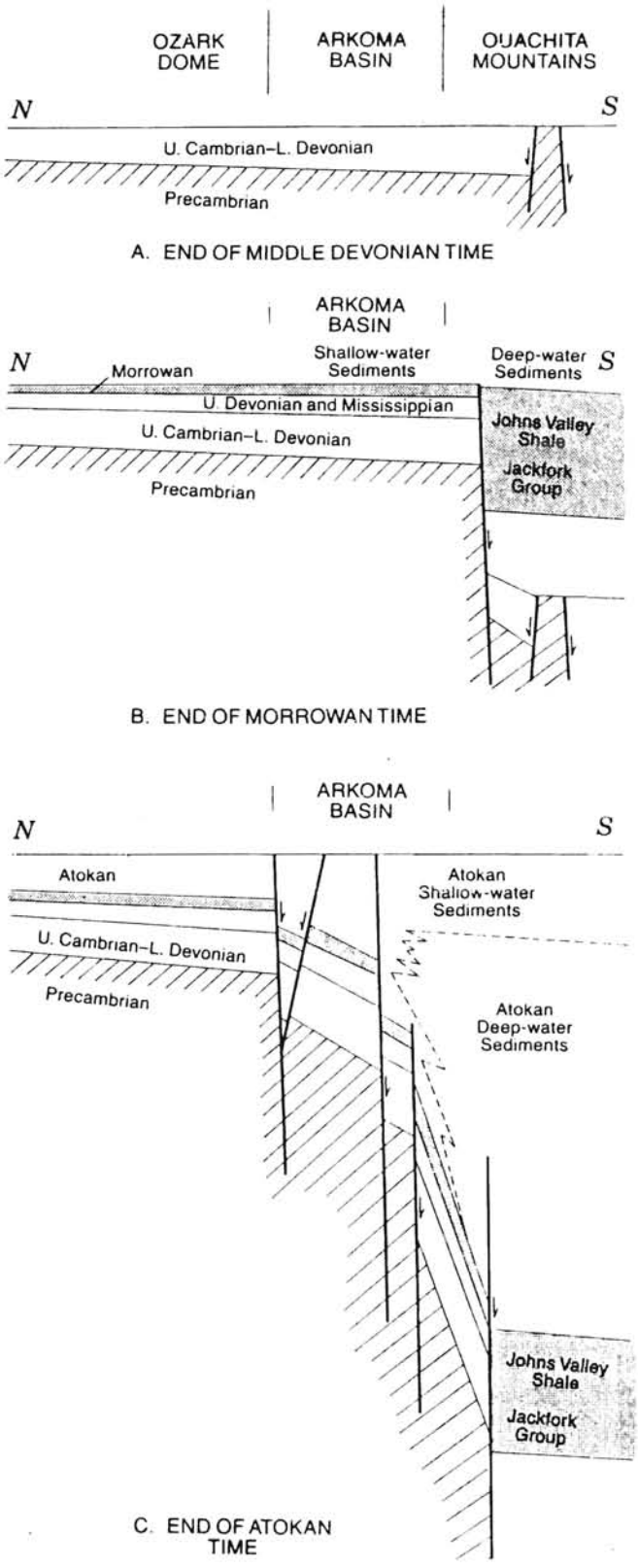

Figure 8: Generalized cross-sections showing the sedimentation in the Arkoma Basin-Ouachita Mountain area from Late Cambrian through Atokan time (From Johnson, 1988)

units of the Arkoma basin resemble deposition in a coal-bearing molasse basin. The structural configuration of the Arkoma-Ouachita system has remained fairly same since the Desmoinesian, although relatively minor folding and thrusting continued after the Desmoinesian (Figure 7e) (Houseknecht and Kacena 1983).

Arkoma Basin

The Arkoma Basin was first characterized as a foreland basin by Buchanan and Johnson (1968) where an incomplete section of Cambrian through Morrowan rocks exist. Arbenz (1989) studied the structural geology of the Ouachita Mountains and the Arkoma Basin as a mixed assemblage of structural styles. He suggested that in the southern two-thirds of the basin, a thin-skinned compressional fold belt detached from the underlying block faulted lower Atokan and older rocks dominates the surface and shallow subsurface geology.

The Choctaw fault is the northernmost exposed thrust fault in the frontal Ouachitas and is commonly accepted as the boundary between the Arkoma Basin and the Ouachita Mountains. Arbenz (1989) observed that the Choctaw fault dies in the western part of Arkansas resulting in an inferred boundary between the Arkoma Basin and the Frontal Ouachita Mountains. The presence of an extensional fault system displacing the Atokan and pre-Atokan Paleozoic section is documented by Buchanan and Johnson (1968) and Berry and Trumbley (1968). These faults are dominantly down-to-the-south and displace the upper crystalline basement (Arbenz, 1989). Houseknecht (1986) suggested the rotation along these normal faults. An abrupt increase in the thickness of the lower and middle Atoka and combined with the presence of turbidite facies along

those normal faults to the south suggest that the faults were active during Atokan sedimentation. However, olistostromal units in older rocks hint that the growth faulting could be occurred as early as Mississippian (Arbenz, 1989). Ferguson and Suneson (1988) proposed that the growth faults acted as barriers which forced the thrusts to ramp over basement rocks.

Hardie (1988), and Perry and Suneson (1990) discussed the presence of a triangle zone marking the transition from the Frontal Ouachitas to the Arkoma Basin. Mazengarb (1995), Akthar (1995), Cemen and others (1995), and Sagnak and others (1996 a,b) accept the presence of a triangle zone at the frontal zone of the Ouachita mountains in southeast Oklahoma.

Oklahoma Geological Survey has published several geological maps and guidebooks describing the geology of the Arkoma Basin and Frontal Ouachita Mountains. These include Johnson (1988), and Suneson and Tilford (1990).

Wilburton Gas Field and Surrounding Areas

Study area of this thesis is located in the Wilburton gas field and surrounding areas which is located in Latimer and Pittsburg counties, Oklahoma (Figure 2). Wilburton gas field is productive since 1929 and the main production is from the Spiro sandstone.

The Wilburton gas field is associated with several structural features (Hendricks, 1939). The Adamson anticline, the Hartshorne syncline, the Wilburton anticline, and the Carbon fault are the prominent structural features in and around the field.

Based on the structural contour maps in the Wilburton gas field area, Berry and Trumbley (1968) concluded that surface structures continue into the subsurface within the middle Atokan. Tilford (1990) suggested that units from the Wapanucka Limestone to the basement rocks flooring the area occur without depositional breaks to the south of the Choctaw fault.

Perry and Suneson (1990) and Cemen and others (1994) made preliminary interpretations of seismic profiles near Wilburton and Hartshorne. These interpretations agree on the presence of duplex structures splaying from a basal detachment. Cemen and others (1994) also pointed out the rough correlation between the pressure data in the Spiro reservoirs and the duplex structures. Wilkerson and Wellman (1993) studied the Gale-Buckeye Thrust System in the frontal Ouachitas which partially coincides with the Wilburton gas filed and suggested that the system might have been formed by a breakforward sequence of thrusting. Akthar (1995) estimated about forty five percent shortening of the Spiro sandstone due to thrusting in the Wilburton area.

Several studies were conducted to understand the petrologic and diagenetic characteristics of the Spiro sandstone in the Arkoma Basin and particularly in the Wilburton gas field area. Lumsden and others (1971) discussed the relationship between chlorite coatings and preservation of porosity in the Spiro sandstone. In a study on the Spiro sandstone in the Wilburton Gas Field area, Al-Shaieb (1988) and Al-Shaieb and others (1995) identified chamosite, an iron-rich chlorite, as the clay coating responsible for preservation of primary porosity. Feller (1995) studied the compartmentation processes and sealing mechanisms.

CHAPTER 2

STRATIGRAPHY OF THE ARKOMA BASIN

The Arkoma Basin is composed of a thick sequence of sedimentary rocks with ages ranging from Cambrian to Pennsylvanian (Figure 9). The Pennsylvanian is represented by Morrowan, Atokan, and Desmoinesian series in the basin. The exposed rock stratigraphic units in Oklahoma are of Atokan and Desmoinesian age. Whether units younger than Pennsylvanian age were deposited and subsequently eroded or were not deposited at all remains unresolved. In this study, the emphasis is on the Spiro sandstone which is the lowermost part of the Atokan series. However, a brief description of the units in the Arkoma Basin is included.

Proterozoic granite and rhyolite is believed to form the basement in the basin (Figure 9). The Upper Cambrian Timbered Hills Group overlies the Proterozoic rocks and is composed of the Reagen Sandstone and the Honey Creek Limestone. The Reagan Sandstone is a time-transgressive basal sandstone deposited in all areas except local topographic highs (Johnson, 1988). The sandstone is succeeded upward by the Honey Creek Formation consisting of thin, trilobite-rich pelmatozoan limestone (Ham, 1978).

The Arbuckle Group conformably overlies the Timbered Hills Group. The sediments continue upward as carbonates of Upper Cambrian to Lower Ordovician age (Ham, 1978). From bottom to top, the Fort Sill Limestone, the Roger Dolomite, the

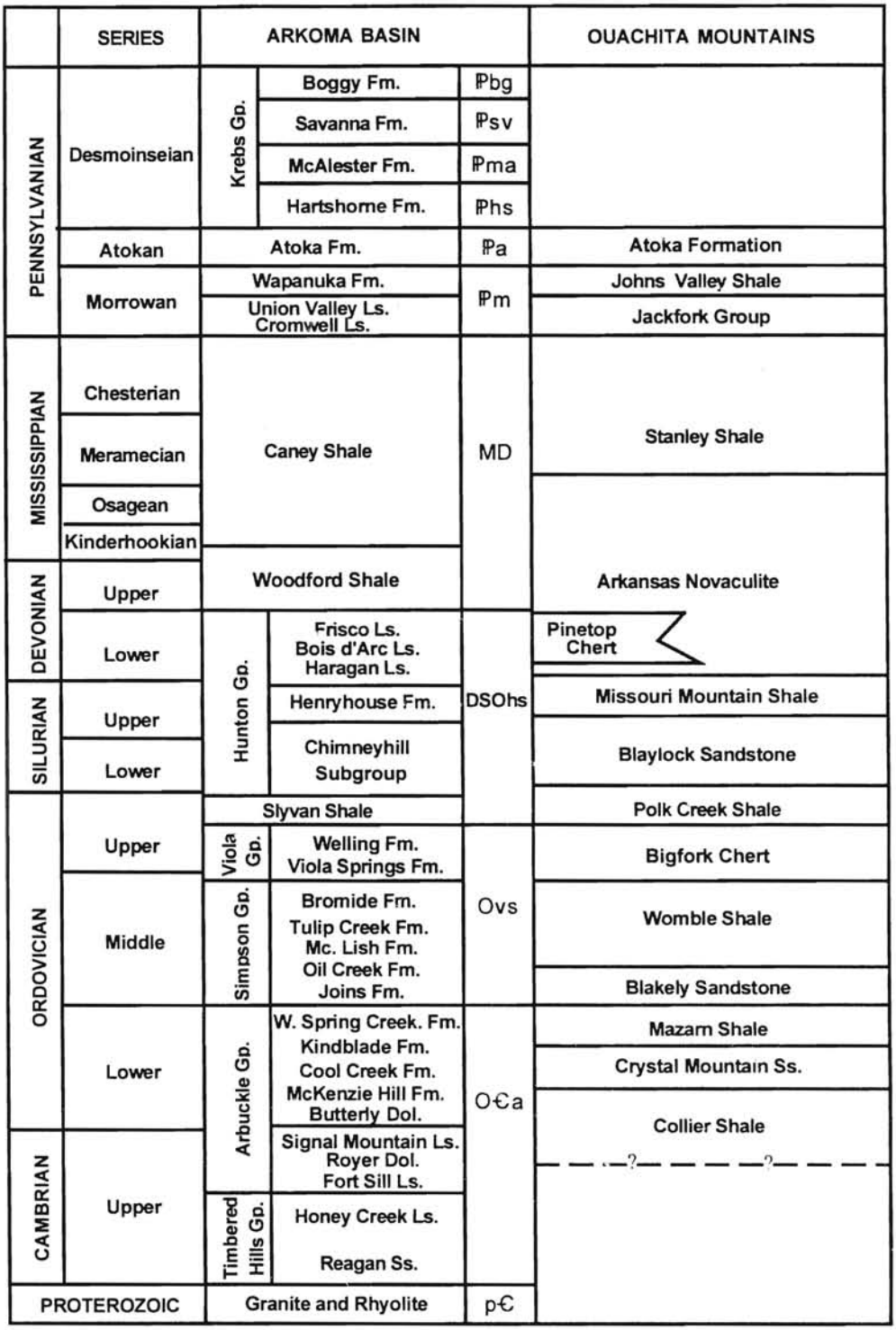

Figure 9: Stratigraphic chart of the Arkoma Basin and the Ouachita Mountains (From Johnson, 1988).

Signal Mountain Limestone, the Butterfly Dolomite, the McKenzie Hill Formation, the Cool Creek Formation, the Kindblade Formation, and the West Spring Creek Formation comprise the Arbuckle Group. These units are of shallow marine origin and are rich in fossils including trilobites, brachiopods, mollusks, pelmatozoans, sponges, and toward the top, graptolites (Ham, 1978).

The Middle and Upper Ordovician rocks include the Simpson Group, the Viola Group, and the Sylvan Shale in an ascending order. Rocks of the Middle Ordovician Simpson Group represent a change in depositional environment over that of the Arbuckle Group. The group is predominantly composed of the alternation of skeletal calcarenites, skeletal carbonates, mudstones, sandstones and shales. Clean sand and greenish gray shale beds are common in the skeletal calcarenites. The Joins Formation is at the base. The Oil Creek, McLish, Tulip, and Bromide Formations succeed towards the top and all have prominent basal sandstones (Ham, 1978). In the shelf environments, the group consists mostly of limestone (Ham, 1978). The Viola Group conformably overlies the Simpson Group and is composed of the Viola Springs Formation and the Welling Formation. The Viola Group represents several different limestone facies including nodular chert-rich mudstones, packstones, porous grainstones, wackestones and dolomitized wackestones (Sykes, 1995). Unconformably overlying the Viola Group, the Upper Ordovician Sylvan Shale is a dark greenish-gray shale with well developed laminations and graptolite and chitinozoan content (Ham, 1978).

The Hunton Group rocks represent Lower Silurian through Lower Devonian rocks. It conformably overlies the Sylvan Shale and unconformably underlies the Woodford shale. Its base is characterized by Ordovician oolites. The Silurian formations

over the base (Subgroup, Chimneyhill and Henryhouse) are mainly composed of skeletal mudstones and skeletal calcarenites. The overlying Devonian formations are the Harragan, Bois d'Arc, and Frisco limestones which are predominantly skeletal mudstones and calcarenites (Ham, 1978).

The Upper Devonian to Lower Mississippian Woodford Shale unconformably overlies the Hunton Group. The Woodford Shale consists of dark fissile shale, beds of vitreous chert, and siliceous chert (Ham, 1978). In the frontal Ouachitas, the Woodford Shale hosts a main detachment surface termed the Woodford Detachment.

The Lower and Middle Mississippian in the Arkoma Basin is represented by the Caney Shale. The main lithology in the Caney Shale is dark gray fissile shales with some local phosphatic nodules. The informal Springer formation is similar to the Caney Shale in appearance. The stratigraphic boundary between the Springer and Caney shales is drawn at the earliest appearance of siderite or clay-ironstone beds in the sequence. Based on the spores and pollens the Springer shale is Late Mississippian (Chesterian) (Ham, 1978). In the Frontal Ouachita Mountains, the Springer shale hosts a main detachment.

The Pennsylvanian rocks unconformably overlie the Mississippian and are divided into Morrowan, Atokan, and Desmoinesian. The Morrowan strata in the basin represent a continuation of shelf-like sediments although they contain significant amounts of sand. These strata range from 300 feet thick in the north, to roughly 1000 feet thick along the southern margin of the basin. Johnson (1988) reported that the Morrowan strata grade into 3000-6000 feet of deeper-water marine (flysch) sediments (Jackfork Group and Johns Valley Shale) in the south within the Ouachita Mountains. In the

Arkoma Basin, the Morrowan rocks are represented by the Union Valley-Cromwell interval and the Wapanucka Formation.

The Union Valley Limestone and Cromwell sandstone are widely present in the Oklahoma part of the Arkoma Basin. They were deposited during a series of transgressions and regressions. They are composed of a series of discontinuous limestones and sands separated by shales (Sutherland, 1988).

Conformably overlying the Union Valley-Cromwell and unconformably underlying the Atoka Formation is the Wapanucka Formation. It contains the Wapanucka shale and the overlying Wapanucka Limestone. In the study area, the Wapanucka Formation is exposed along the thrust faults.

The thickest unit in the Arkoma Basin of Oklahoma is the Atoka Formation of the Atokan Series. It is divided into lower, middle, and upper Atokan (Figure 10). The division is based on the effects of syndepositional normal faults on the amount of sediments that accumulated in the Arkoma Basin. The Atoka Formation is roughly seventy percent shale in the central and southern parts of the Arkoma Basin. It also contains lenses and tongues of sandstone and siltstone along with several thin coal beds (Cardott and others, 1986). Atokan deposition in the basin was characterized by a series of meandering fluvial systems and deltas that had their origin in the north and northwest. The thickness of the Atoka ranges from several hundred feet to 10,000 feet in the basin (Johnson, 1988).

There is a regional unconformity between the Atoka and Morrowan in the northern margin of the basin. However, in the southern section of the basin, the pre-Atokan unconformity is absent. The lower Atokan is represented by the Spiro sandstone

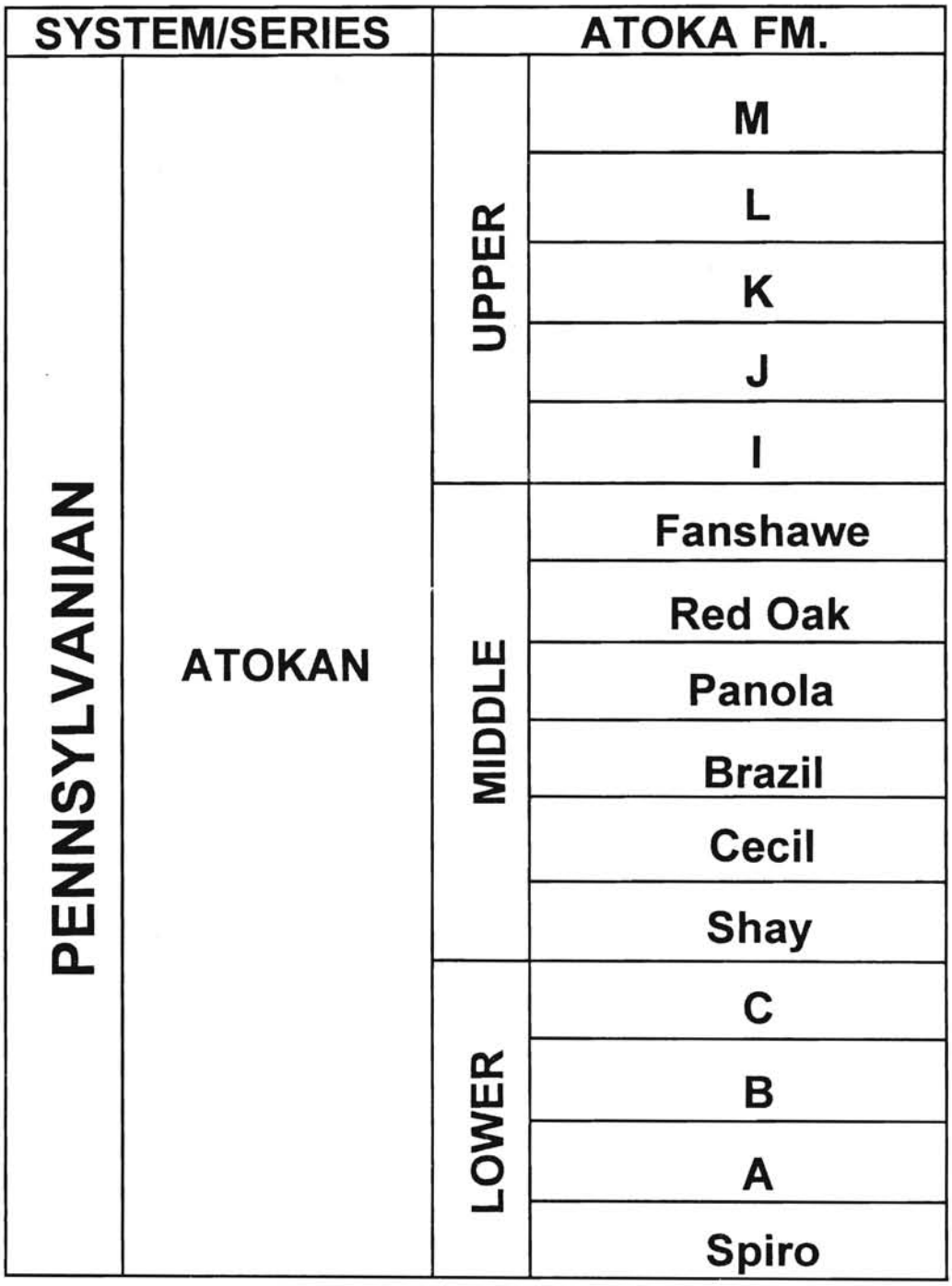

Figure 10: Stratigraphic chart illustrating the Atokan Series in Arkoma Basin in Oklahoma (From Feller, 1995).

and an overlying persistent shale (Sutherland, 1988). Sedimentation in this interval was initiated in Oklahoma with a source from the northwest by the development of fluvial systems and small deltas on the eroded surface of the underlying Wapanucka Formation (Sutherland, 1988).

The middle Atokan interval in Oklahoma is composed predominantly of shale with a few thick sandstone units. The Red Oak sandstone is a major sandstone which continues to the south of the San Bois Fault. According to Vedros and Fisher (1978), the Red Oak sand was deposited in a submarine fan environment. The upper Atokan strata is are not cut by normal faults. The predominant lithologies in the upper Atoka are shallow shelf and deltaic rocks (Sutherland, 1988).

The Desmoinesian series in the Arkoma Basin and adjacent areas to the northwest consist of the Krebs, Cabaniss, and Marmation Groups (Figure11). In the study area only the Krebs Group crop out. Rocks of the Cabaniss and Marmation Group are found along the northwest margin of the basin.

The Krebs Group is composed of the Hartshorne Formation, the McAlester Formation, the Savanna Formation, and the Boggy Formation. The Hartshorne Formation, gradationally overlies the Atoka Formation, and was deposited in high constructive tidally-influenced deltaic systems. The overlying McAlester to Boggy Formations are comprised of the rocks of fluvial/deltaic sedimentation which were deposited during series of transgressions and regressions. The Boggy Formation was deposited in a deltaic complex (Sutherland, 1988).

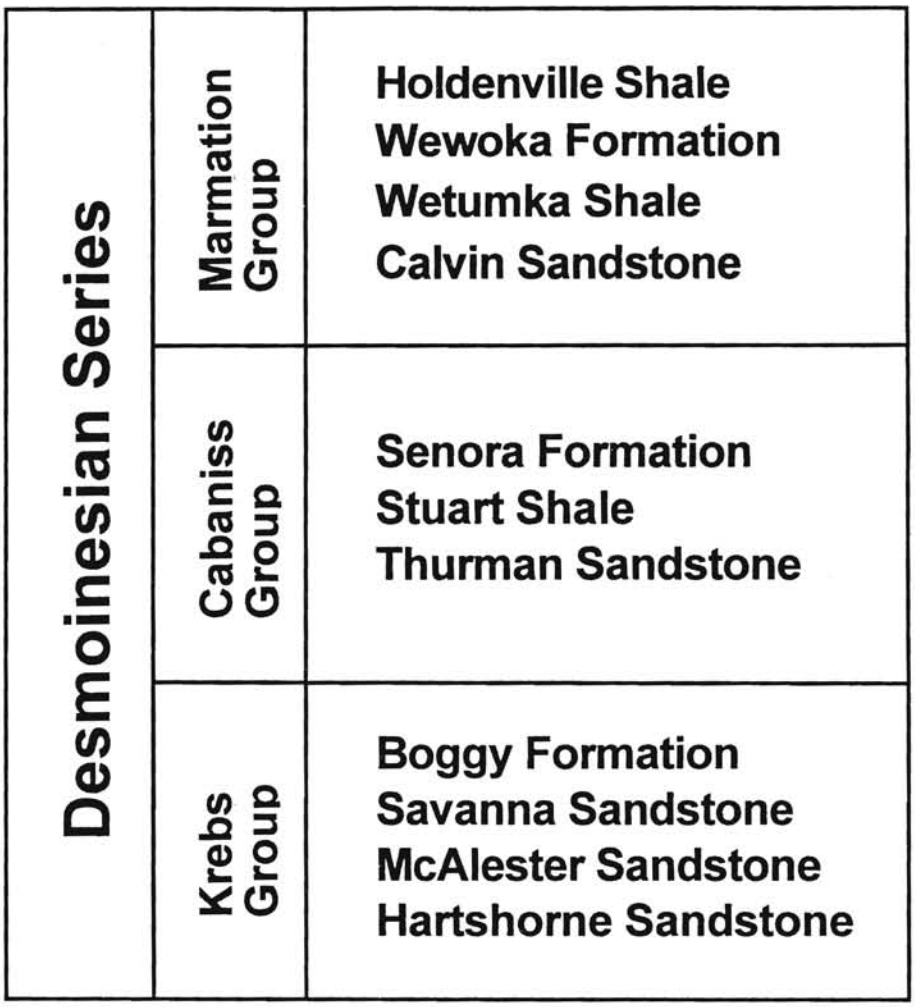

Figure 11: Stratigraphy of the Desmoinesian in the Arkoma Basin of Oklahoma (From Sutherland, 1988)

CHAPTER 3

PETROLOGY, DIAGENESIS AND DEPOSITIONAL ENVIRONMENT OF THE SPIRO SANDSTONE

An extensive petrographic study of the Spiro sandstone is beyond the scope of this study. However, a core interval of the Spiro sandstone obtained from the Pan-American Petroleum Company, Reusch #1 well is examined in order to infer petrologic characteristics and depositional environment of the sandstone within the study area. Thirteen thin sections prepared from this core were examined under a petrographic microscope in addition to visual examination of the core for primary sedimentary structures.

Petrology and Diagenesis

Detrital Constituents

Detrital constituents identified include quartz, rock fragments, skeletal fragments, phosphate, zircon, muscovite, and biotite.

The most abundant detrital grain in the Pan-American Reusch #1 core samples is monocrystalline quartz (Figure 12). It comprises about 95% of the total quartz in the thin-sections. The monocrystalline quartz grains mostly exhibit straight extinction but

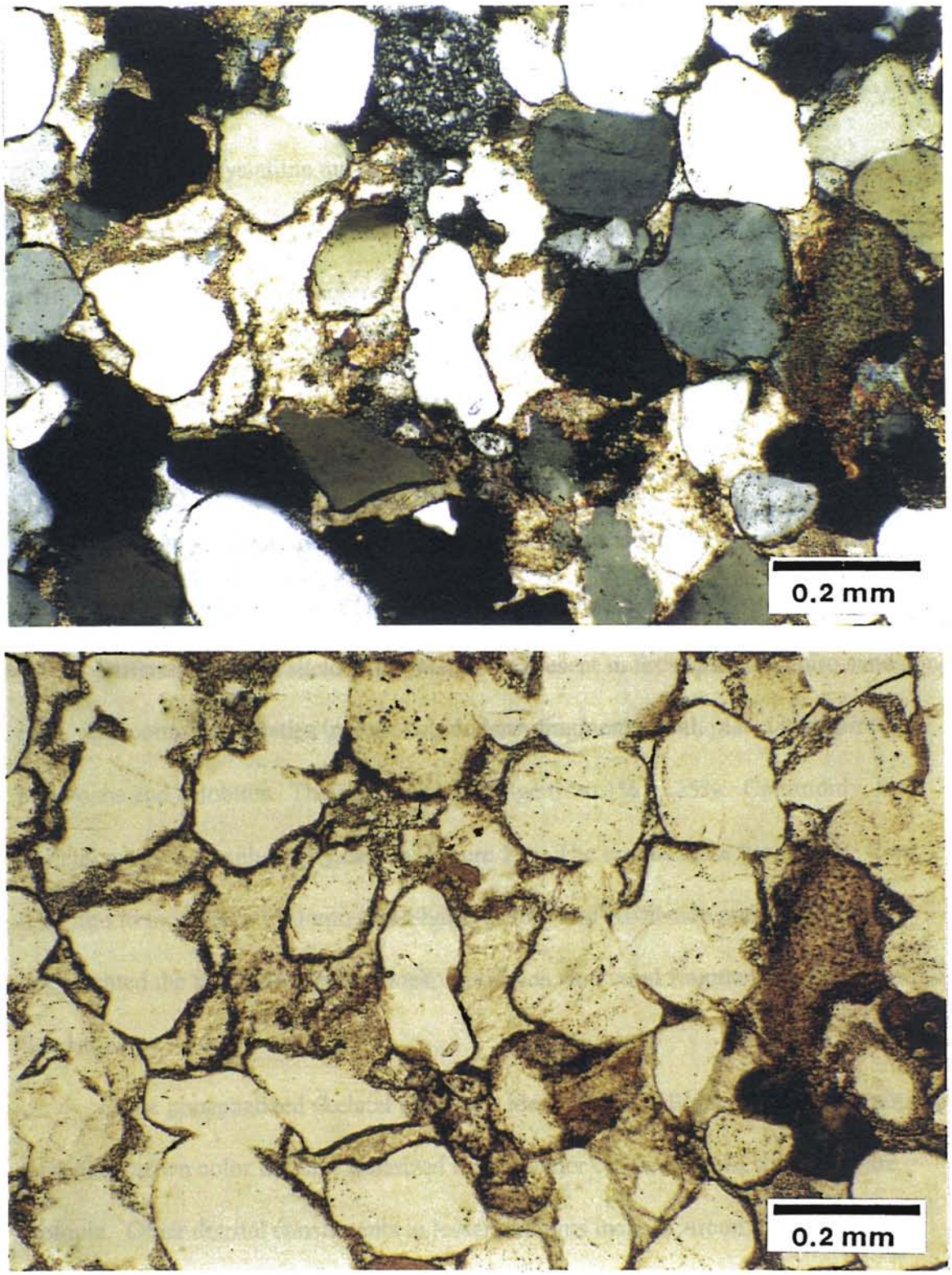

Figure 12: Subrounded quartz grains and calcite cement
(XN, PPL, 100X)

slightly undulose extinction showing grains are also present in much lesser quantities. The average total quartz content ranges from 43% to 64% of the total detrital constituents. Polycrystalline quartz occurs in minor quantities. Inclusions and vacuoles are also present in quartz grains in minor amounts. The quartz grains are mostly medium grained and well sorted with subrounded to rounded shapes. Quartz grains are easily recognizable by their first order birefringence color, low relief, and lack of twining and alteration.

Although no feldspars are observed in the thin sections, the presence of plagioclase and potassium feldspar in minor amounts are documented by Al-Shaieb (1988), Carlson (1988), Hooker (1988), and Al-Shaieb and others (1995).

Different types of skeletal fragments are present in the examined Spiro sandstone core. The common varieties include echinoderm fragments (both plates and spines), bryozoans and trilobites. Their percentages range from 1% to 25%. Commonly, the skeletal grains are replaced by calcite (Figure 13). The size of these grains vary from 0.05 mm to more than 1.00 mm. Al-Shaieb (1988) and Al-Shaieb and others (1995) documented the presence of ostracodes, fussilinids, and coral fragments in the Spiro Sandstone.

Some phosphatized skeletal grains are identified as collophane. These grains have a reddish brown color in plane polarized light. Under crossed nicols, the grains are isotopic. Other detrital constituents in lesser amounts include zircon, muscovite, and biotite (Figure 14). The presence of illite, and pseudomatrix formed by ductile

deformation of chamosite, glauconite, and shale fragments are documented by Al-Shaieb (1988), Al-Shaieb and others (1995) and Feller (1995).

Diagenetic Constituents and Features

Cement

Silica and carbonate cements are the main cement types observed in the Spiro sandstone. Silica cement occurs as syntaxial quartz overgrowths. Clay rims separate the grains from overgrowths. The rims are mainly composed of an early diagenetic product such as chlorite (Al-Shaieb and others, 1995). The early chlorite coating on quartz grains inhibits the formation of quartz overgrowths and retards the pressure solution features (Lumsden and others, 1971). This event is observed in several thin sections. In the areas of less and/or no clay coating, the syntaxial quartz overgrowths are common.

Carbonate minerals are the main cements observed in the Pan-American Petroleum Company, Reusch #1 core. Calcite is the dominant cement type. It is of variable size, and in the areas of widespread cementation, it is poikilotopic. In such areas, quartz grains and skeletal fragments float in the cement and are commonly replaced by calcite or less commonly by dolomite (Figure 15). The second most abundant carbonate cement is dolomite. Dolomite is observed as forming rhombs. Al-Shaieb (1988) differentiated two different stages of dolomite cementation and identified minor siderite cement. Trace amounts of pyrite cement are also observed in the thin sections.

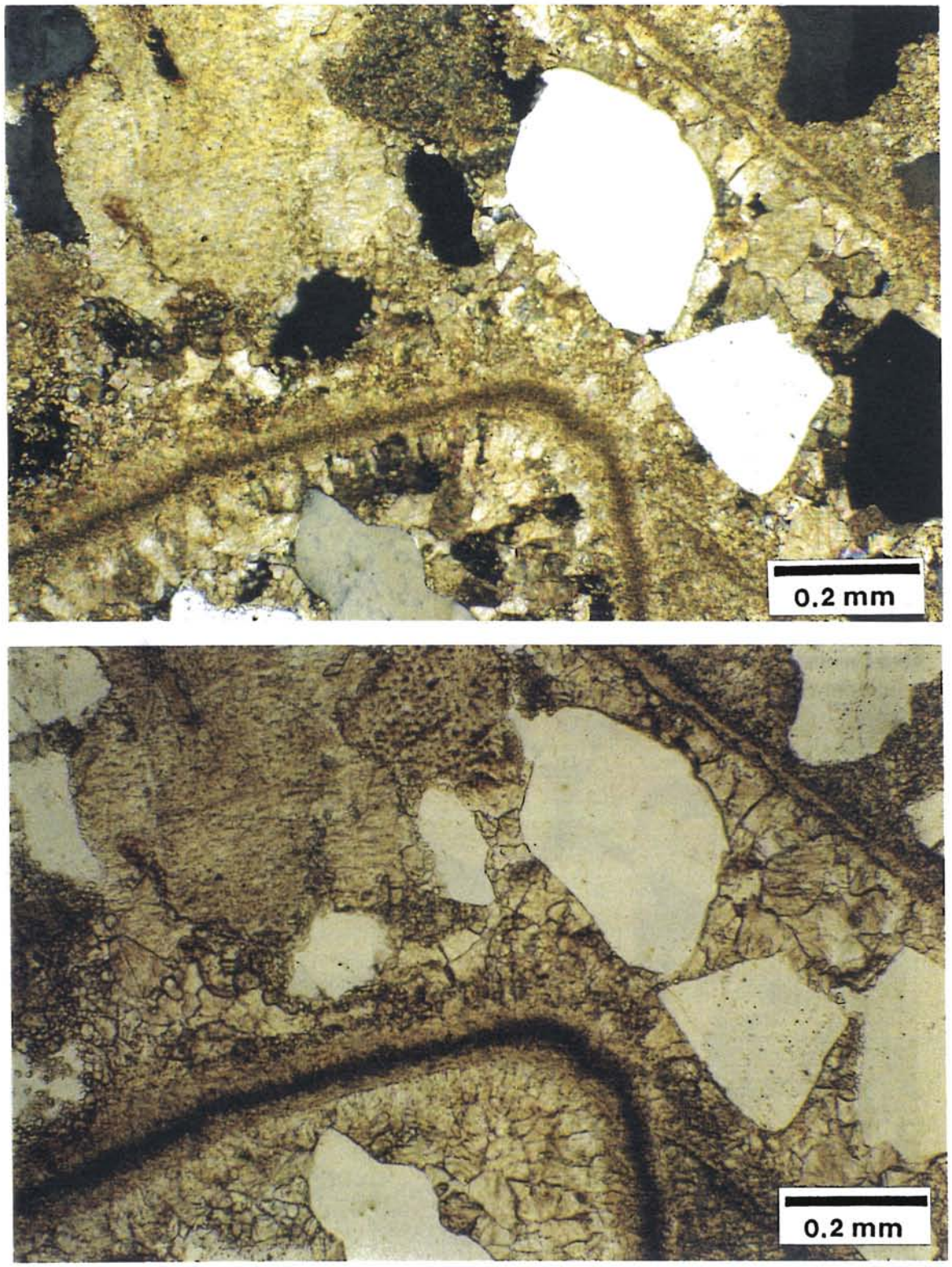

Figure 13: Skeletal fragments replaced by calcite
(XN, PPL, 100X)

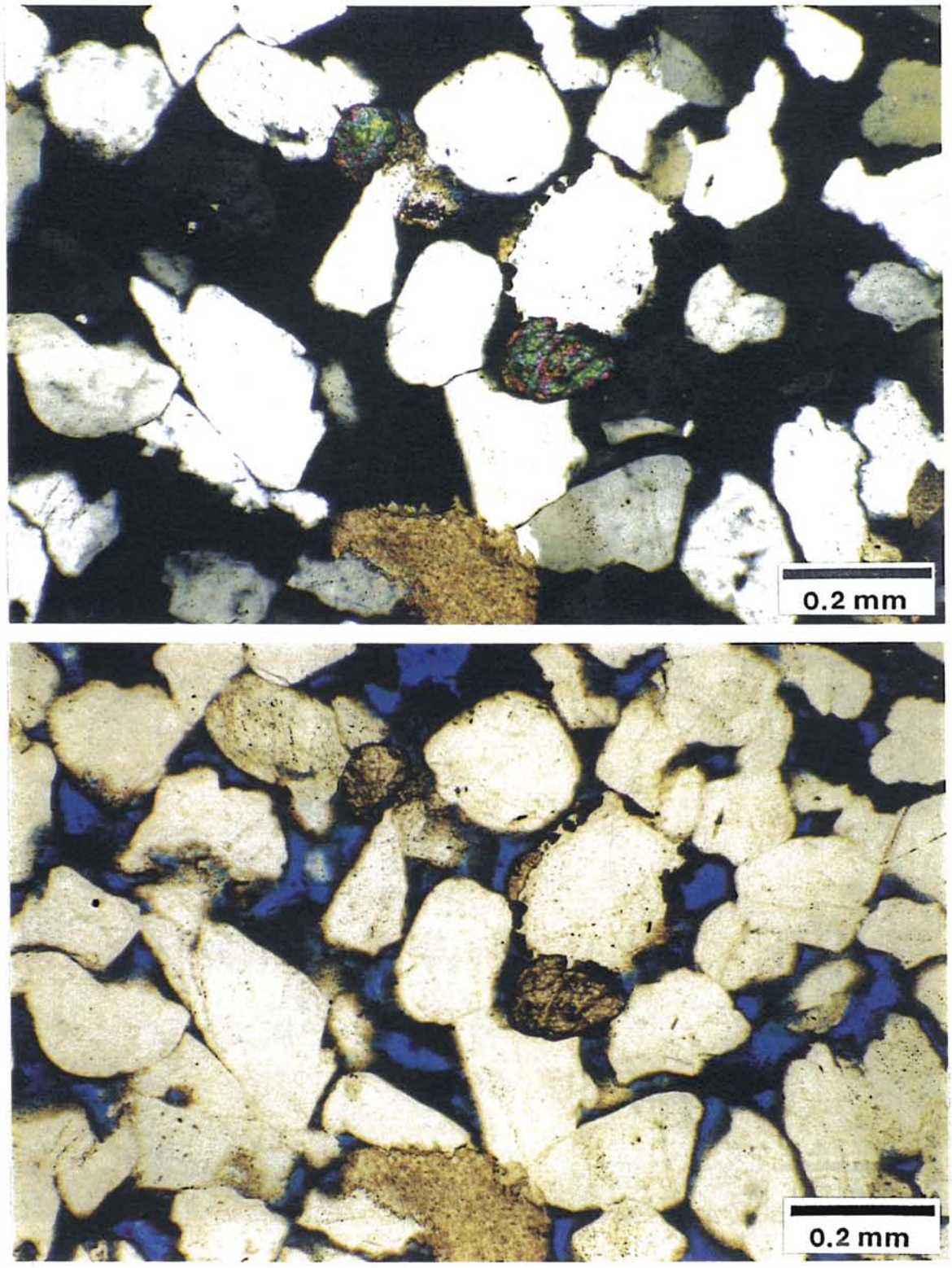

Figure 14: Chamosite coated quartz grains and minor zircon
(XN, PPL, 100X)

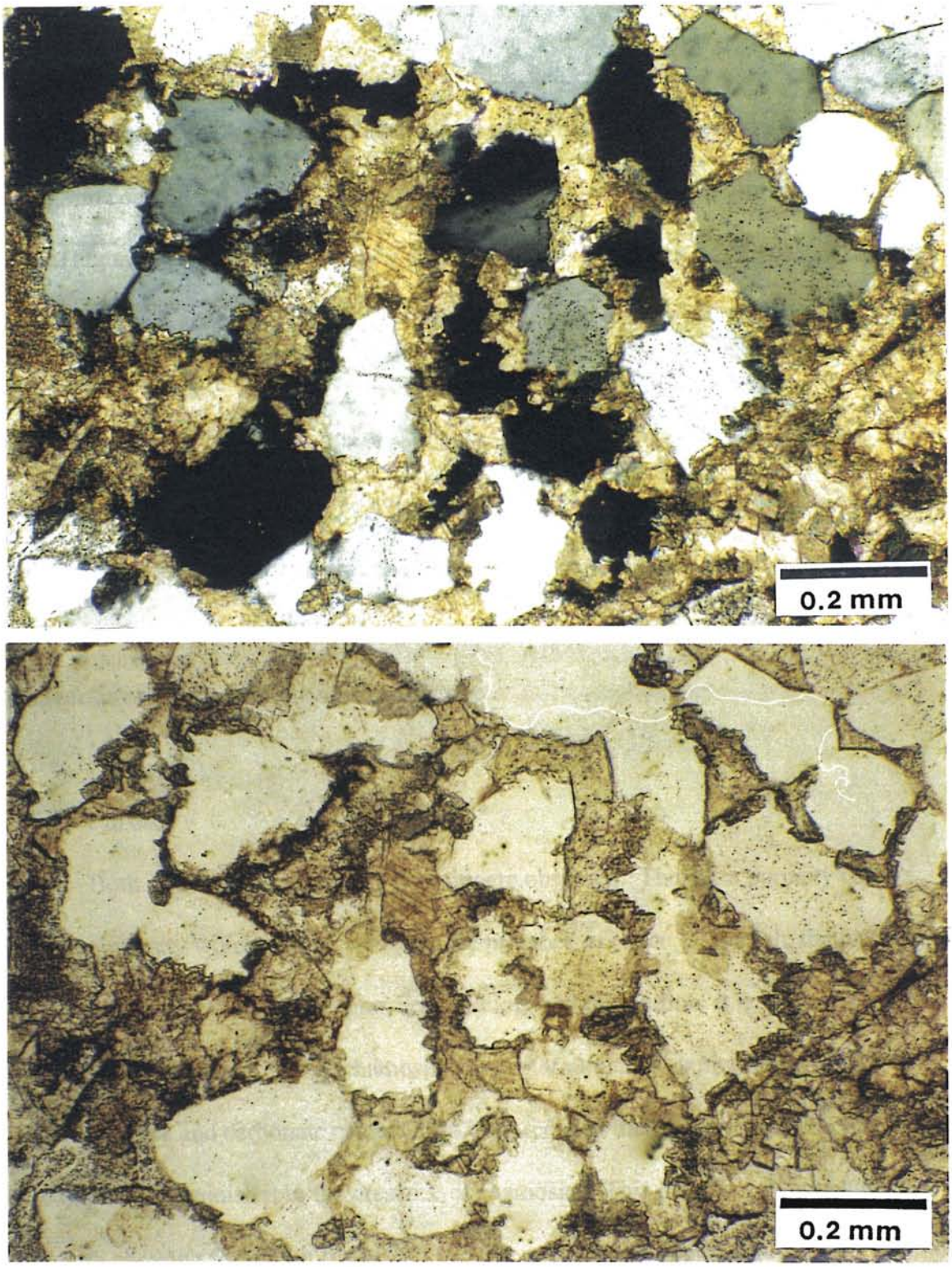

Figure 15: Heavily carbonate cemented (calcite and dolomite) area. Note the replacement of quartz grains by carbonate cement (XN, PPL, 100X)

Diagenetic Clays

Chamosite is the most abundant clay mineral in the examined core. It occurs both as a grain coating and individually as pellets. It is typically green to brownish green in color (Figures 14 and 16). If partially altered, the pellets are dark brown or even opaque. In areas of thick chamosite coating, cementation is limited. The chamosite coating around the quartz grains is the main contributor to the preservation of intergranular primary porosity.. Al-Shaieb (1988) concluded that two stages of chamosite precipitation occur in the Spiro sandstone. The other diagenetic clay observed is chlorite. Chlorite is identified as a pore filling mineral. Al-Shaieb (1988) and Al-Shaieb and others (1995) documented the presence of illite in the low chamosite content and discussed the diagenesis of the clays in the Spiro sandstone.

Porosity

Both primary and secondary porosity are observed. The main porosity type is primary porosity which was preserved in the presence of clays. Although, the primary porosity is modified by compaction, cementation, and dissolution, it is well preserved in the areas where there is a thick chamosite coating around the quartz grains (Figures 14 and 16). Silica and carbonate cementation have reduced the primary porosity but failed to completely diminish it in the presence of chamosite. This primary porosity acted as conduits allowing formation fluids to move through and eventually dissolve the metastable grains resulting in the generation of secondary porosity (Figure 17) (Al-Shaieb, 1988).

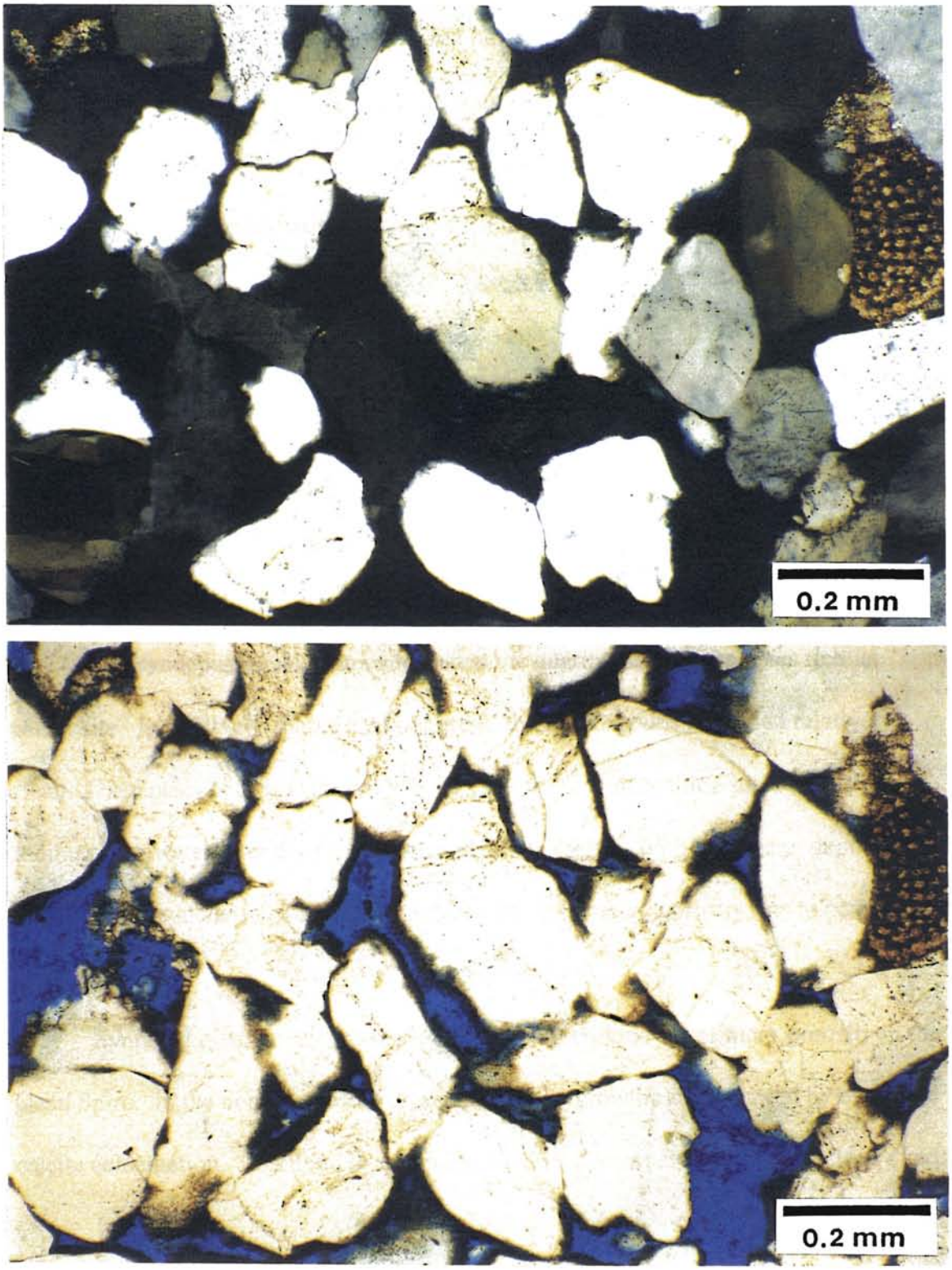

Figure 16: Chamosite coating surrounding quartz grains preserves the primary porosity. (XN, PPL, 100X)

Secondary porosity is present as moldic porosity and oversized and elongated pores. Al-Shaieb (1988) and Al-Shaieb and others (1995), documented that secondary porosity is volumetrically as significant as primary porosity. It can be attributed to the partial and/or complete dissolution of metastable constituents. Dissolution of chamosite pellets and skeletal grains are the major contributors to the secondary porosity.

Diagenesis

Diagenesis of the Spiro sandstone in Arkoma Basin of Oklahoma is studied in detail by Lumsden and others (1971), Al-Shaieb (1988), and Al-Shaieb and others (1995). A short summary of the diagenetic history of the Spiro sandstone is mainly compiled from these studies.

The syndepositional chamosite coated the quartz grains in the areas rich in chamosite. In relatively chamosite poor areas, the quartz grains remained relatively clean. Diagenesis of Spiro sandstone began shortly after deposition just below the sediment sea water interface (Al-Shaieb and others 1995). With increasing depth, the burial pressure increased resulting in decrease in the primary porosity due to compaction related effects.

Syntaxial quartz overgrowths significantly decreased the primary porosity in the clean Spiro. In the non-chamositic areas, quartz overgrowths are followed by extensive calcite cementation. Poikilotopic and mosaic calcite cement are common in clean quartz

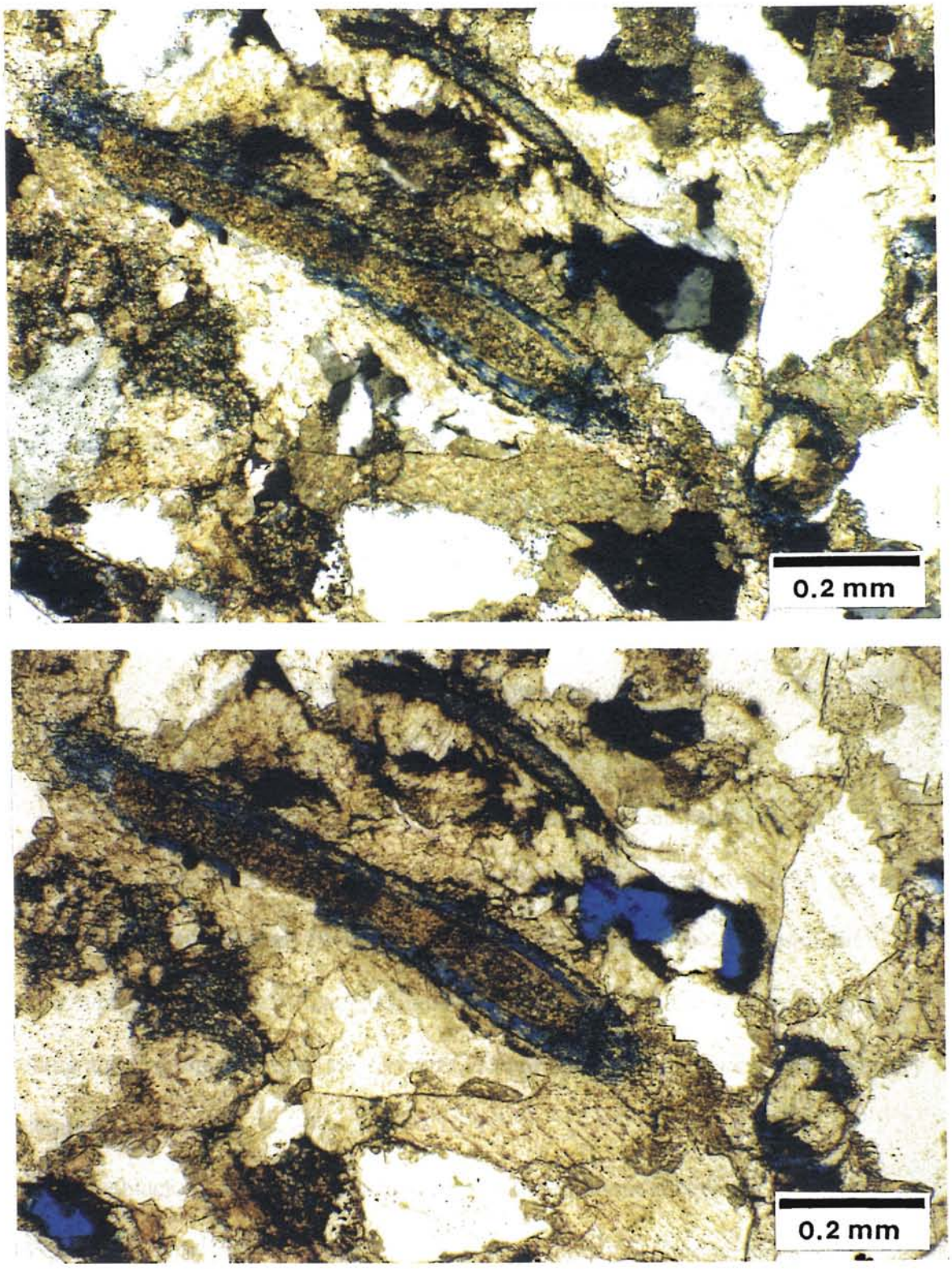

Figure 17: Secondary porosity formed from dissolution of echinoderm spines (XN, PPL, 100X)

areas. Both types of cementation reduce primary porosity. On the other hand, the quartz grains with thick chamosite coating remained relatively unaffected. Later, the preserved pores provided the necessary conduits for the fluids generated during the thermal maturation of organic matters. These acidic fluids were able to partially dissolve chamosite, other clays, and skeletal grains generating secondary porosity. Moldic porosity is abundant where there is a high concentration of skeletal grains (Figure 17). Hydrocarbon migration followed the secondary porosity generation. A late stage chamosite precipitation with well developed crystals filled the pores as a later diagenetic event. Figure 18 shows a diagram about the evolution and/or preservation of porosity as suggested by Al-Shaieb (1988).

Depositional Environment

The Spiro Sandstone in the Pan-American Petroleum Company, Reusch # 1 core is a light gray, light brown, grayish brown and brownish tan colored, fossilliferous, fine to medium grained sandstone (Appendix I). Carbonate and silica are the dominant cement types. Among the primary sedimentary structures, medium scale trough cross-bedding and flowage structures are common. Minor stylolites are observed as secondary structures.

The black, fissile, laminated sub-Spiro shale is present at between 11519 and 11533 feet. Burrows exist towards the silty top portion of this interval, and the gradational contact between sub-Spiro shale and Spiro Sandstone shows no feature. The 11505-11519 feet interval is characterized by a fine grained silty-sand lithology and

possesses widespread bioturbation and flowage structures. This portion of the core is the gradation between the sub-Spiro shale and the Spiro sandstone. The Spiro sandstone is present from 11505 feet to the top of the cored interval (11468 feet). It is a brown to grayish brown, well sorted, predominantly medium grained sandstone. Sedimentary structures include trough cross-bedding. Minor stylolites are observed as secondary features. The thin-sections from various depths of this interval show the presence of chamositic facies.

Lumdsen and others (1971) identified four major sand channels in the Oklahoma part of the Arkoma Basin and referred to them as Foster sand. They postulated that the Spiro sandstone deposited in a shore line environment and the Foster sand was in the central part of the basin. Sutherland (1988) concluded that the interchannel deposits are composed of fine grained sand and shale, organized into ripple bedded and thoroughly bioturbated sequences and represent shallow through tidal flat environments.

The findings from the limited amount of petrologic and core exmainations of this study are supportive of the previous interpretations. Detrital constituents including chamosite, skeletal grains, and collophane as well as the primary sedimentary structures like trough cross-bedding, bioturbation, and burrows suggest a shallow marine environment. Clean, medium-grained sandstone facies with cross-bedding and current ripples indicate a tidal channel. The tidal flat environment is suggested by shale/siltstone alternation, bioturbation, burrows, and flow structures. The black fissile shale below the Spiro sandstone indicates a swamp environment. Sandstone with significantly decreasing amounts of skeletal grains towards the top is indicative of channel facies.

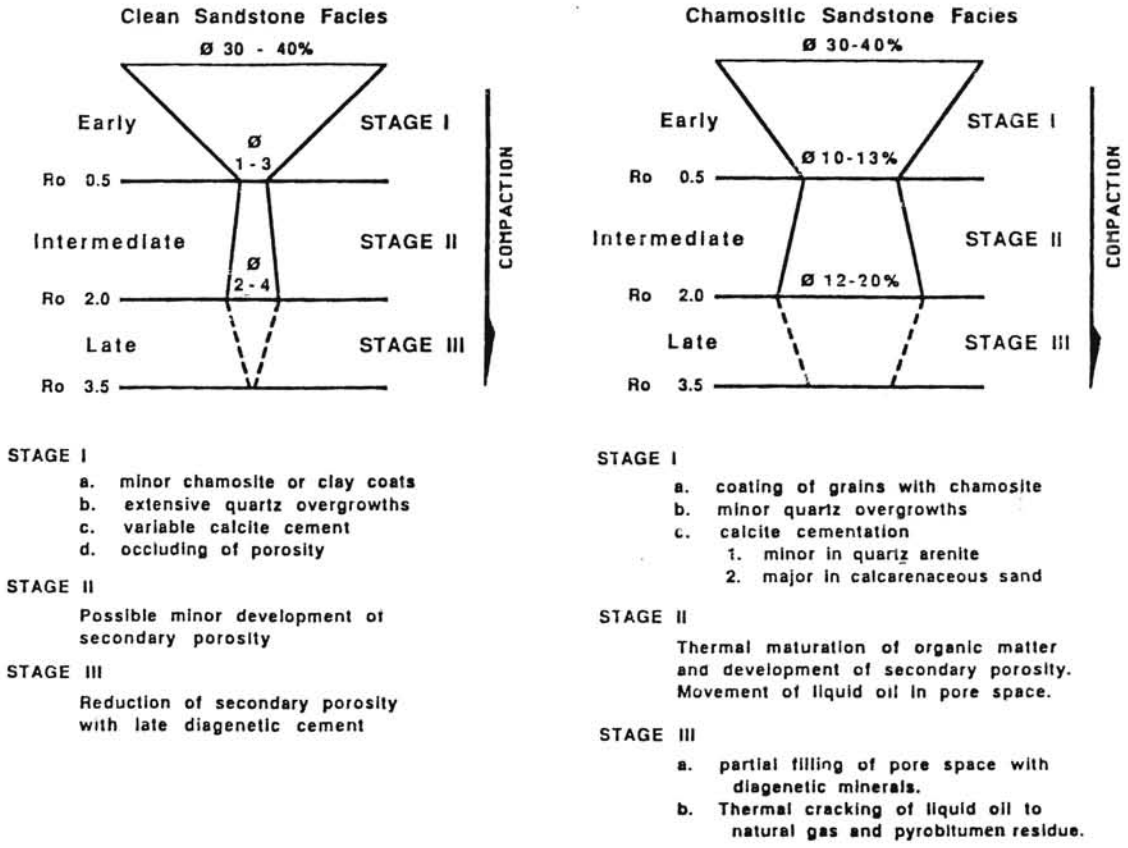

Figure 18: Preservation and/or development of porosity as related to diagenetic evolution (From Al-Shaieb, 1988)

CHAPTER 4

GEOMETRY OF FOLD AND THRUST ASSEMBLAGES

Compressional mountain belts contain fold and thrust assemblages which occur as wide zones of deformed sedimentary cover on the external side, or outer fringe. Gradations to basement thrusting are common toward the internal or core regions.

Fold and thrust belts contain complex listric thrusts which almost always cut upsection in the tectonic transport direction. Anticlines with imbricate thrusts and broad folded-thrust faults occur across the breadth of a fold and thrust belt. The latter are usually located where faults step up in sedimentary cover (Lowell 1985). Thrust faults which are directed against the tectonic transport direction are commonly observed and are called the back-thrusts which bound belts at their fronts and lead to the formation of the triangle zones.

Thrust Systems

In a fold and thrust belt several nearby faults may arrange in a closely related branching array known as a thrust system (Boyer and Elliot, 1982). Marshak and Mitra (1988) described a thrust system as an array of kinematically related faults that develop in

sequence during a single regional deformation and are associated with deformation above a basal detachment. The first comprehensive classification of thrust systems was done by Boyer and Elliot (1982). According to them, there are two basic types of thrust systems; a) Imbricate fans and b) Duplexes (Figures 19).

Imbricate Fans

In a thrust system, if the faults repeat the size and shape of the neighboring faults, an overlap of thrust sheets occurs with the same general dip direction. This kind of thrust systems are classified as Imbricate Fans (Boyer and Elliot, 1982).

The faults in an imbricate fan (Figures 19 and 20) cut up-section from a basal detachment but do not rejoin at a higher stratigraphic level (Marshak and Mitra, 1988). In an imbricate fan, a sole thrust serves as a lower common thrust where several thrust faults splay upward like a fan (Boyer and Elliot, 1982).

An imbricate fan that has most of its displacement on the leading thrust is called a leading imbricate fan (Figures 19 and 20). If the maximum displacement is at the trailing thrust fault, a trailing imbricate fan forms (Boyer and Elliot 1982). McClay (1992) described a blind imbricate complex as a buried imbricate fan (Figure 20) such that the displacement on the imbricate faults below is compensated at a higher structural level by folding, cleavage development, or another set of structures.

A problem may arise in distinguishing between imbricate systems formed from duplexes which have had the leading branch lines eroded (Figure 20) and those imbricate systems formed from branching of thrusts that die out into tip lines and were subsequently eroded (McClay, 1992).

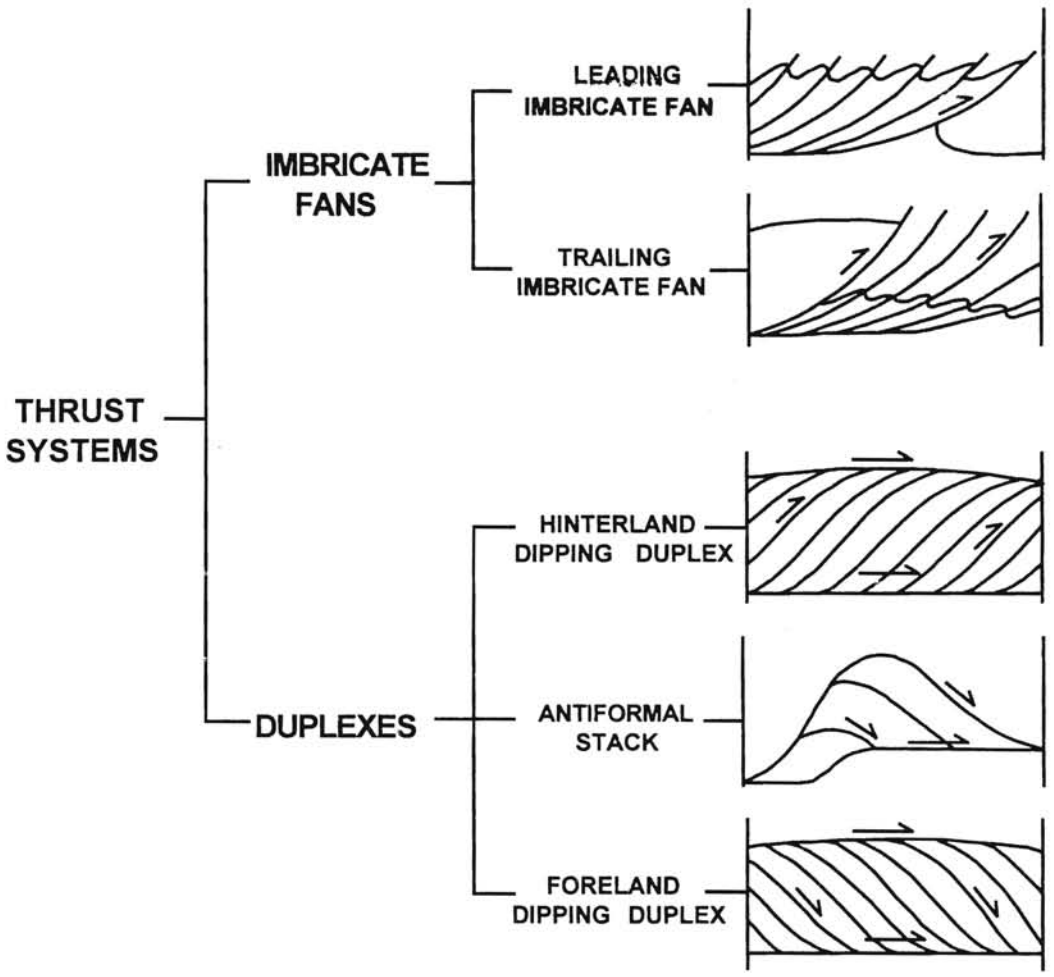

Figure 19: Classification of thrust systems (From Boyer and Elliot, 1982)

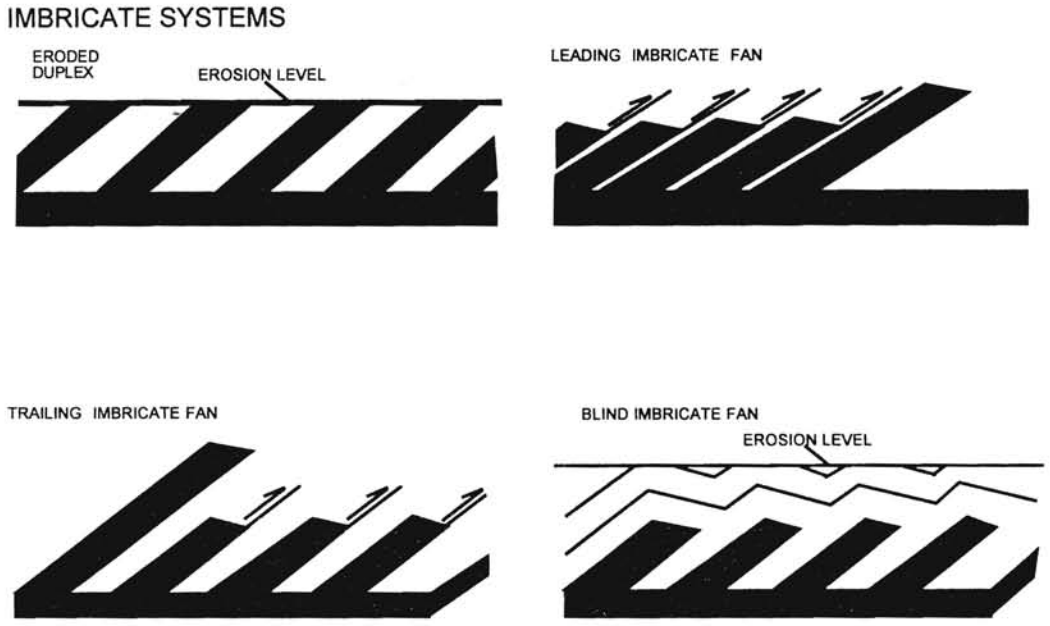

Figure 20: Imbricate systems (From McClay, 1992).

Duplexes

A thrust system with imbricate faults curved towards a sole (bottom) and an upper thrust is called a duplex (Boyer and Elliot, 1982). The thrust faults in a duplex cut up-section from a basal detachment and merge at a higher stratigraphic level to form another continuous detachment (Figures 19 and 20). In a duplex, the lower detachment is called the floor thrust and the upper detachment is called the roof thrust. The faults that cut up from the floor to the roof thrust surround bodies of rock. These rock bodies bounded on all sides by faults are called horses (Marshak and Mitra, 1988).

Models for duplex development by Boyer and Elliot (1982) and Mitra (1986) assume a forward breaking sequence. Butler (1987) proposed an alternative break backward development sequence. Boyer and Elliot (1982) subdivided the duplexes into: a) hinterland dipping duplex; b) antiformal stack; and c) foreland dipping duplex (Figure 19). In their classification, hinterland and foreland refer to the final attitudes of imbricate thrusts. Mitra (1986) also classified the duplexes in three main types: a) independent ramp anticlines; b) true duplex; and c) overlapping ramp anticlines leading to antiformal stack development (Figure 21). Unlike Boyer and Elliot (1982), he used the terms hinterland and foreland dipping duplexes to define the attitude of the roof thrust at the contact between horses.

A hinterland dipping duplex (Figures 19) is formed when the initial spacing of the thrust faults and the displacement of the horses are relatively small. The final geometry involves imbricate thrust faults splaying from a floor thrust and joining a roof thrust with a general dip towards the hinterland. According to Mitra (1986), in independent ramp anticlines, the final spacing between the thrusts is much greater than the displacement on

the individual thrusts and the structure formed consists of independent ramp anticlines separated by broad synclines (Figure 21). With increasing displacement hinterland sloping duplexes are formed from independent ramp anticlines where the initial spacing of the thrust faults is small such that, at the contact between horses, the roof thrust slopes towards the hinterland.

Mitra (1986), defines a true duplex as a duplex with parallel floor and roof thrusts at the contact between adjacent horses (Figure 21). They are subdivided into three classes depending upon their position with respect to larger thrusts. They may occur in the footwall of a ramp anticline, in the hanging wall of a ramp anticline, and in front of a ramp anticline (Figure 21). The true duplex of Mitra (1986) is similar to the hinterland dipping duplex of Boyer and Elliot (1982) in the sense of the general dip direction of the individual thrusts but differ by definition which requires a floor and a roof thrust that are parallel to each other.

Antiformal stacks form when a duplex has a displacement similar to the spacing between the ramps which eventually juxtapose the branch lines (Butler, 1987). This leads the higher horse to fold over the lower ones (Figures 19 and 21). Downward in the duplex the folding dies which implies of the sequence of events (Boyer and Elliot, 1982). For the development of the hinterland dipping structures and the antiformal stack structures, a coherent roof thrust is not always necassary. Both may occur within duplexes or imbricate fans (Butler, 1987).

When the displacement on the individual thrust is greater than the spacing between ramps, foreland dipping duplexes form (Boyer and Elliot, 1982). They consist

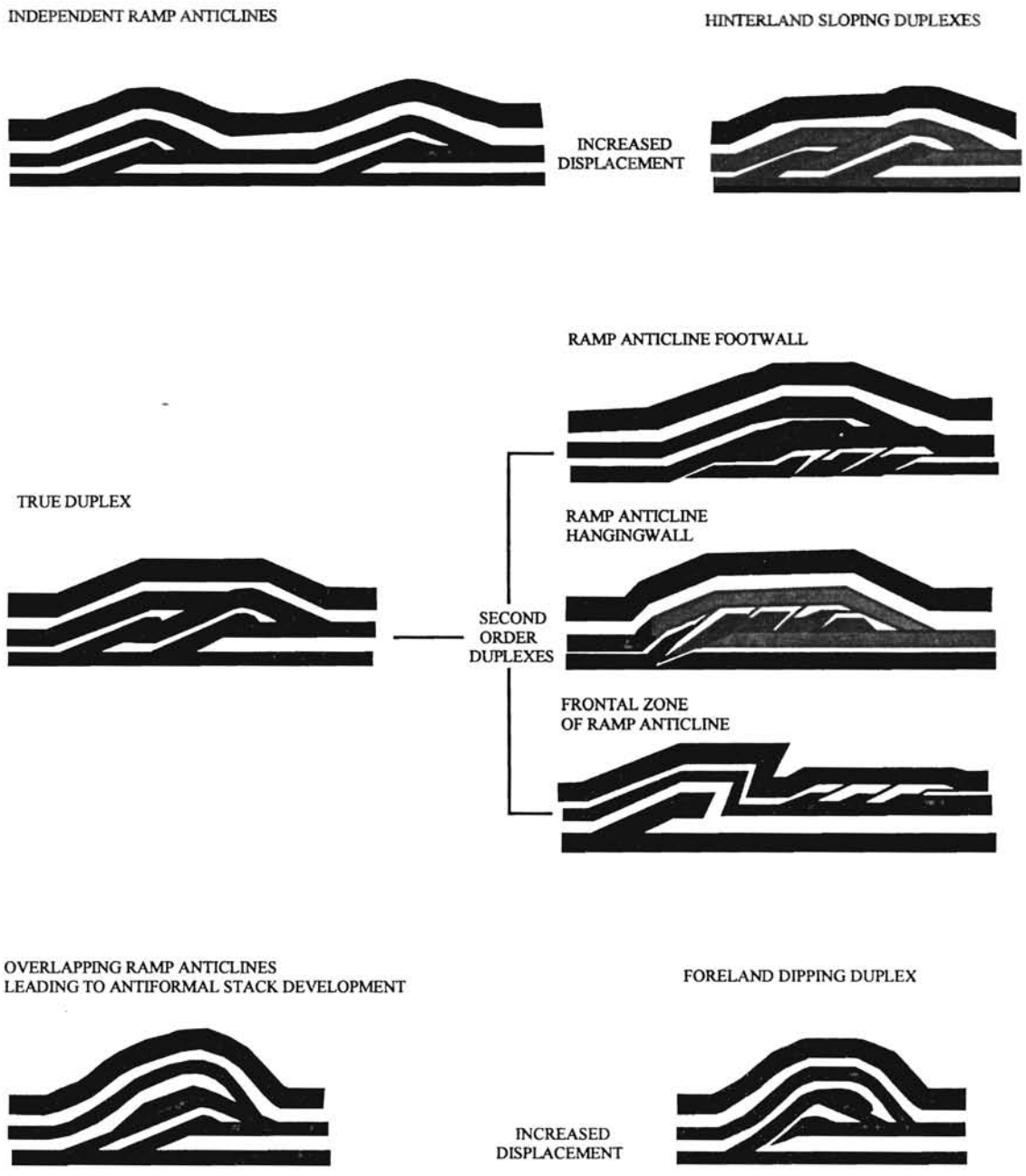

Figure 21: Duplex classification (From McClay, 1992)

of downward-facing horses (Figures 19 and 21). Butler (1987) suggested that the foreland dipping duplexes form in a break-backwards sequence where the earliest horse is toward the foreland and the latest one is on the hinterland side. Mitra (1986) proposed that an overlapping ramp anticline forms where the crests of successive ramp anticlines partially or completely overlap (Figure 21). He termed a system of completely overlapping ramp anticlines in which the trailing branch lines are coincident an antiformal stack similar to classification of Boyer and Elliot (1982) and suggested that the increased displacement in antiformal stacks form foreland dipping duplexes (Figure 21).

A duplex in which out of sequence movement on the link thrusts have breached or cut through the roof thrust is called a breached duplex (Figure 22). A corrugated or bumpy roof duplex (Figure 23) forms when the roof thrust is corrugated or folded (McClay, 1992). Link thrusts (Figure 24) are imbricate thrusts that link the floor thrust to the roof thrust of the duplex. Link thrusts are commonly sigmoidal in shape (McClay, 1992). The link thrusts in this study (Figures 37 through 44 and Plates III through X) show similar geometries to the example suggested by McClay (1992).

The stacking arrangement of the of the horses and the duplex shape depends upon ramp angle, thrust spacing, and displacement on individual link thrusts (McClay, 1992). A horse can change along strike into splay, and it is also possible that a duplex can change along strike into an imbricate fan (Boyer and Elliot, 1982).

Above and below a duplex, the bedding planes may be relatively undisturbed. A particular stratigraphic unit may be present in the hanging wall of the roof or the footwall

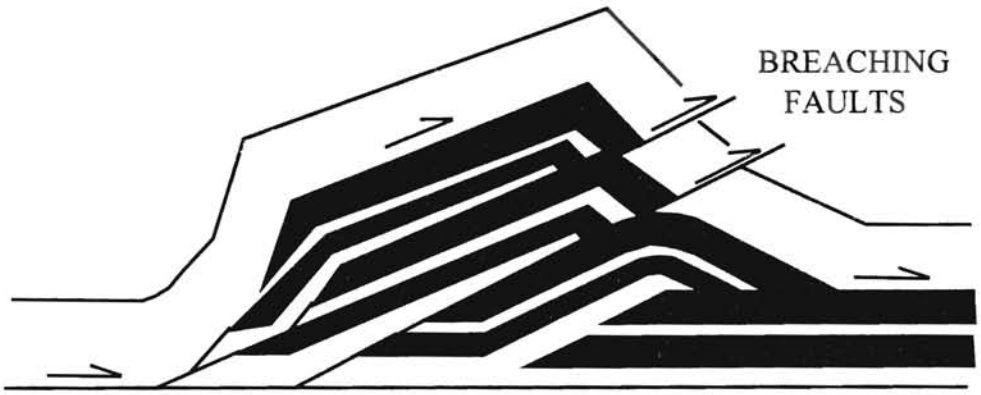

Figure 22: Breached duplex (From McClay, 1992).

Figure 23: Corrugated duplex (From McClay, 1992)

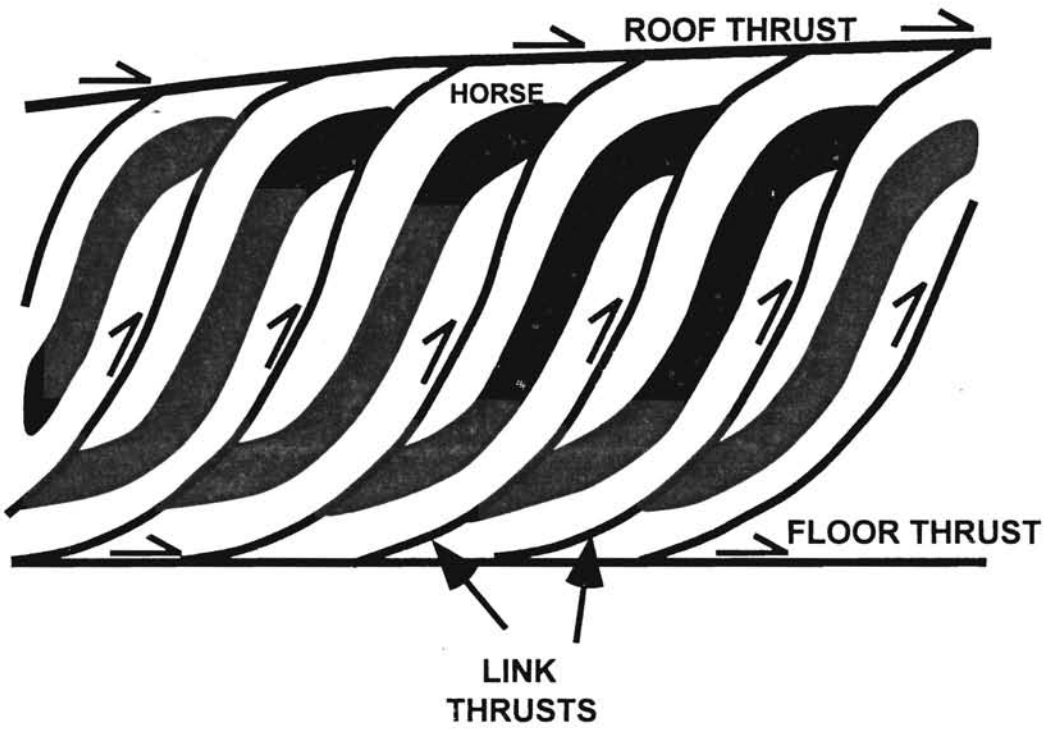

Figure 24: Link thrusts (From McClay, 1992)

of the floor thrusts for long distances. The fold pairs within any of the duplexes usually have similar shape and size (Boyer and Elliot, 1982).

Sequence of development of duplexes look at fig 63

Two different models for the sequential development of duplexes are the brake-forward and brake-backward sequence models. The duplex classifications of Boyer and Elliot (1982) and Mitra (1986) both agree on a brake-forward development towards the foreland. Boyer and Elliot's (1982) model was constructed on typical dimensions and angles of observed duplexes assuming plain strain, constant bed lengths, and kink folding (Figure 25). According to their model, an initial thrust with a slip (S_o) cuts steeply through a more competent sequence, forming a footwall ramp, and reaches to an upper gliding horizon. The next fault follows the same geometry and propagates from the base of the ramp and cuts up-section, eventually reaching the preexisting major thrust. Later, while the overlying fault segment remains fixed, a new fracture slips (S_2). The major thrust slips by $S_0 + S_1$ both behind and in front of the new horse. This kind of movement transfers the slip to a new and lower fault, while the major fault rides passively. The result is a new folded horse and a major thrust folded in the inactive portion. The process continues as the movement is transferred to new faults. This leads to the formation of the first duplex. As the slip is transferred to the new and lower fault, a portion of the major thrust is deactivated and remains passive. The characteristic features of such duplexes include elongate folds within imbricate horses and beds parallel to the thrust faults. Above the roof thrust, the stratigraphic units remain undisturbed and the same unit may continue for long distances.

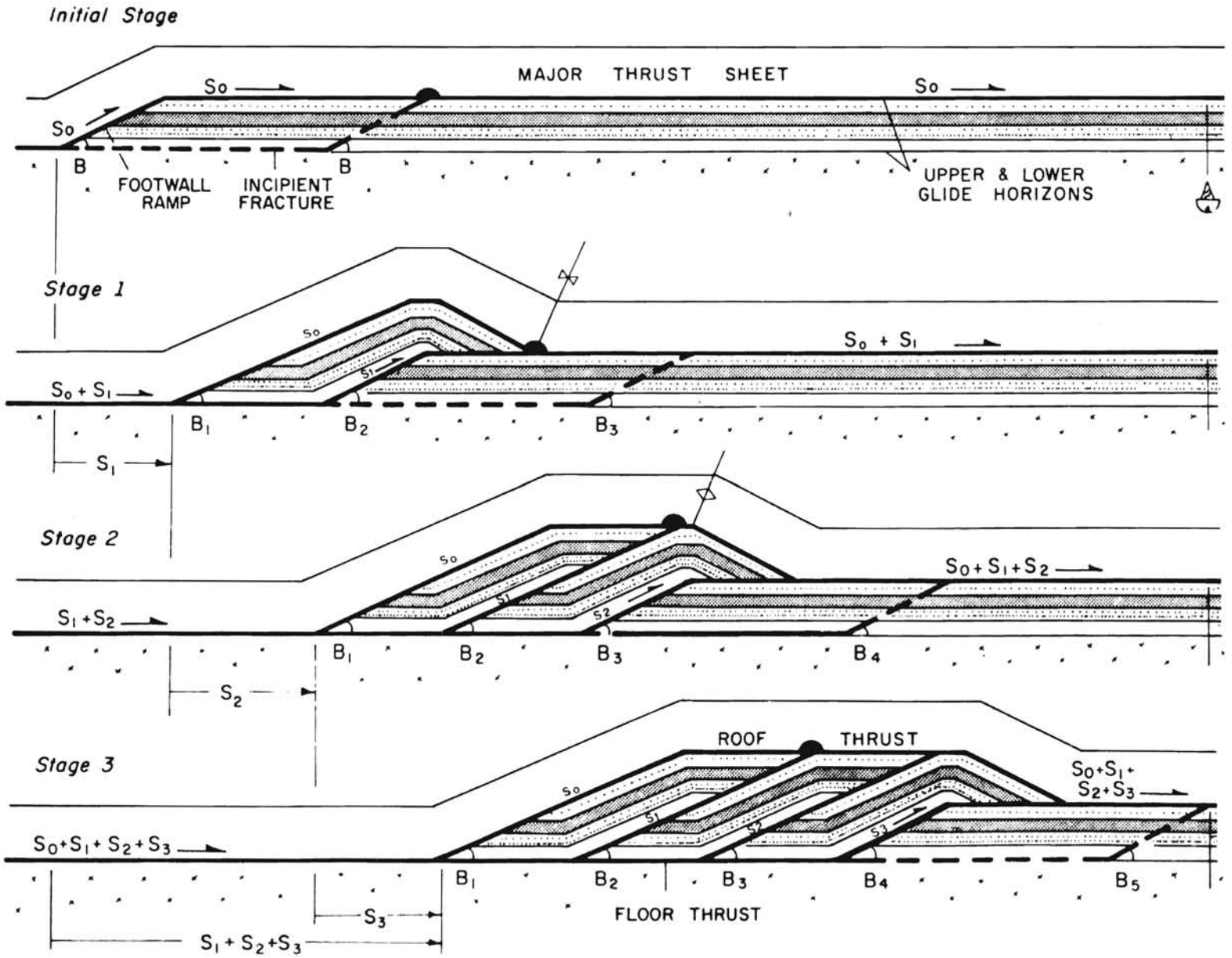

Figure 25: Sequential development of duplexes (From Boyer and Elliot, 1982)

Butler (1987) argues the viability of break-forward development of hinterland dipping duplexes, unless the geometric relations at the roof between leading branch lines and the internal stratigraphy of the individual horses are exposed. He agrees that the antiformal stack development must be the result of a foreland-directed propagation because the higher level thrust sheets are back rotated by the lower thrust sheets. According to Butler (1987), the foreland dipping duplexes form in a break-backwards propagation, because their trailing branch lines are carried beyond the base of the next footwall ramp.

Triangle Zones

The widely recognized usage of "Triangle Zones" (Figure 26) refers to a combination of two thrusts with opposing vergence, such that they form a triangular zone (McClay, 1992). The triangle zone arrangement of faults along a foreland margin of a fold and thrust belt is common (Jamison, 1994). Although, the triangle zones may show differences in their internal structures, each marks the tectonic delamination of a foreland basin. The size of a triangle zone may range from micro to crustal scale (Price, 1994). A triangle zone is often associated with a duplex or an antiformal stack in the axial part. A passive roof duplex describes this kind of triangle zone and such zones are basically intercutaneous wedges (Figure 27) (Mc.Clay 1992). Price (1986) defines an intercutaneous thrust wedge as a thrust bounded by a sole or floor thrust at the base and by a passive roof thrust at the top. Couzens and Wiltschko (1994) proposed that three end member geometries dominate the triangle zones (Figure 28).

Figure 26: Triangle Zone (From McClay, 1992).

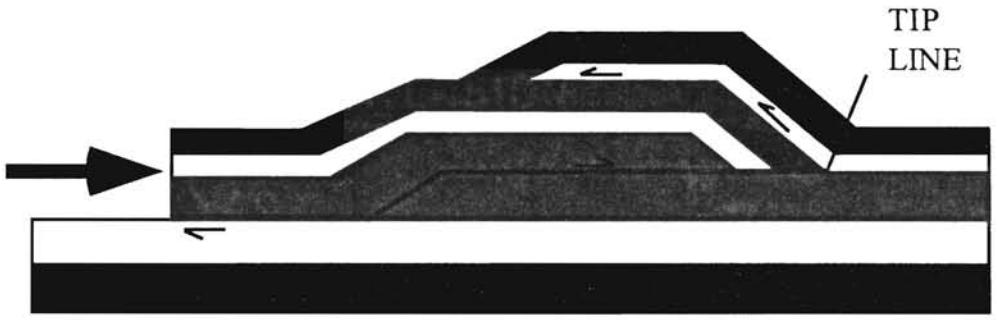

Figure 27: Intercutaneous thrust wedge (From McClay, 1992).

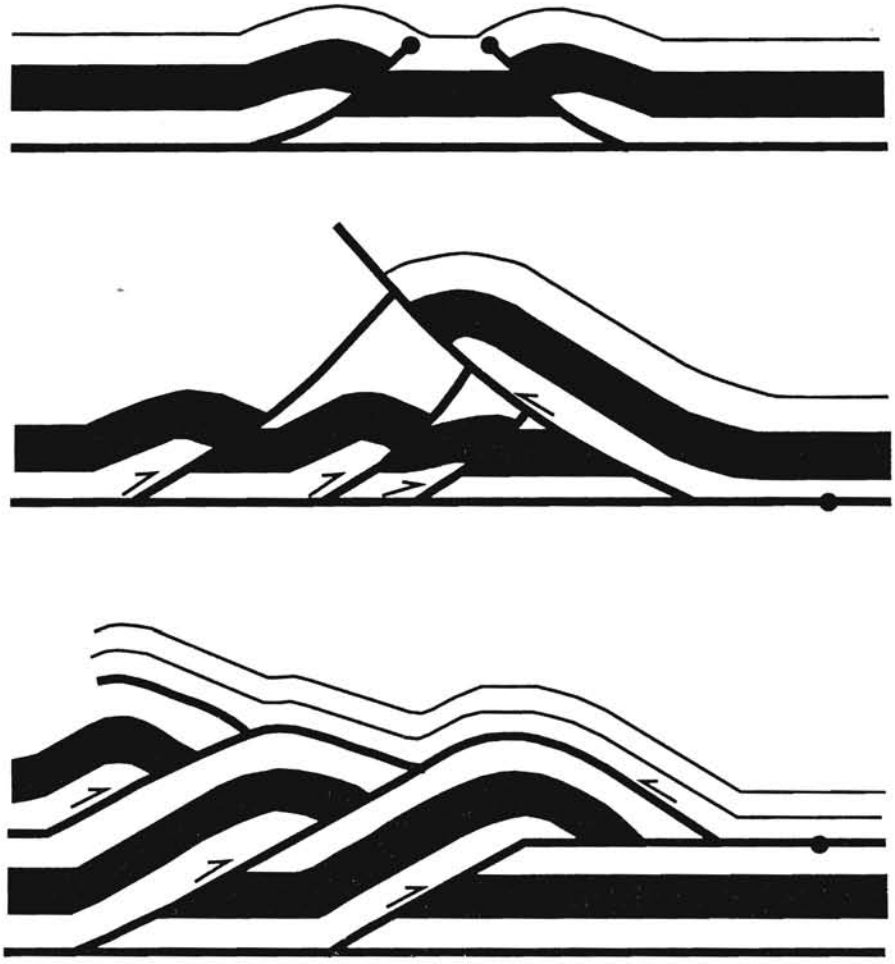

Figure 28: Three end member geometries for triangle zones
(From Couzens and Wiltschko, 1994)

Each thrust at the leading edge of a foreland-propagating belt of deformation can form a triangle zone, and this thrust wedging is repeatable. Several buried thrust fronts, or stacked triangle zones, can be found in a sequence of separate tectonostratigraphic units, the basal detachment of one unit becomes the upper detachment of the underlying one (Price, 1994).

CHAPTER 5

PROPOSED STRUCTURAL GEOMETRY OF FRONTAL THRUST BELT OF OUACHITA MOUNTAINS

The complex structural geometry of the transition zone between the Arkoma Basin and the Frontal Ouachita Mountains has long been debated. Several workers proposed different interpretations about the transition zone. The main debate concerning the structural geometry has been over the nature of the imbricate thrust faults and the presence of a triangle zone. In his recent work, Suneson (1995) summarized various interpretations of the transition zone between the Arkoma Basin and the frontal belt of the Ouachita fold and thrust belt. The following is a summary of these interpretations based mostly on Suneson (1995).

Arbenz (1984) is the first author to recognize the south dipping thrust faults, the blind imbricate thrust faults, and the bedding parallel detachment surface serving as a floor thrust for the imbricate thrusts (Figure 29). He interpreted the detachment surface as gradually rising northward with Cambrian to Devonian preorogenic strata to the south and Middle Pennsylvanian strata to the north, at the footwall.

The presence of a triangle zone in the Arkoma Basin was first introduced by Hardie (1988). He identified the Blanco thrust, located to the southwest of Hartshorne,

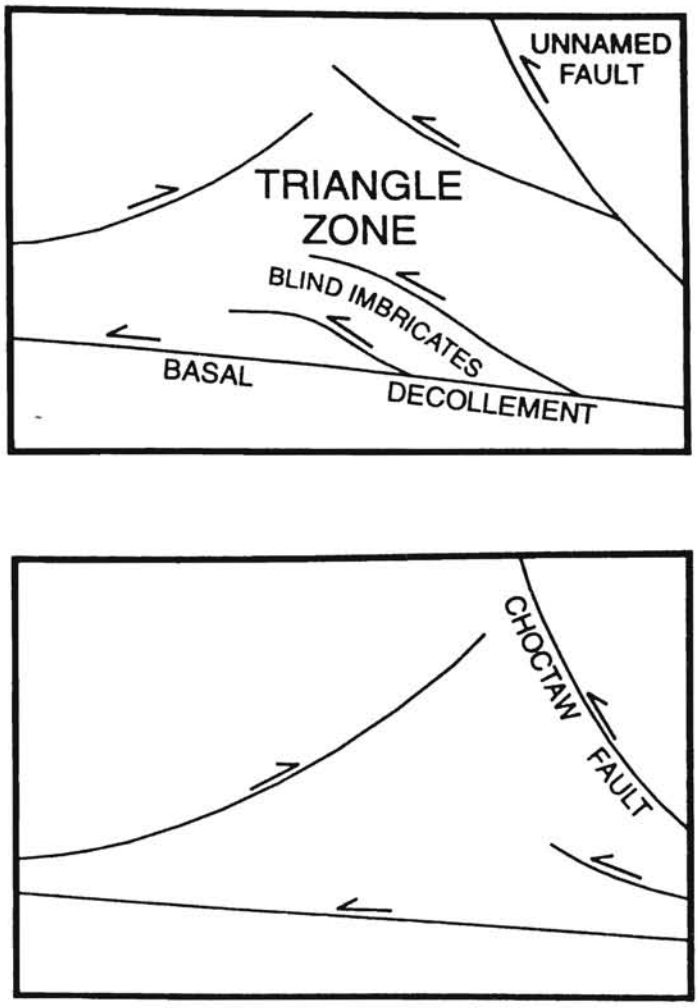

Figure 29: Sketch cross-section showing styles of deformation in the subsurface at the transition zone between the Arkoma Basin and Ouachita Mountains as proposed by (a) Arbenz (1984) (b) Arbenz (1989) (From Suneson, 1995)

as a basinward roof of a relatively thick triangle zone. His cross-sections showed blind imbricate thrusts and backthrusts and north-directed overturned folds beneath the Choctaw fault, as well as a basal decollment at the base of the Pennsylvanian Springer Formation (Figure 30).

Milliken (1988) showed a thin triangle zone floored by south dipping imbricate thrust faults (Figure 31). He interpreted several small displacement imbricate thrust faults and backthrusts and termed them "detached bivergent imbricates". He showed these structures beneath a major decollment within the Atoka Formation, which reaches the surface as the Carbon fault.

Camp and Ratliff (1989) identified a thick triangle zone floored by blind imbricate thrust faults and backthrusts. They also suggested a deep, north directed decollment, climbing from Mississippian shales in the south to Middle Pennsylvanian strata to the north (Figure 32).

Reeves and others (1990) suggested a thin triangle zone floored by two north-directed duplex structures (Figure 33), and a decollment in the lower Atokan strata. They also showed a complex series of blind imbricates and associated small displacement backthrusts, similar to the detached bivergent imbricates proposed by Milliken (1988).

A shallow triangle zone, overlying a deeper triangle zone or a passive roof duplex was proposed by Perry and Suneson (1990). Later, Perry and others (1990) revised the original interpretations and concluded that the deep triangle zone consists of two north-directed imbricates, a floor thrust and a north-directed roof thrust that gradually reaches a shallower depth within the Atoka Formation (Figure 34).

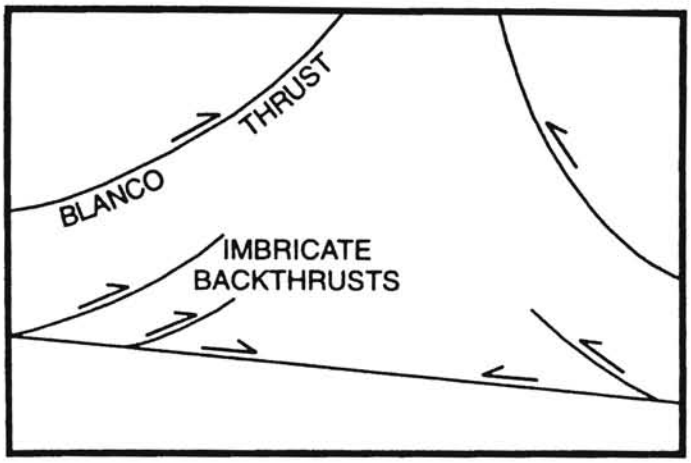

Figure 30: Sketch cross-section showing styles of deformation in the subsurface at the transition zone between the Arkoma Basin and Ouachita Mountains as proposed by Hardie (1988) (From Suneson, 1995)

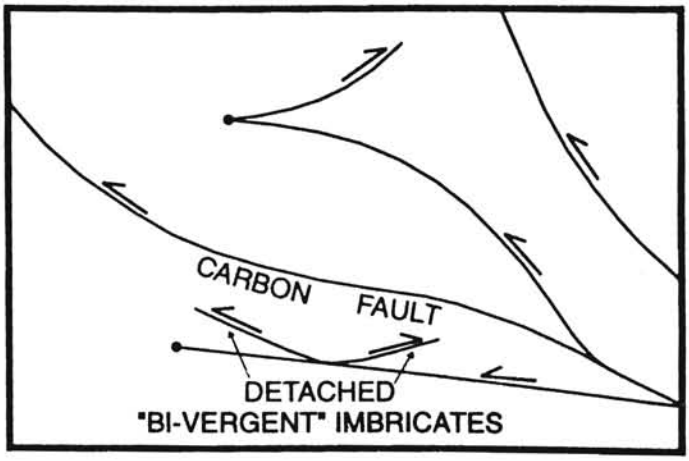

Figure 31: Sketch cross-section showing styles of deformation in the subsurface at the transition zone between the Arkoma Basin and Ouachita Mountains as proposed by Milliken (1988) (From Suneson, 1995)

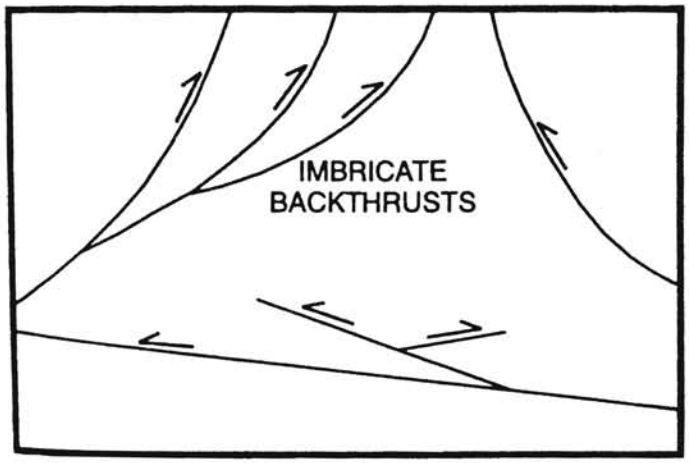

Figure 32: Sketch cross-section showing styles of deformation in the subsurface at the transition zone between the Arkoma Basin and Ouachita Mountains as proposed by Camp and Ratliff (1989) (From Suneson, 1995)

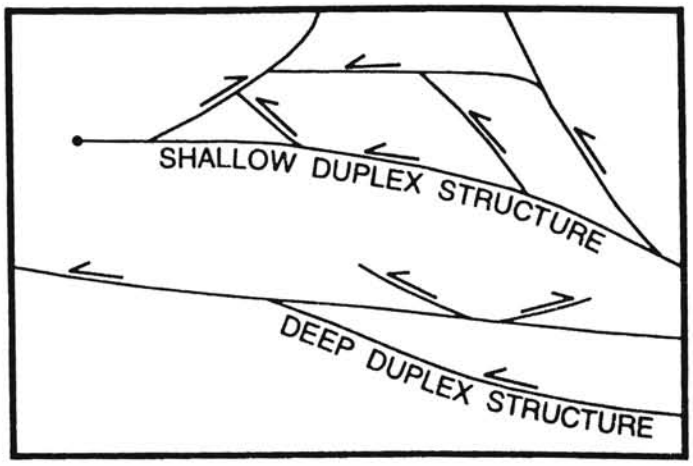

Figure 33: Sketch cross-section showing styles of deformation in the subsurface at the transition zone between the Arkoma Basin and Ouachita Mountains as proposed by Reeves and others (1990) (From Suneson, 1995)

Roberts (1992) interpreted the folds exposed in the southern part of the Arkoma Basin as a result of underlying duplex structures. He showed a decollment in the lower part of the Atoka Formation which extends into the basin (Figure 35).

The presence of a thin triangle zone and the duplex structures is also suggested by Wilkerson and Wellman (1993) (Figure 36). Their interpretation also included blind imbricate thrusts and transverse structures such as oblique ramps and tear faults.

Cemen and others (1994) suggested the presence of duplex structures in the Wilburton gas field area and pointed out a rough correlation between pressure gradients and the duplex structures in the lowermost Atokan Spiro sandstone. They proposed that "thrusting in the duplex structures in the subsurface has acted as seals for gas in the Spiro sandstone" and suggested the possibility that the Carbon fault may be a south dipping thrust fault. Akhtar (1995) and Cemen and others (1995) concluded that both duplex structures and a triangle zone exist in the area. Akhtar (1995) calculated that the amount of shortening in the Wilburton area is about 45%.

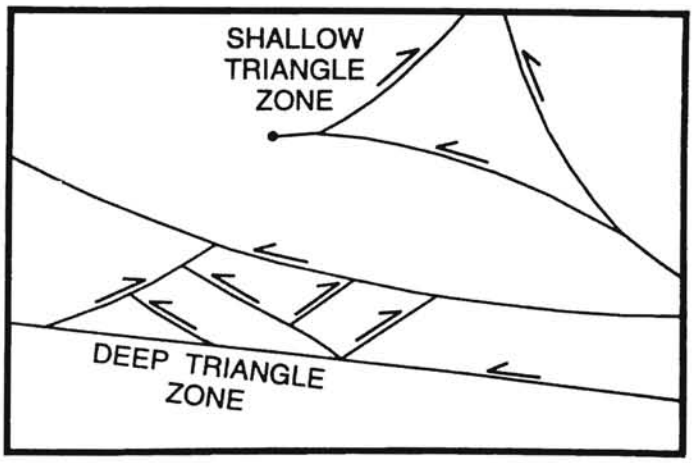

Figure 34: Sketch cross-section showing styles of deformation in the subsurface at the transition zone between the Arkoma Basin and Ouachita Mountains as proposed by Perry and others (1990) (From Suneson, 1995)

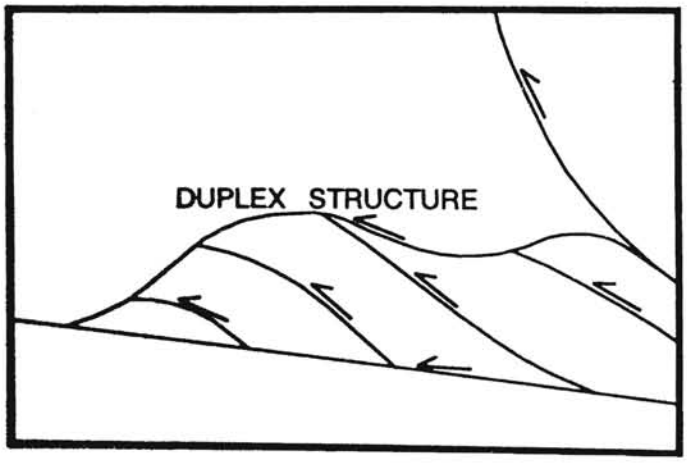

Figure 35: Sketch cross-section showing styles of deformation in the subsurface at the transition zone between the Arkoma Basin and Ouachita Mountains as proposed by Roberts (1992) (From Suneson, 1995)

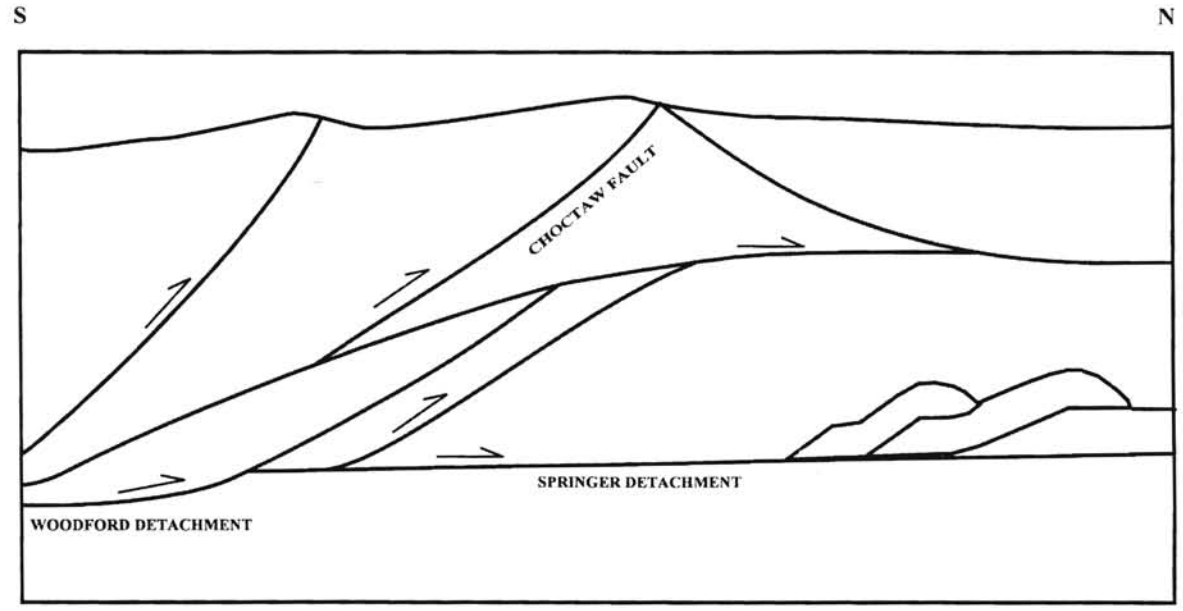

Figure 36: Sketch cross-section showing the geometry in the west of Wilburton gas field (From, Wilkerson and Wellman, 1993)

CHAPTER 6

STRUCTURAL GEOLOGY

The structural geometry of the study area is delineated by constructing eight balanced structural cross-sections using available wire-line well log data, well completion cards, interpretations of seismic profiles donated by EXXON and updated surface geological maps of N.H. Suneson, C.A Ferguson, and L.R. Hemish of the OGS. A structural contour map on top of the Spiro sandstone has also been constructed (Plate 1). The cross-sections are restored in order to measure the amount of shortening in the study area. The estimated locations of chamosite facies rocks are plotted both on the cross-sections and the restored sections, in order to find the extend of chamositic reservoir rocks. The data regarding the presence of chamosite and glauconite in wells are taken from the X-Ray diffractometer and thin section examinations of Feller (1995). The locations of the cross-sections are plotted on simplified geological map (Plate II). The cross-sections show the interpreted subsurface structural geometry of all structural features.

In the study area, both compressional and extensional structural features are present. The down-to-the-south normal faults are the observed extensional features. These faults have a general trend of east-west to east-northeast, paralleling the trend of

the basin (Figures 37 through 44 and Plates III through X). The limited number of wells in this normal faulted area prevents any detailed interpretation. However, it has been suggested by Koinm and Dickey (1967) that an abrupt increase in the thickness of the middle and lower Atoka, along the normal faults, reveals that these faults were formed as growth faults during subsidence of the basin. They also regard the presence of the turbidite facies rocks present in the lower and middle Atoka as another line of evidence for active growth faults during the Atokan sedimentation.

In all cross-sections, growth faults are observed in the lower and middle Atoka to the north of the leading duplex but there is no evidence of displacement due to normal faulting in the upper Atoka. The Hartshorne sandstone is also observed unfaulted in the cross-sections. The seismic profiles show normal faulting in the units below the detachment surfaces but, because of the unavailability of enough wells drilled deep enough, this cannot be confirmed by well data and is not shown on the cross-sections. In the areas of no well control to the north of the leading duplex, the structure is inferred by using the information on the adjacent cross-sections.

The seismic profiles are located in the southern part of the study area and their area of coverage along the cross-sections are shown with as hatch marks on the surface. The seismic lines coincide with the area where the south dipping imbricate thrust faults and the Gale-Buckeye thrust system of Wilkerson and Wellman (1993), are present. The seismic profiles perpendicular to the major structures are interpreted to provide seismic control for the cross-sections. Two of the interpreted seismic profiles are shown in figures 45 and 46.

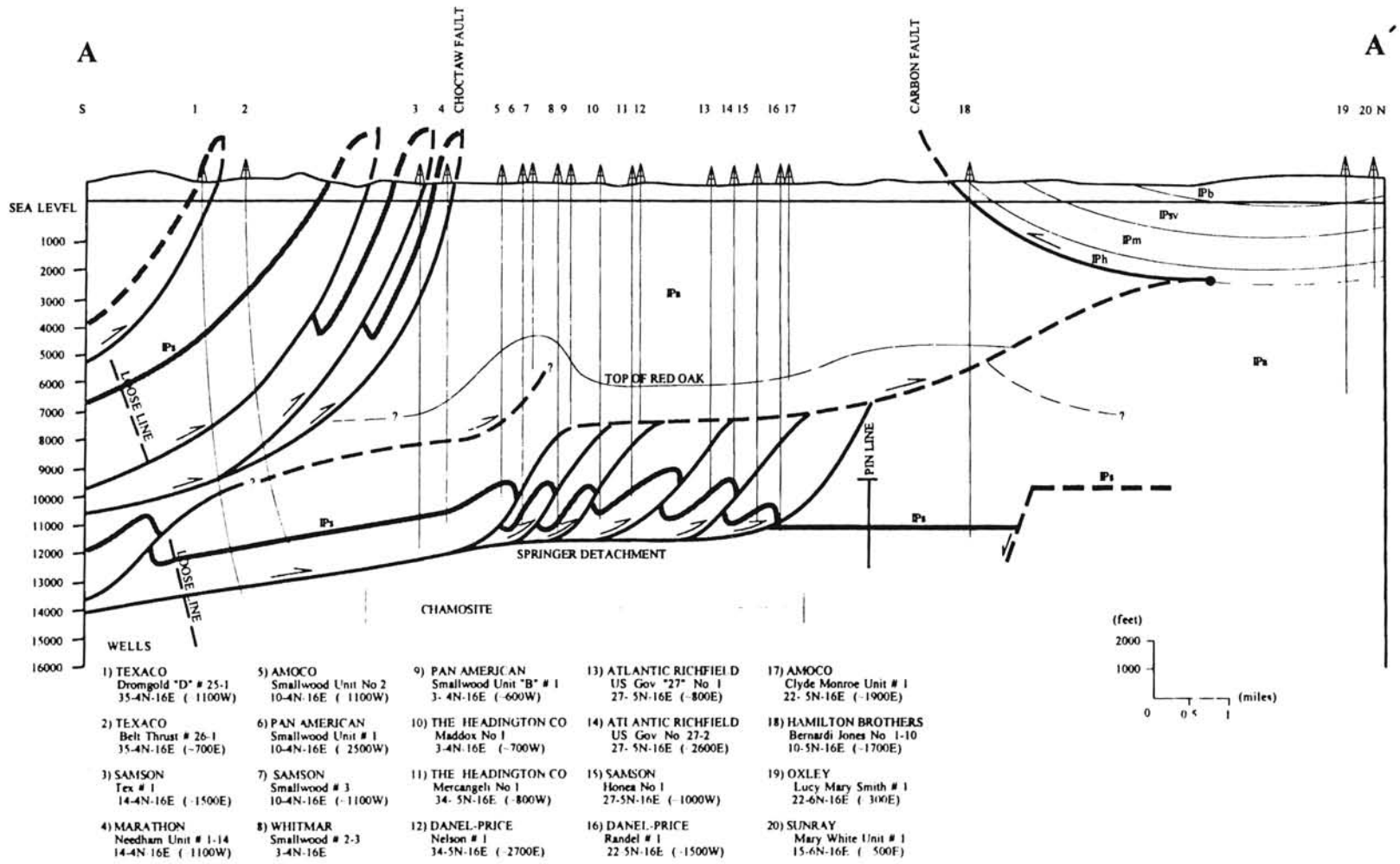

Figure 37: Structural cross-section A-A'

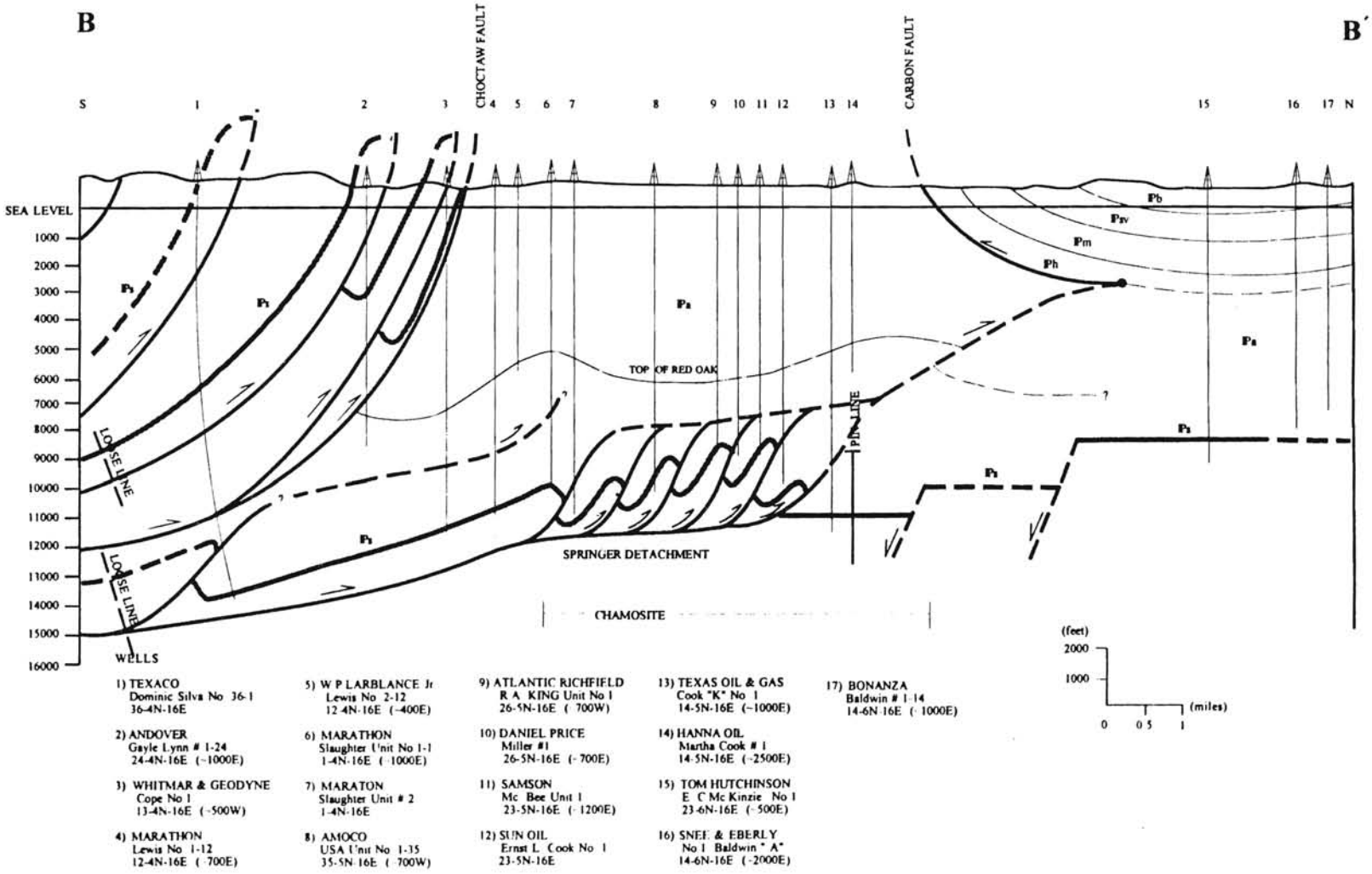

Figure 38: Structural cross-section B-B'

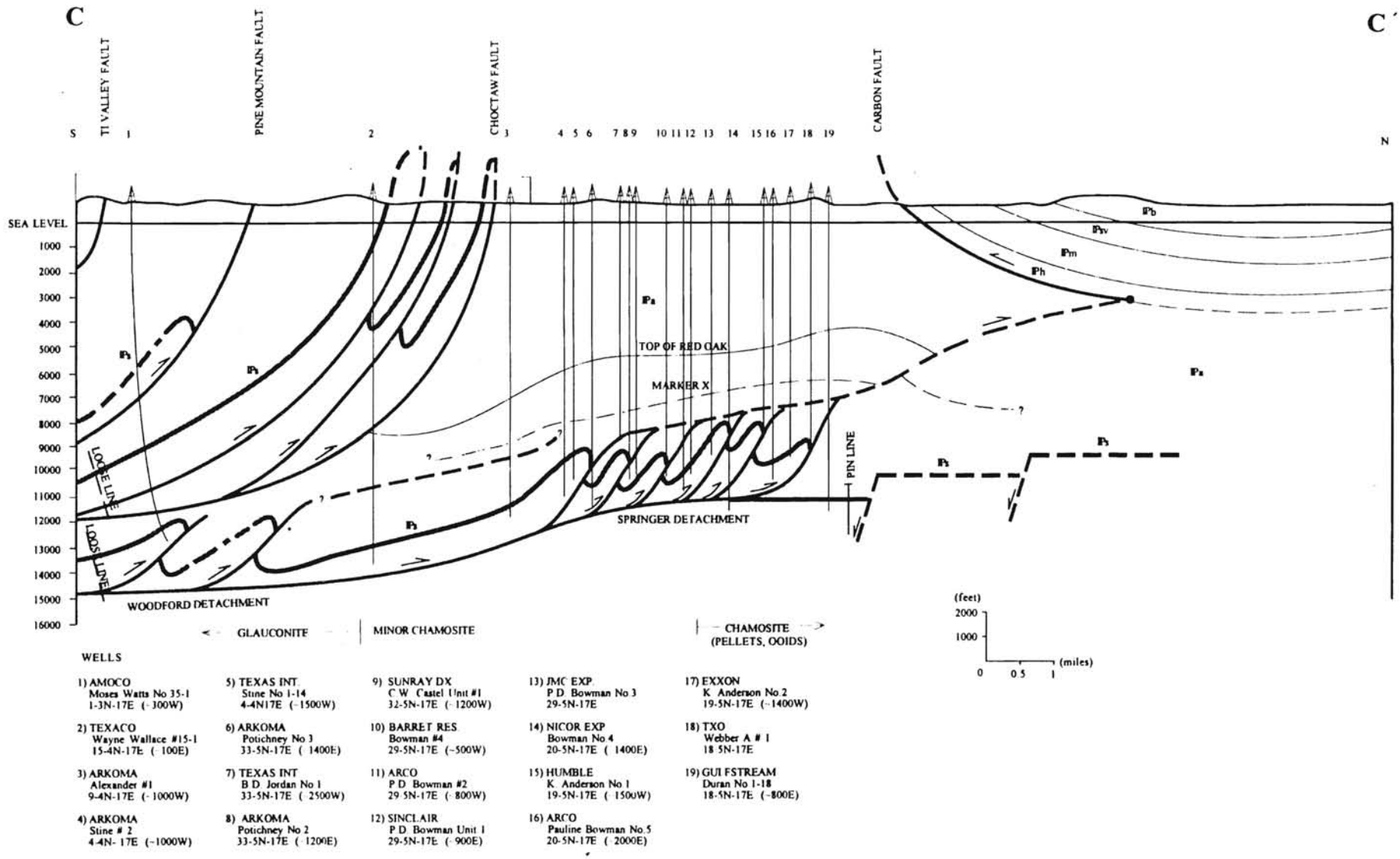

Figure 39: Structural cross-section C-C'

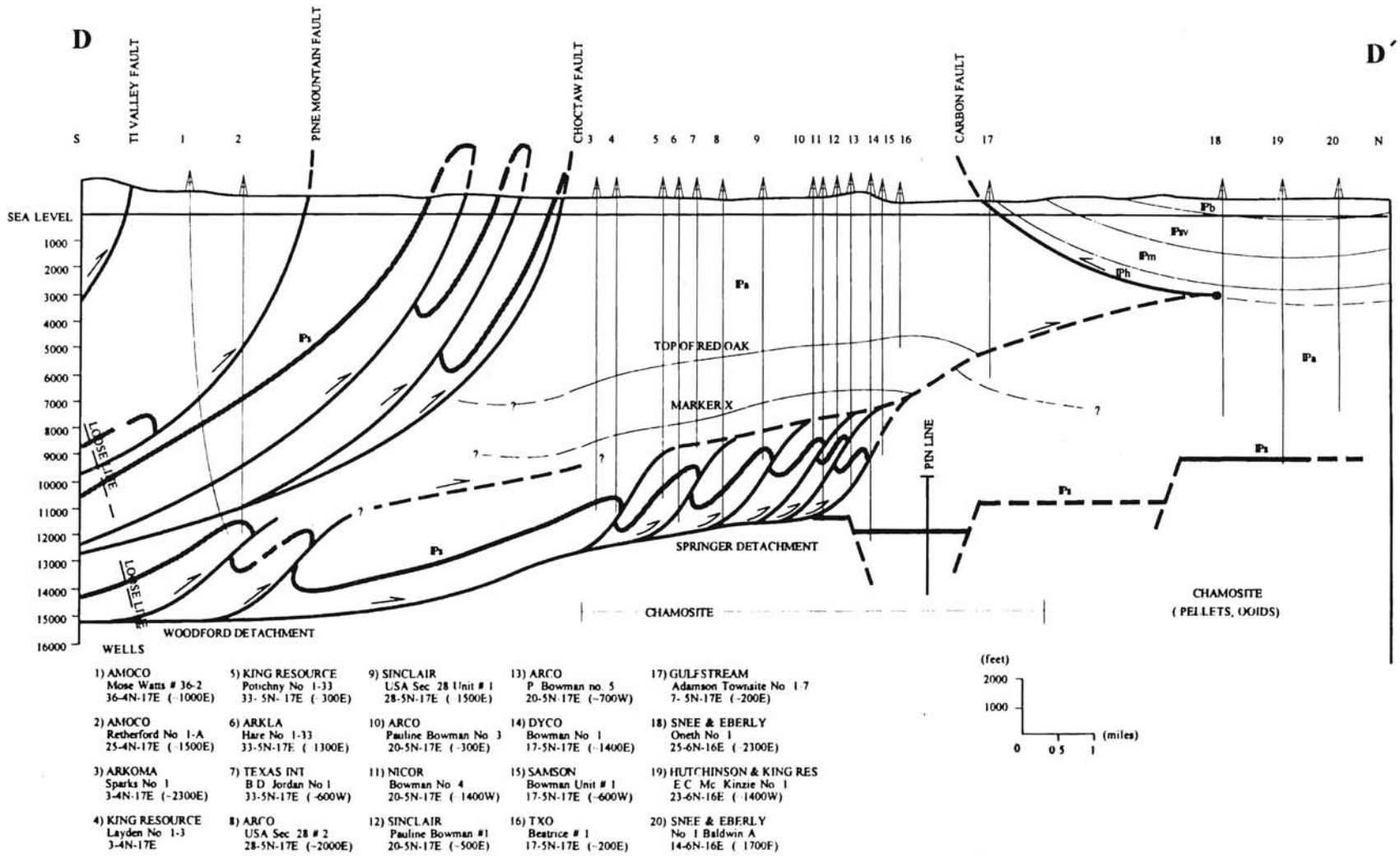

Figure 40: Structural cross-section D-D'

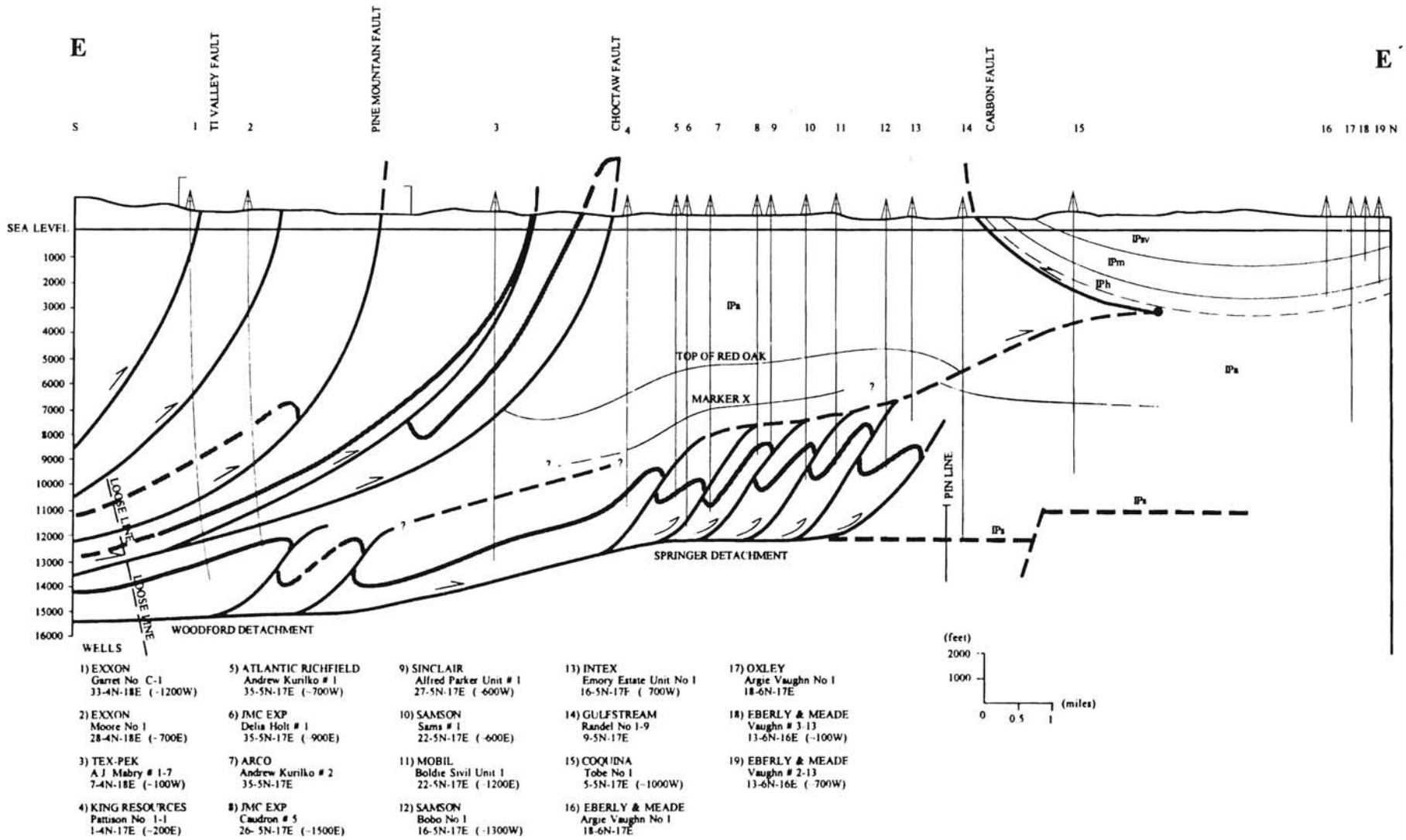

Figure 41: Structural cross-section E-E'

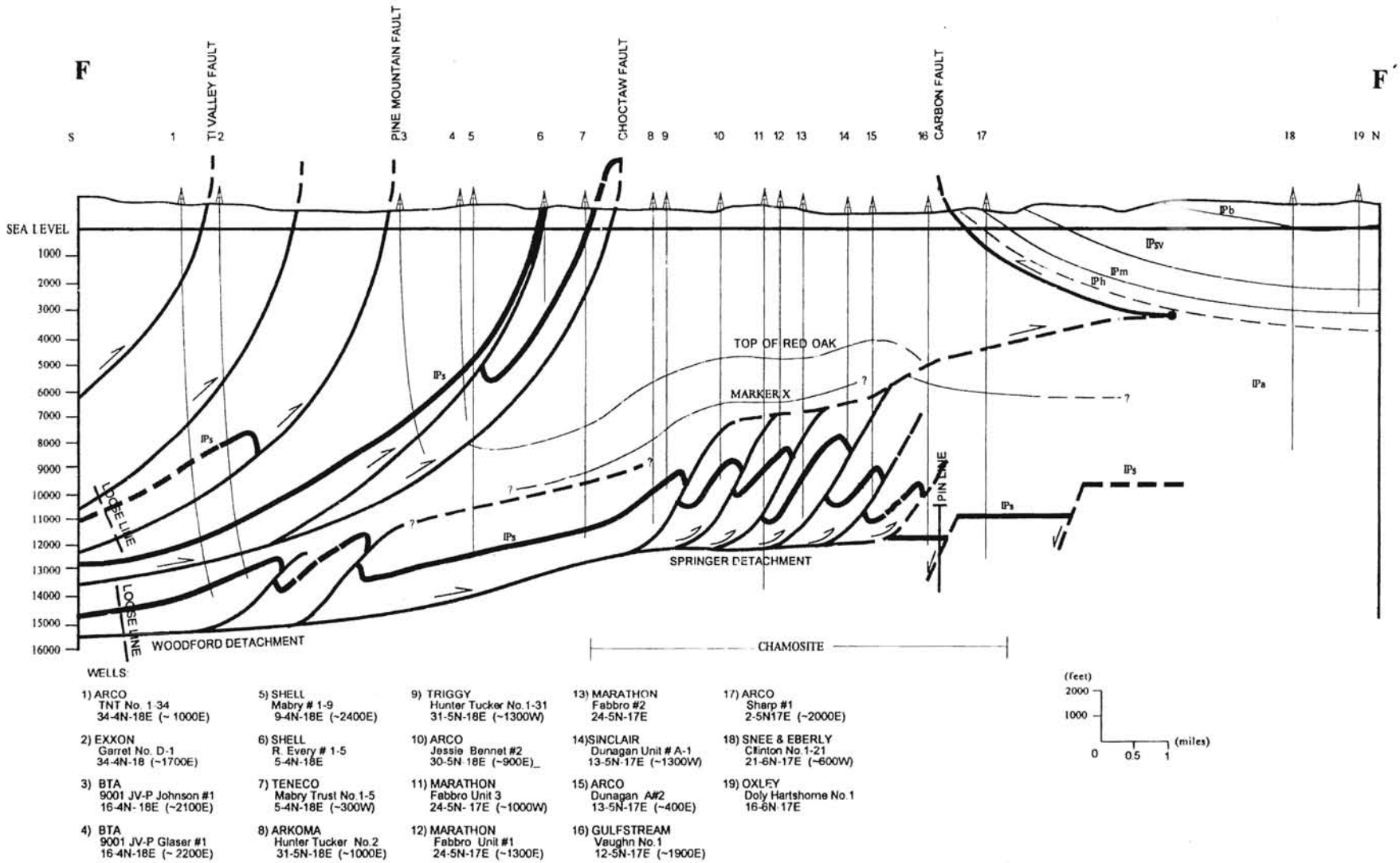

Figure 42: Structural cross-section F-F'

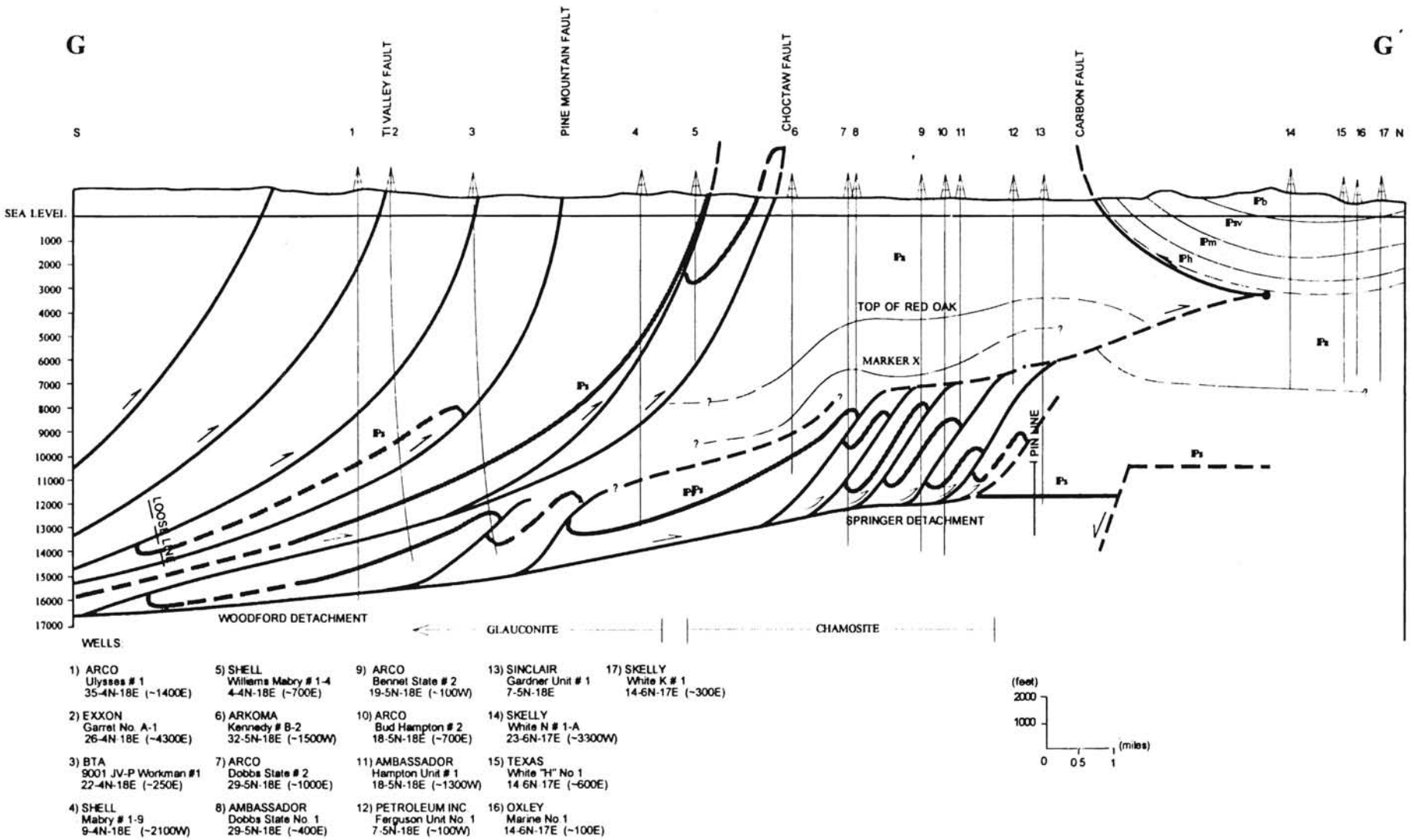

Figure 43: Structural cross-section G-G'

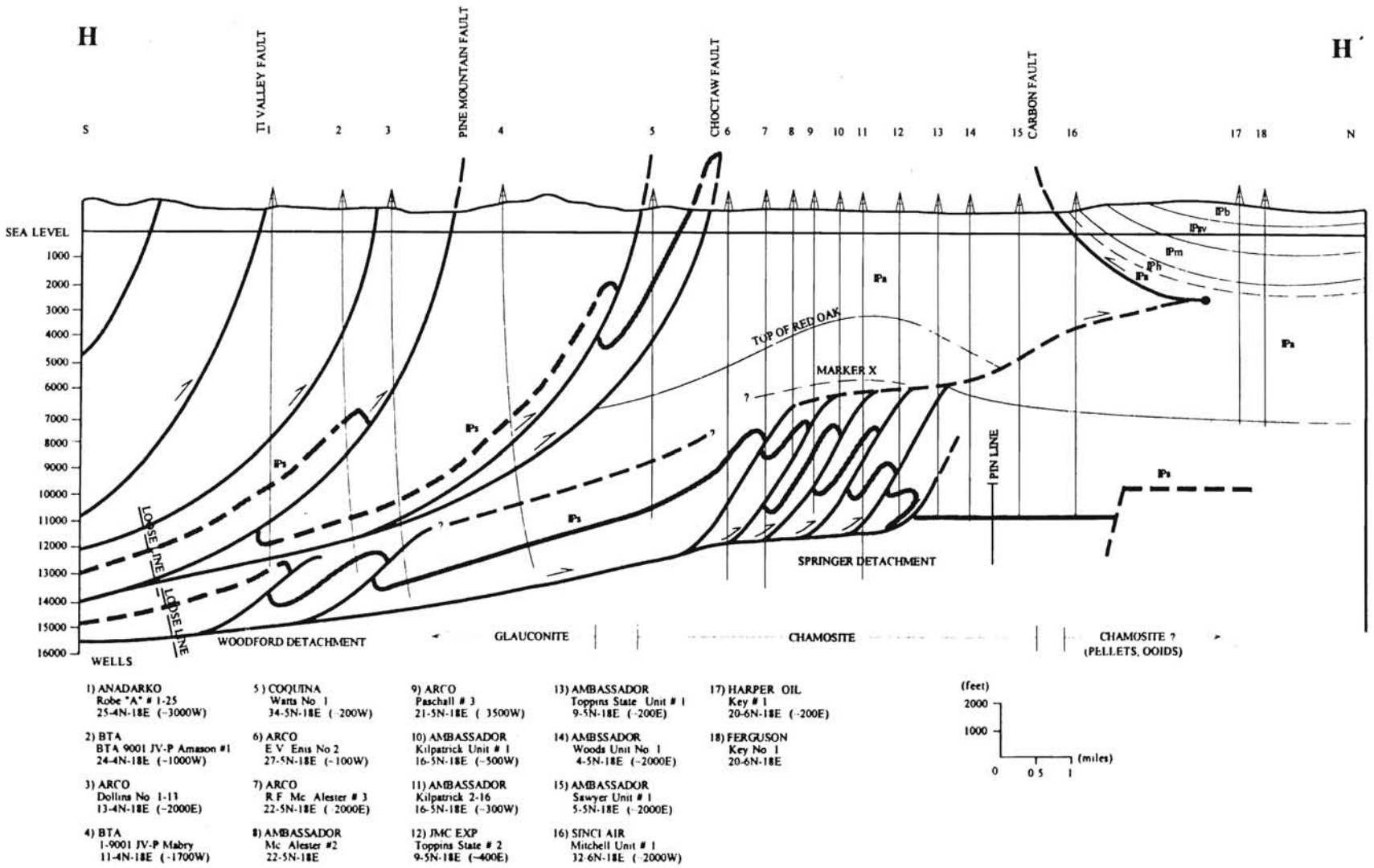

Figure 44: Structural cross-section H-H'

In the structural cross-sections, the Spiro sandstone is used as the key bed to determine the structural geometry. The Wapanucka Formation and the Spiro sandstone are not identified individually, but the entire thickness is referred to as the Spiro and is assumed to have uniform thickness in the study area. Other units identified in the cross-sections include the Red Oak sandstone, a marker called "Marker X", the Hartshorne Sandstone, the McAlester Fomation, the Savanna Formation, and the Boggy Formation. Like the Spiro sandstone, the Red Oak sandstone and Marker X are identified in the logs at their tops, and their thickness are considered to be constant throughout the study area.

The cross-sections depict two different deformation styles, separated from each other by the Choctaw fault. The hanging wall block (upper block) of the Choctaw fault contains many south dipping listric thrust faults, splaying both from the Choctaw fault and the main detachment surface within the Woodford Shale. The footwall block (lower block) of the Choctaw fault displays two detachment surfaces, duplex structures, and a triangle zone.

Major Thrust Faults

In the hanging wall of the Choctaw fault, there are many south dipping listric thrust faults exposed on the surface. The Spiro sandstone is displaced by these faults and crops out along the surface trace of several of these faults. Some of the thrust faults are named in the literature, but there are several other unnamed thrust faults that are mapped (Plates I and II). These faults are probably thrust faults splaying from the major detachment surface or from the other major thrust faults (Figure 47).

Ti Valley Fault

The Ti Valley fault is the southernmost major thrust fault in the study area (Plates I and II). Only two of the structural cross-sections show both the Ti Valley fault and an unnamed thrust fault to the south of it. The Ti Valley fault is one of the major thrust faults in the Ouachita fold and thrust belt, with a length of about 240 miles extending from near Atoka, Oklahoma to near Jacksonville, Arkansas (Suneson, 1988). In the study area, the Atoka Formation is the only unit present both on the north and the south of the Ti Valley fault.

In the study area, the Ti Valley Fault has a steep dip of about 70 to 80 degrees, as mapped on OGS maps, and flattens at depth, as interpreted on the cross-sections. Its trend is west-southwest to east-northeast. The displacement along the Ti Valley fault could not be measured from the cross-sections, because of the lack of a piercing point to locate a bed on the hanging wall and footwall of the thrust fault. Like the other faults in the hanging wall block of the Choctaw fault, the interpreted geometry of the Ti Valley fault displays a south-dipping imbricate listric thrust fault geometry (Figures 40 through 44) and Plates VI through X). Using this inferred similarity, it is possible to assume that the Spiro sandstone is also displaced along the Ti Valley fault, although it cannot be measured from the cross-sections.

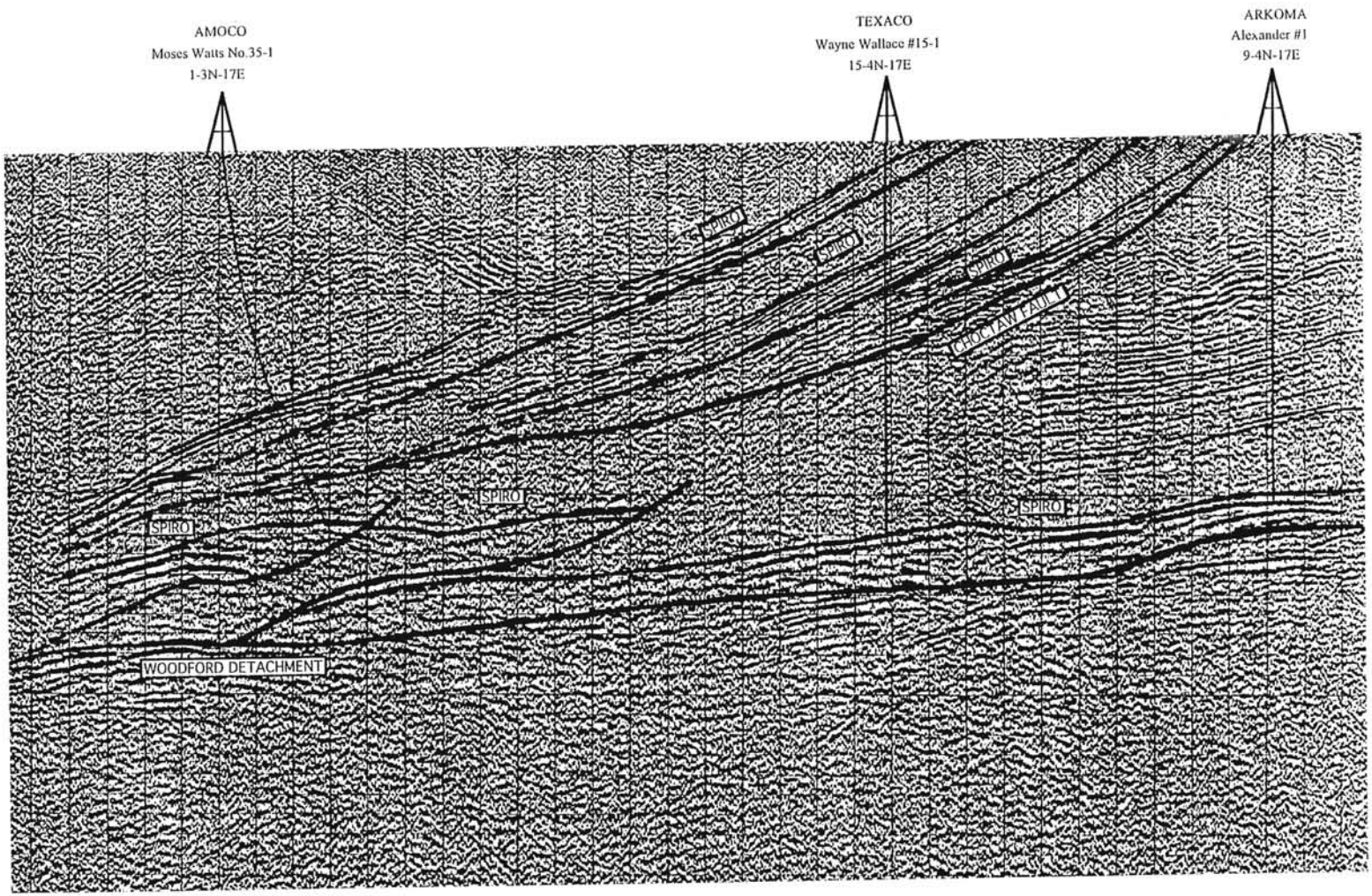

Figure 45: Interpreted seismic profile along the cross-section C-C'.

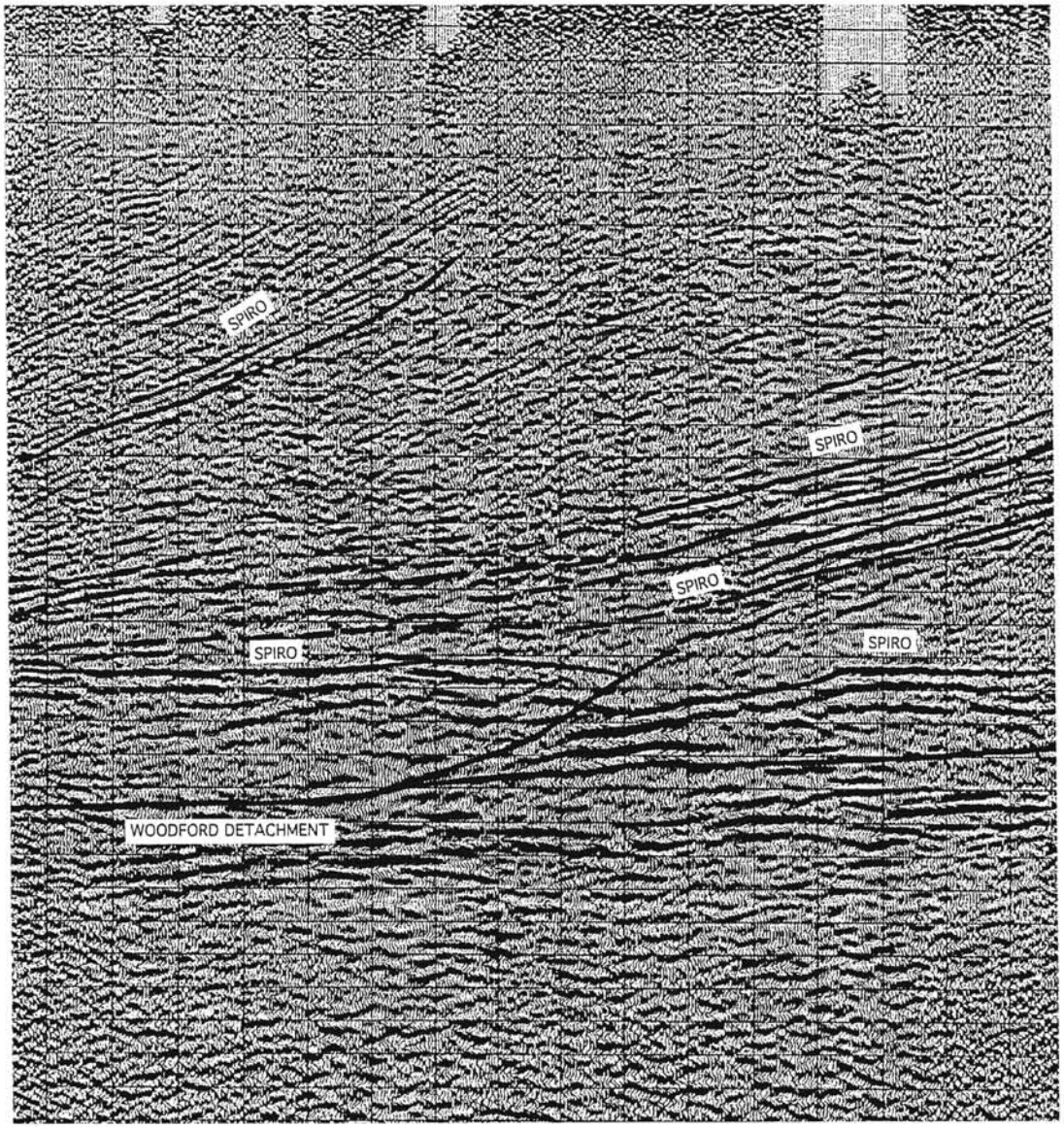

Figure 46: Interpreted seismic profile along the cross-section E-E'

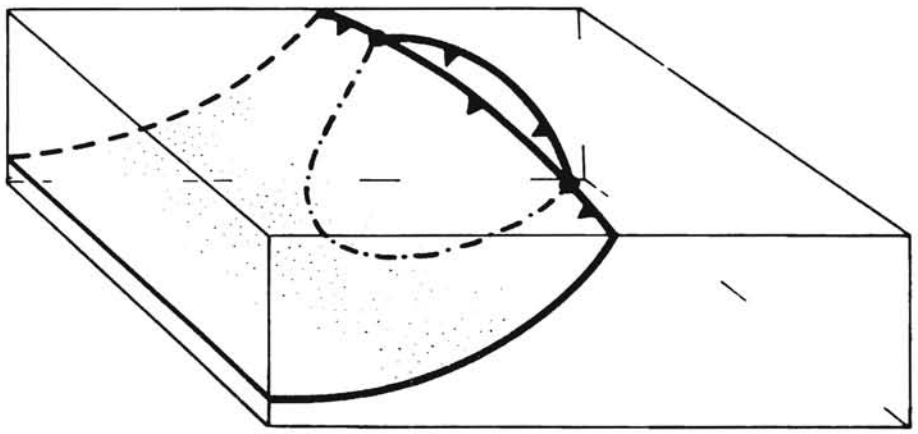

Figure 47: Major thrust fault and a splay (From Boyer and Elliot, 1982)

Pine Mountain Fault

Like the Choctaw and Ti Valley faults, the Pine Mountain fault is located in the southern part of the study area, with a west-southwest to east-northeast trend. The surface trace, as mapped on OGS maps is not continuous in the western part of the study area and is mostly inferred to the east where it is mostly covered with alluvium (Plates I and II). The surface trace of the Pine Mountain fault is subparallel to the Ti Valley and Choctaw faults, and dips roughly 70 to 80 degrees to the south. The geometry of the Pine Mountain fault is interpreted using seismic profiles and wire-line log data. They are suggestive that the fault loses its dip at depth and is a splay from either the Woodford detachment or the Choctaw fault (Figures 43 and 44, Plates IX and X). The cross-sections C-C' through H-H' are constructed perpendicular to the tectonic transport direction. Therefore, these cross-sections could be assumed to show displacement along the thrust faults. The displacement measured from the cross-sections shows a minimum of 4100 feet to a maximum of more than 7500 feet of displacement (Figures 43 and 44).

Choctaw Fault and Associated Structural Features

The Choctaw Fault serves as a boundary between the Arkoma Basin and the Ouachita Mountains. In the subsurface, it separates the two different styles of deformation. As mentioned earlier, in the hanging wall block of the Choctaw fault, there are several named and unnamed south-dipping, imbricate thrust faults. Two of these unnamed thrusts are located between the Ti Valley-Pine Mountain faults and the Pine Mountain-Choctaw faults (Figures 37 through 44 and Plates III through X). In the cross-sections, the latter fault is interpreted as a splay from the Choctaw fault. The Spiro

sandstone is present in the hanging wall of this unnamed fault and is displaced by it. The southern extent of the Spiro sandstone in the hanging wall of this fault is interpreted as continuing southward as suggested by the wells cutting through it, but it is unclear how far it continues towards the south. Figures (37 through 40) and Plates (III through VI) suggest another thrust fault splaying from the Choctaw Fault between the northern unnamed fault and the Choctaw fault. The Spiro sandstone is also present in the hanging wall of this thrust splay.

The southern unnamed thrust fault, mapped between the Ti Valley and Pine Mountain faults (Figures 41 through 44 and Plates VII through 44) suggest not only displacement of the Spiro sandstone but shows a similar geometry to the other south dipping imbricate faults in the hanging wall block of the Choctaw fault.

The Choctaw fault is the northern most south dipping thrust fault in the area. Like the other imbricate thrust faults, the Choctaw fault has a west-southwest to east-northeast trend. It extends more than 120 miles within Oklahoma. Perry and Suneson (1990) suggested about six miles of shortening along the Choctaw fault.

Based on the cross-sections, the displacement along the Choctaw fault appears to be increasing to the east. Cross-section G-G' (Figure 43 and Plate IX) in the eastern part of the study area, suggests a piercing point along the Woodford detachment approximately 4.5 miles south of the surface trace of the Ti Valley fault in the subsurface. This cross-section yields the maximum displacement in excess of 17,000 feet.

In the cross-sections, the Choctaw fault and the Spiro sandstone in the hanging wall were extrapolated into the air in order to estimate the amount of displacement in the

eroded part. This rough estimation suggests a minimum of 2000 feet of displacement. The other thrust faults, and the Spiro sandstone present in their hanging walls were similarly extrapolated.

Similar to the other faults in the imbricate series, the Spiro sandstone is present in the hanging wall of the Choctaw fault. It has a similar geometry in all of the cross sections and is similar to the geometry of the south-dipping thrust faults which are steep near the surface, but flatten out at depth (Figures 37 through 44 and Plates III through X).

Basal Detachment Surfaces

Two basal detachment surfaces found in the study area are the Woodford and Springer detachments. The Woodford detachment propagates within the Woodford shale and is named after the host formation (Hardie, 1988). It is a relatively flat detachment surface lying at about 15,000 feet below sea level. In the southern part of the study area, it serves as the floor for imbricate thrust faults and is referred to as the Gale-Buckeye thrust system by Wilkerson and Wellman (1993). Further north, the Woodford detachment makes a ramp and reaches a shallower depth in the Springer shale (Figures 39 through 44 and Plates V through X). At the base of the Springer shale, the basal detachment (Springer detachment) is present. It is approximately 12,000 to 13,000 feet below sea level and continues northward in the Springer shale until it is cut by a thrust fault, leading to the formation of the northern most duplex structure (Figures 37 through 40 and Plates III through VI) or the leading member of an imbricate fault system

(Figures 41 through 44 and Plates VII through X). The Springer detachment is interpreted as the floor thrust of the duplex structures in the study area.

Locating these two detachment surfaces in the subsurface was primarily dependent on the availability of data. The seismic profiles (Figures 45 and 46) examined cover the southern part of the study area and depict the Woodford detachment above the Hunton Group rocks. The Springer detachment was located primarily by using a limited number of deep well-logs.

In the southern part of the study area, two imbricate thrust faults which use the Woodford detachment as their floor are also depicted. These thrust faults probably form the Gale-Buckeye thrust system of Wilkerson and Wellman (1993). It has been suggested by Wilkerson and Wellman (1993) that the faults in this system have a fault length to displacement ratio of about 10:1 and, at least locally, are formed in a break-backward sequence.

Duplex structures and the Lower Atokan Detachment

In this study, the term duplex is used on the condition that the imbricate thrust faults splay from a basal detachment (floor thrust) and merge into an upper detachment (roof thrust). Duplex structures are found in the footwall block of the Choctaw fault (Figures 37 through 44 and Plates III through X). They are hinterland dipping duplexes floored by the Springer detachment and bounded on top by a roof thrust termed the Lower Atokan detachment (LAD) by Akthar (1995) and Akthar and others (1995). The duplexes are classified as the hinterland dipping duplexes of Boyer and Elliot (1982).

Horses found within the duplexes are probably formed by the upward propagation of the imbricate thrust faults splaying from the basal detachment. These imbricate faults join to the Lower Atokan detachment which serves as the roof thrust for the duplexes.

The Lower Atokan detachment is a south to north propagating detachment and is located at approximately 8000-9000 feet below sea level in the western part and 7000-8000 feet below sea level in the eastern part of the study area. The Lower Atokan detachment makes a gradual ramp to the north of the leading duplex and reaches a shallower depth. During its northward propagation, it displaces the Red Oak sandstone (Figures 41, 42, 44 and Plates VII ,VIII, X) and eventually reaches the Hartshorne sandstone where it probably forms the Carbon fault as a backthrust.

The presence and location of a roof thrust is suggested by the great difference in geometry above and below the interval between the imbricately thrusted Spiro sandstone and a sand unit in the Atoka Formation named Marker X. In the wire-line well logs, Marker X is identified by its higher gamma ray and resistivity values (Figure 5). The attempt to distinguish this sand unit from the other sand units within the Atoka Formation was unsuccessful because of the unavailibility of type well log signatures. In some cross-sections, it is not clearly distinguishable in the well logs (Figures 37, 38 and Plates III and IV). In other cross-sections, however, a sand unit at approximately the same depth is inferred as Marker X (Figures 39, 44 and Plates V and X). Whether it is clearly identified in the well logs or simply inferred, Marker X is similar to the geometry of the Red Oak Sandstone above it. On the other hand, below Marker X the Spiro sandstone is imbricately thrusted and is found to be forming horses in the hanging walls

of the thrusts and dipping towards the hinterland. This great difference in geometry strongly suggests the presence of a roof thrust.

It should be noted that, the location of the Lower Atokan Detachment is arbitrarily chosen to be in the middle of the interval separating two different structural geometries and is depicted neither from the seismic profiles nor from the well-log signatures. The seismic profiles do not provide a well developed velocity contrast and the well logs do not suggest a characteristic log signature for the roof thrust. The absence of supporting evidence for the roof thrust most probably arises because the Lower Atokan detachment is propagating within the shales of the Atoka Formation.

Up to five duplexes are depicted in the cross-sections. The eastern cross-sections suggest that the leading imbricate thrust is actually a blind thrust that does not form a duplex (Figures 41 through 44 and Plates VII through X). Cross-section F-F' suggests two blind thrusts (Figure 42 and Plate VIII). The western cross-sections do not show blind thrusts, but consist of up to five duplexes (Figures 37 through 40 and Plates III through VI). According to the cross-sections, the displacements along the hinterland dipping thrust faults are not constant. Besides the differences along the thrust faults, the horses in the duplexes show slight changes in their dips. This change is most pronounced in the leading duplex (Figures 38, 39, 41 and Plates IV, V, VII).

The duplex structures were first proposed by Arbenz (1984) in the Wilburton Gas Field Area. Other workers who proposed duplex structures in the Frontal Ouachita Mountains include Hardie (1988), Perry and Suneson (1990), Wilkerson and Wellman (1993), Cemen and others (1995), Akthar (1995), Akthar and others (1995), and Sagnak and others (1996 a,b).

Carbon Fault

The Carbon fault is present throughout the study area. Its surface trace is prominent and is mostly located at or adjacent to the boundary between the Atoka Formation and the Hartshorne Sandstone (Plates I and II). On a more regional scale, the Carbon fault is present in the west but disappears immediately east of the study area. It trends east-west, more or less paralleling the major thrust faults and exhibits a dip of about 30-40 degrees parallel to the bedding of the Hartshone Sandstone and units above it (Figures 37 through 44 and Plates III through X).

The cross-sections A-A' through H-H' represent the proposed geometry in the study area. All of the cross-sections show that the Carbon fault is a north dipping thrust fault. The surface geometry and well log data indicate that it dips about 30-40 degrees to the north and flattens at about 3000-4000 feet below sea level. It follows the geometry of the Hartshorne sandstone and the overlying Desmoinesian units. This kind of geometry is common for thrust faults where, in thick incompetent units, the thrusts tend to be near the contact with competent units (Dahlstrom, 1970).

As a whole, the study area is characterized by a foreland-verging thrust movement. Duplexes and a roof thrust are at the frontal part of this thrust belt. This kind of tectonic transport should be "accommodated by backthrusting with opposite vergence, in the section overlying the upper detachment" (Jones, 1994). The Carbon fault is believed to have formed in order to accommodate thrust movement in the study area.

Using evidence from the cross-sections and the surface geological maps, the Carbon fault is interpreted as being formed by the continued upward and southward propagation of the roof thrust (Lower Atokan detachment) within the Atoka shale. Within an incompetent unit like the Atoka shale, the propagation of a detachment is quite easy, so the Lower Atokan detachment propagates within the Atoka shale with a low angle and forms a gentle ramp. Eventually, the detachment reaches the competent and coarse grained Hartshorne Sandstone. At this point, detachment is likely to form either a back thrust following the boundary of the sandstone, or a steep ramp within the sandstone. In the study area, utilizing the surface geological maps and well log data the Carbon fault is interrpreted as forming a backthrust, which has an upward and southward propagation, parallel to the Hartshorne Sandstone and the overlying units (Figures 37 through 44 and Plates III through X).

In the western part of the study area, the surface trace of the Carbon fault on OGS maps is mostly inferred in alluvium or in water bodies (Plates I and II). The cross-sections coinciding with this area (Figures 37 through 40 and Plates III through VI) show the Carbon fault as following the boundary between the Atoka and Hartshorne Formations. To the east, where the fault is mapped within the Atoka Formation, the cross-sections (Figures 41 through 44 and Plates VII through X) suggest that the Carbon fault is propagating close to the Atoka-Hartshorne boundary within the Atoka Formation.

The Desmoinesian units above the Carbon fault are folded gently, forming the southern limb of the San Bois syncline. They show no evidence of displacement by thrust faulting. This also can be used as evidence for backthrusting. The geometry

formed by the south dipping Choctaw fault, the Lower Atokan detachment, and the north dipping Carbon fault can be characterized as a triangle zone.

Triangle Zone

This study suggests the presence of a shallow triangle zone in the study area (Figures 37 through 44 and Plates III through X). The zone is floored by the Lower Atokan detachment. The two opposing flanks of the triangle zone are formed by the south dipping Choctaw fault and the north dipping Carbon fault. All of the cross-sections are suggestive that a triangle zone is present and exhibit similar geometry throughout the study area.

To the east, adjacent to the eastern boundary of the study area, the Carbon fault disappears. The reduction in the size of the triangle zone, as the Choctaw and the Carbon faults get closer to each other towards the east may be indicative of the start of the termination of the triangle zone to the east. Akthar (1995) documents the absence of a triangle zone to the immediate east of the study area.

Normal Faults and Strike Slip Faults

Normal faults are depicted at the northern part of the study area (Figures 37 through 44 and Plates III through X). They are north of the leading duplex, or the blind thrust fault, where the effects are not seen. Based on the cross-sections, the normal faults probably same direction as the major thrust faults

but they are not mapped on the structural contour map because of the unavailability of sufficient well control in the northern part of the study area. The cross-sections show that the normal faults displace the Spiro sandstone, but their extent into the pre-Atokan units could not be examined because of the limited amount of data. The seismic profiles are suggestive of the presence of normal faulting below the detachment. In the absence of enough well control, the normal faults and the Spiro sandstone are mostly inferred from the adjacent cross-sections. The cross-sections suggest a maximum of 2000 feet of vertical displacement. Ferguson and Suneson (1988) proposed that the growth faults acted as barriers, which forced the thrusts to ramp over basement rocks.

Three strike slip faults are suggested by the structural contour map. These strike slip faults have a right lateral movement and they can be classified as tear faults. The tear faults trend in a northwest to southeast direction and are depicted in the southern two thirds of the structural contour map.

Folds

The anticlines and synclines in the study area trend generally in a east-northeast-west-southwest direction following the trend of major thrust faults (Plates I and II). To the south of the Choctaw fault, the folds are found in the hanging walls of the individual thrust faults, folding the thrust sheets above them (Figures 37 through 44 and Plates III through X). The folds formed by the thrust faults are asymmetrical to the north. North of the Choctaw fault, the Hartshorne syncline, the Adamson anticline and the San Bois syncline are the prominent folds.

The Red Oak sandstone and Marker X are gently folded above the Lower Atokan detachment. The anticline in the Red Oak sandstone at the western most part of the study area may be due to a blind thrust fault (Figures 37, 38 and Plates III, IV).The Carbon fault is interpreted as following the Hartshorne-Atoka boundary, which forms part of the southern limb of the San Bois syncline.

Restored cross-sections and amount of shortening

The structural cross-sections are restored using the key bed restoration method to calculate the amount of shortening for the Spiro sandstone (Figures 48 through 55). In the study area, especially to the south of the Choctaw fault, the Atoka shale dominates the rock units both at the surface and in the subsurface. Shales have characteristic responses to deformation. Because they are incompetent, they can be easily deformed and to select the bed boundaries within shales could be very difficult. While constructing the cross-sections this situation is encountered and only the Spiro sandstone is used to define the subsurface structural geometry because of its recognizable well log signature.

The pin lines for the restored cross-sections are located to the north of the leading duplex or the blind thrust, where the Spiro sandstone is not affected by shortening in the frontal zone. The loose lines are located to the south where there is no piercing point for the thrusted Spiro sandstone.

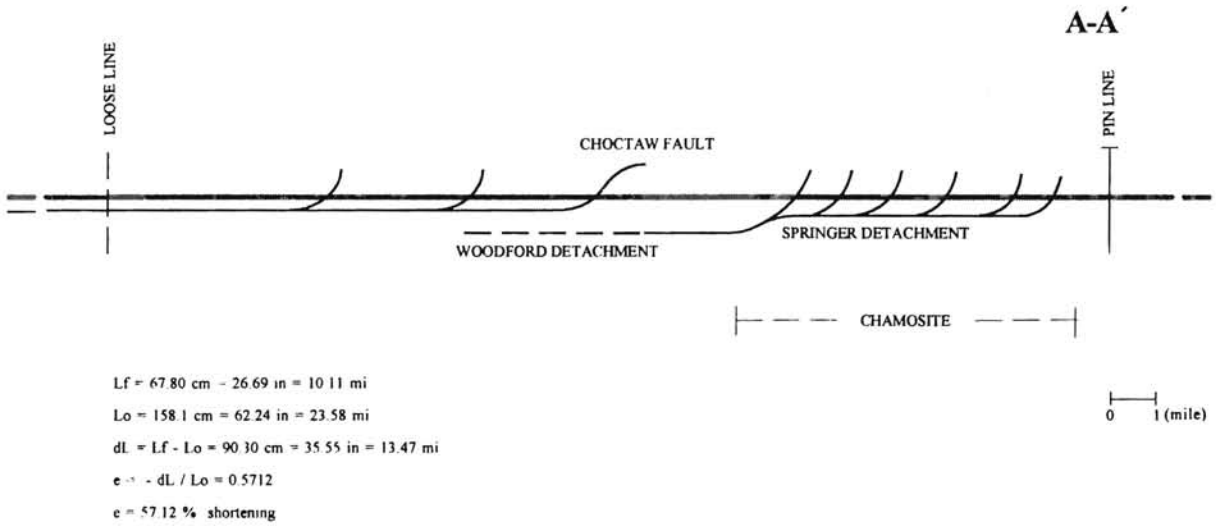

Figure 48: Restored cross-section A-A'

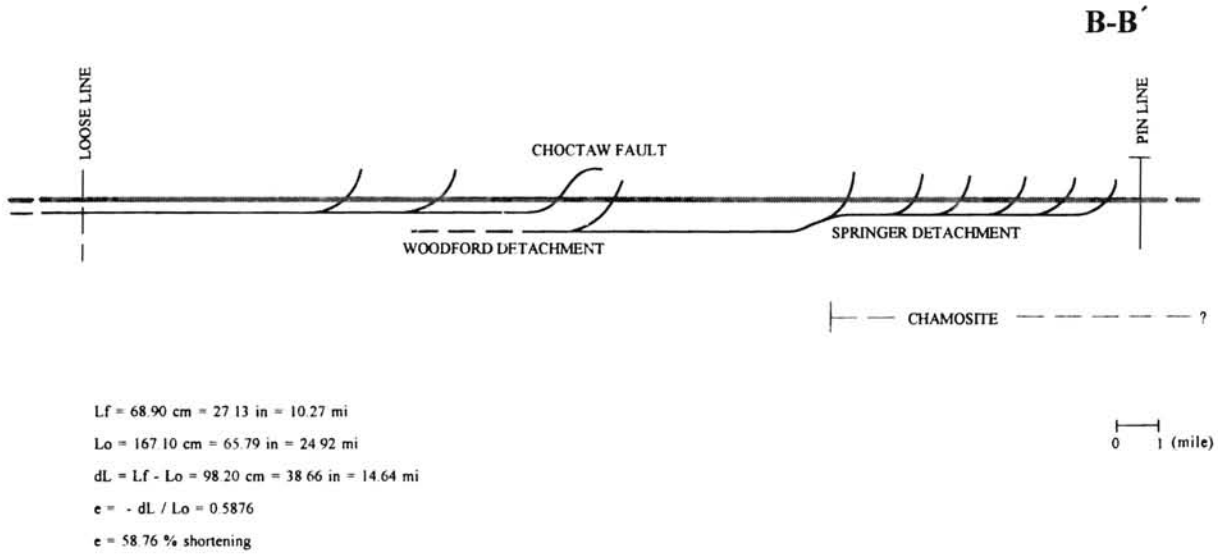

Figure 49 : Restored cross-section B-B'

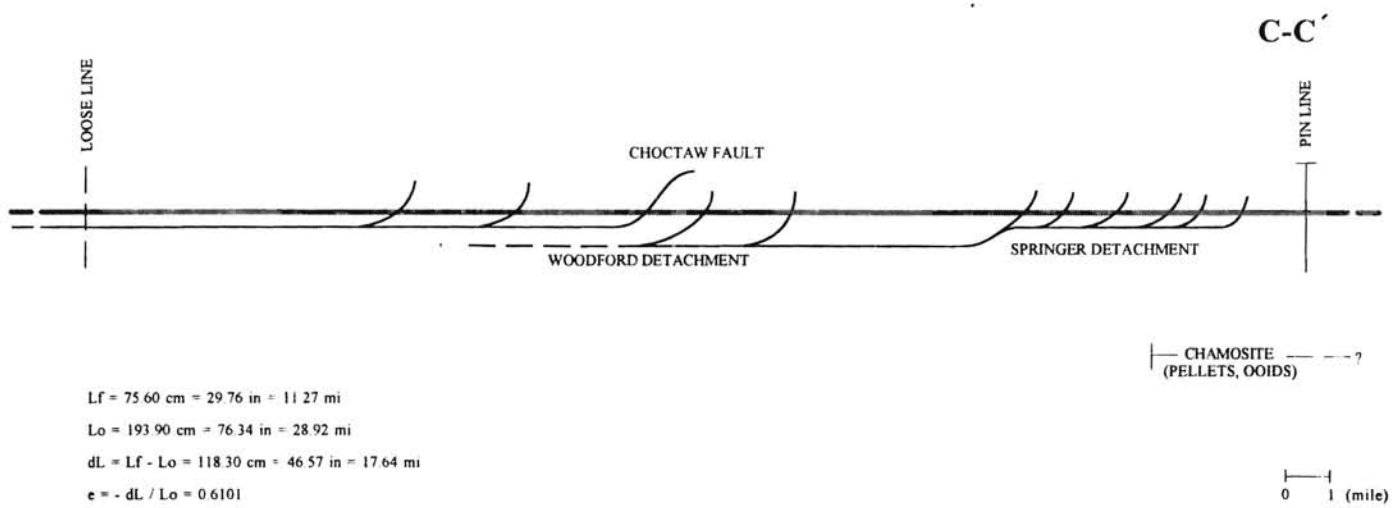

Figure 50: Restored cross-section C-C'

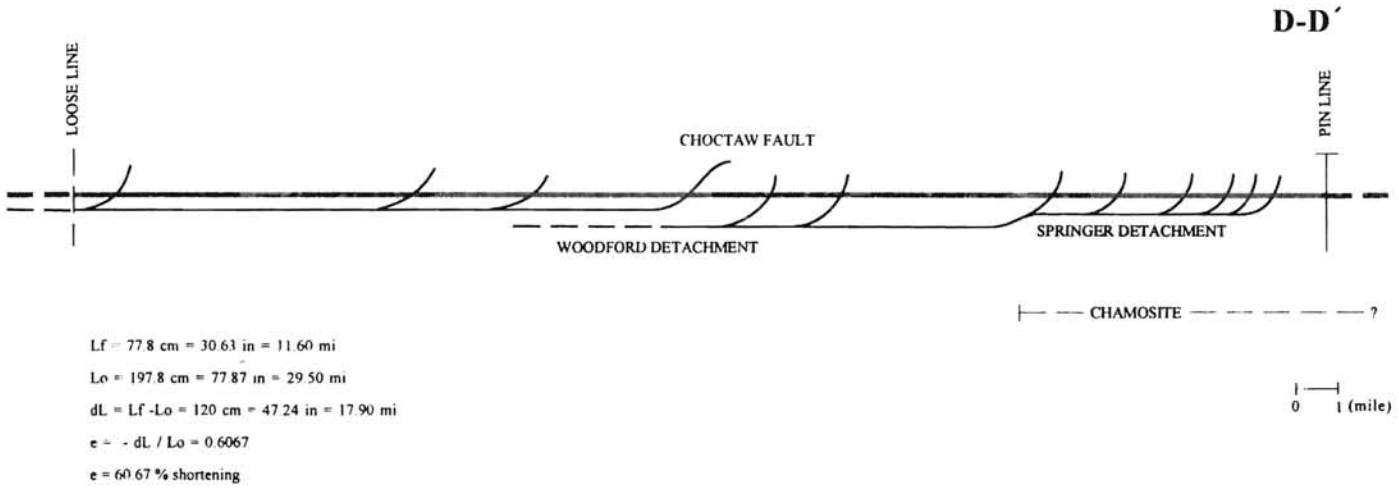

Figure 51: Restored cross-section D-D'

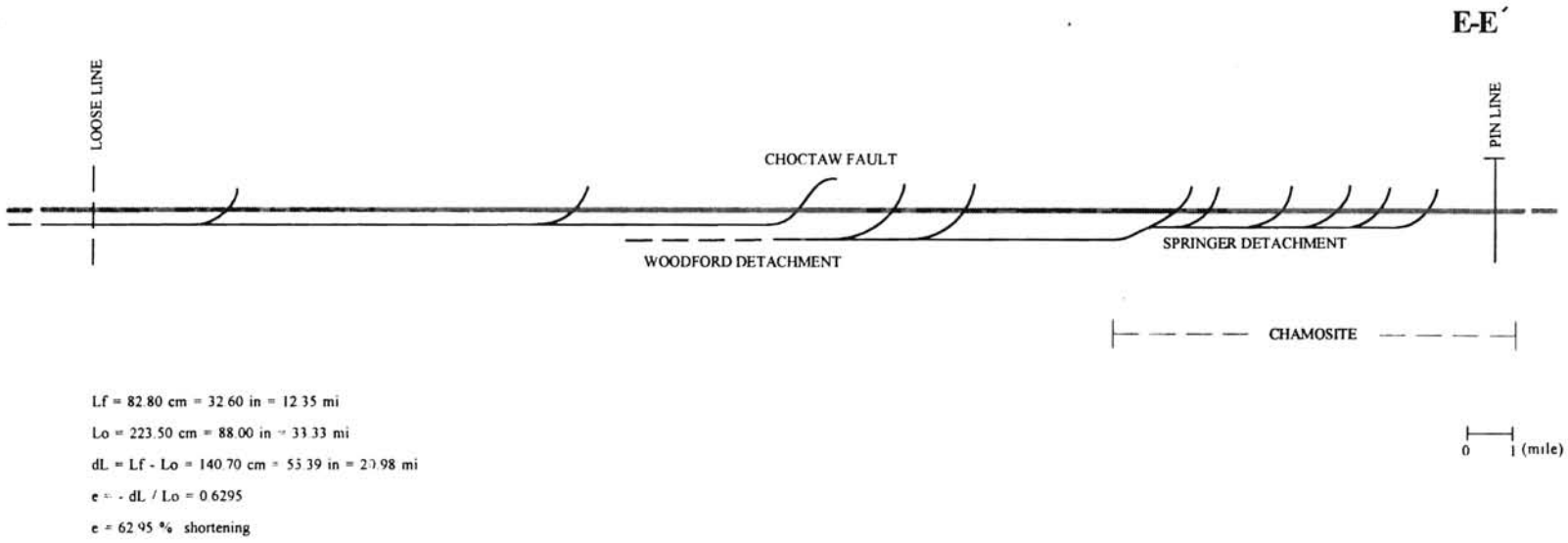

Figure 52: Restored cross-section E-E'

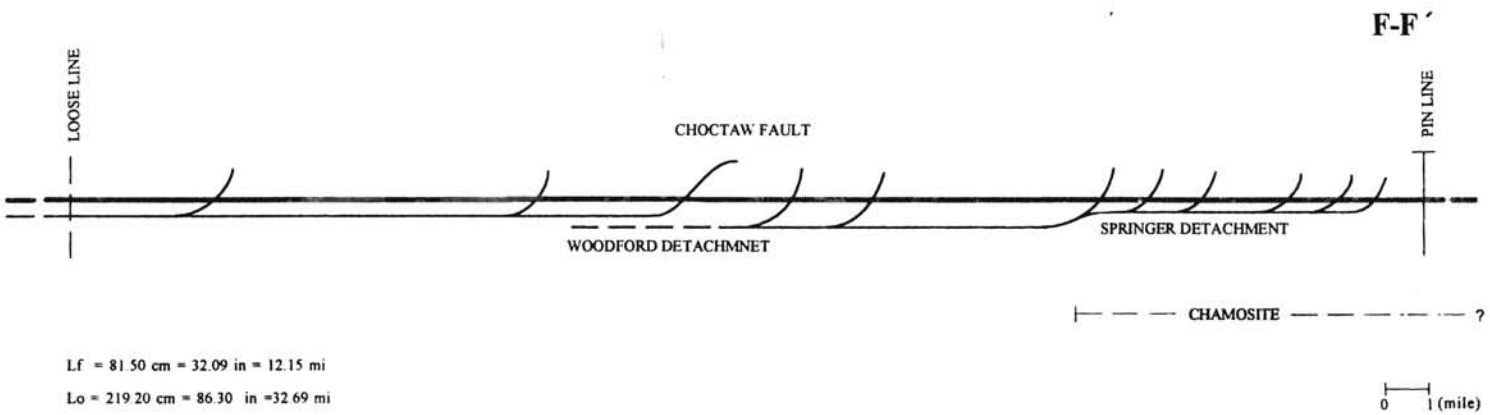

Figure 53: Restored cross-section F-F'

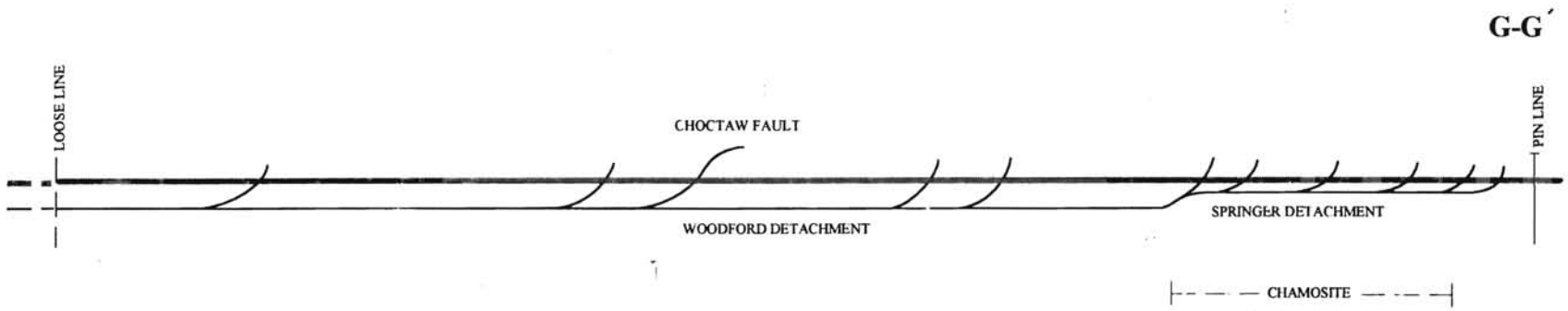

Figure 54: Restored cross-section G-G'

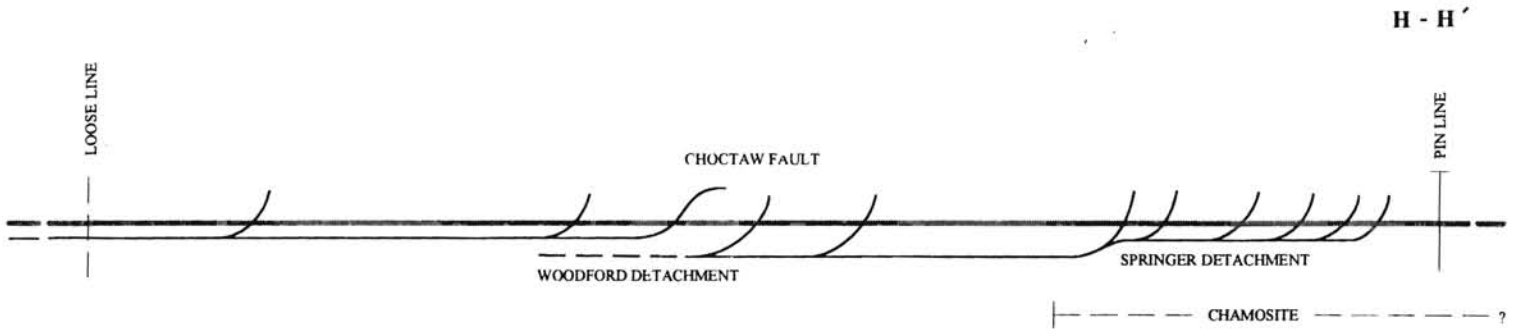

Lf = 82.1 cm = 32.32 in = 12.24 mi

Lo = 216.20 cm = 85.12 in = 32.24 mi

dL = Lf - Lo = 134.1 cm = 52.80 in = 20.00 mi

e = - dL / Lo = 0.6203

e = 62.03 % shortening

Figure 55: Restored cross-section H-H'

The calculations suggest about 60% shortening for the Spiro sandstone. The calculations for the amount of shortening in the cross-sections are done from 1:24000 scale geological maps. The scales for the cross-sections and their restorations are not the same. The restorations are reduced in order to be in a reasonable size to be shown with the cross-sections on the plates (Plates III through X). The centimeter and inch values on the calculations are the measured lengths from the original 1:24000 scale maps. The calculations for the shortening of the cross-sections are as follows:

Cross-section A-A':

Lf = 67.80 cm = 26.69 in = 10.11 mi

Lo = 158.1 cm = 62.24 in = 23.58 mi

dL = Lf - Lo = 90.30 cm = 35.55 in = 13.47 mi

e = - dL / Lo = 0.5712

e = 57.12 % shortening

Cross-section B-B':

Lf = 68.90 cm = 27.13 in = 10.27 mi

Lo = 167.10 cm = 65.79 in = 24.92 mi

dL = Lf - Lo = 98.20 cm = 38.66 in = 14.64 mi

e = - dL / Lo = 0.5876

e = 58.76 % shortening

Cross-section C-C':

Lf = 75.60 cm = 29.76 in = 11.27 mi

Lo = 193.90 cm = 76.34 in = 28.92 mi

dL = Lf - Lo = 118.30 cm = 46.57 in = 17.64 mi

e = - dL / Lo = 0.6101

e = 61.01 % shortening

Cross-section D-D':

Lf = 77.8 cm = 30.63 in = 11.60 mi

Lo = 197.8 cm = 77.87 in = 29.50 mi

dL = Lf -Lo = 120 cm = 47.24 in = 17.90 mi

e = - dL / Lo = 0.6067

e = 60.67 % shortening

Cross-section E-E':

Lf = 82.80 cm = 32.60 in = 12.35 mi

Lo = 223.50 cm = 88.00 in = 33.33 mi

dL = Lf - Lo = 140.70 cm = 55.39 in = 20.98 mi

e = - dL / Lo = 0.6295

e = 62.95 % shortening

Cross-section F-F':

Lf = 81.50 cm = 32.09 in = 12.15 mi

Lo = 219.20 cm = 86.30 in =32.69 mi

dL = Lf -Lo = 137.7 cm = 54.21 in = 20.54 mi

e = - dL / Lo = 0.6282

e = 62.82 % shortening

Cross-section G-G':

Lf = 91.80 cm = 36.14 in = 13.69 mi

Lo = 252.30 cm = 99.33 in = 37.63 mi

dL = Lf - Lo = 160.50 cm = 63.19 in = 23.94 mi

e = - dl / Lo = 0.6361

e = 63.61 % shortening

Cross-section H-H':

Lf = 82.1 cm = 32.32 in = 12.24 mi

Lo = 216.20 cm = 85.12 in = 32.24 mi

dL = Lf - Lo = 134.1 cm = 52.80 in = 20.00 mi

e = - dL / Lo = 0.6203

e = 62.03 % shortening

CHAPTER 7

CONCLUSIONS

The major accomplishments of this study are listed below;

1) The study area contains two different geometries of structural deformation above and below the Choctaw fault.

2) The hanging wall block of the Choctaw fault contains many south dipping imbricate thrust faults that displace the Spiro sandstone.

3) The footwall block shows well developed duplex structures and imbricate thrust faults floored by detachment surfaces at two different depths (Woodford and Springer detachments).

4) A floor (Springer detachment) and a roof thrust (Lower Atokan detachment) form the lower and upper boundaries of the duplexes.

5) The Carbon fault is a north dipping thrust fault.

6) The leading edge of the Ouachita fold and thrust belt is terminated by a shallow triangle zone, which is bounded by the Choctaw fault, the Lower Atokan detachment, and the Carbon fault.

7) The average amount of shortening in the Wilburton-Hartshorne area approximates 60%.

8) Chamosite coatings aid in the preservation of primary porosity.

REFERENCES

Akhtar, S., 1995, The Geometry of Thrust Systems in Wilburton Gas Field and Surrounding areas, Latimer County, Oklahoma: unpublished M.S. thesis, Oklahoma State University, Stillwater, OK 97 p.

Akhtar, S., Cemen, I, and Al-Shaieb, Z., 1995, Geometry of Thrust Systems in Wilburton Gas Field and Surrounding Areas, Arkoma Basin, Oklahoma; Geological Society of America North; South-Central Section Meeting Abstracts with Programs, v. 27, no. 3, p. 33.

Al-Shaieb, Z., 1988, The Spiro sandstone in Wilburton field area: Petrology, Diagenesis, Sedimentology, Porosity and Reservoir Quality: unpublished report, 139p.

Al-Shaieb, Z., Shelton, J., Puckette, J., and Boardman, D., 1995, Sandstone and Carbonate Reservoirs of the Mid-Continent; Syllabus for Short Course, OCGS-OSU Core Workshop: Oklahoma City Geological Society, 194 p.

Arbenz, J.K., 1989, Ouachita Thrust Belt and Arkoma Basin: in Hatcher, R.D,, Jr., Thomas, W.A., and Viele, G.W., eds., The Geology of North America, vol. F-2, The Appalachian-Ouachita Orogeny in the United States, Geological Society of America, Boulder, Colorado, p. 621-634.

Buchanan, R.S., and Johnson, F.K., 1968, Bonanza Gas Field-a model for Arkoma Basin Growth Faulting. In Cline, L.M., ed., Geology of the Western Arkoma Basin and Ouachita Mountains: Oklahoma City Geol. Society Guide, p. 75-85.

Berry, R.M. and W.D. Trumbly, 1968, Wilburton Gas Field; in Cline, L.M., ed., A Guidebook to the Geology of the Western Arkoma Basin and Ouachita Mountains: Dallas Geol. Soc. and Ardmore Geol. Soc. Symposium Guidebook, p. 65-68.

Butler, R.W.H., 1987, Thrust Sequences: Journal of the Geological Society, London, v. 144, p. 619-634.

Boyer, S.E., and Elliot, D., 1982, Thrust Systems: AAPG Bull., v 66, p. 1196-1230.

Camp. W.K. and Ratliff, R.A., 1989, Balanced Cross-Section Through Wilburton Gas Field, Latimer County, Oklahoma: Implications for Ouachita Deformation and Arbuckle (Cambro-Ordovician) Exploration in Arkoma Basin (abstract): AAPG Bull, v. 73, p.1044.

Cardott, B.J., Hemish, L.A., Johnson, C.R., and Luza, K.V., 1986, The Relationship Between Coal Rank and Present Geothermal Gradient in the Arkoma Basin, Oklahoma: Oklahoma Geol. Survey Special Publication 86-4, p. 65.

Carlson, M.C., 1988, A Petrologic Analysis of Surface and Subsurface Atoka For (Lower Pennsylvanian) Sandstone, Western Margin of the Arkoma Ba ɔma Oklahoma: unpublished M.S. thesis, The University of Tulsa, Tul· 196 p.

Cemen, I., Al-Shaieb, Z., Akhtar, S., and Feller, R., 1994, Prelimiiity of the a Seismic Profile and the Spiro Reservoir Pressure Datcal Survey: Wilburton Gas Field and Surrounding Areas, Okla' Guidebook 29, p. 249-252.

Cemen, I, Al-Shaieb, Z., Hess, F., Akthar, S., and Feller, R., 1995, Geometry of thrusting in Wilburton Gas Field and Surrounding Areas, Arkoma Basin, Oklahoma; Implications for Gas Exploration in the Spiro Sandstone Reservoirs; (Abstract): AAPG Bull. v. 79, no. 9, p. 1401.

Couzens, B.A., and Wiltschko, D.V., 1994, Some Constraints for Mechanical Models of Triangle Zones; (Abstract): Western Canadian and International Expertise, Exploration Update; A Joint Convention of CSEG and CSPG, Calgary, Alberta, 1994, p. 370-71.

Dahlstrom, C.D.A. , 1970, Structural Geology in the Eastern Margin of the Canadian Rocky Mountains: Bulletin of Canadian Petroleum Geology, 18, p. 332-406.

Ferguson, C.A. and N.H. Suneson, 1988, Tectonic Implications of Early Penssylvanian Paleocurrents from Flysch in the Ouachita Mountains Frontal Belt, Southeast Oklahoma; in Johnson, K.S., ed., Shelf to Basin Geology and Resources of Pennsylvanian in the Arkoma Basin and Frontal Ouachita Mountains of Oklahoma: Okla. Geol. Survey Guidebook 25, p. 49-63.

Feller, R., 1995, Characteristics of Abnormally-Pressured Gas Compartments and Potential Sealing Mechanisms in the Spiro Sandstone, Arkoma Basin, Oklahoma: unpublished M.S. thesis, Oklahoma State University, Stillwater, Oklahoma.

Ham, W.E., 1978, Regional Geology of the Arbuckle Mountains, Oklahoma: Oklahoma Geological Survey Special Publication 73-3, 61p.

Hardie, W., 1988, Structural Styles of the Frontal Thrust Belt of the Ouachita Mountains, southern Pittsburg County, Oklahoma: Oklahoma Geology Notes, v. 48, no. 6, p.232-246.

Hemish, L.R. and Suneson N.H. Geologic map of the Adamson Quadrangle, Pittsburg County, Oklahoma (unpublished): Oklahoma Geological Survey, scale 1:24000.

Hemish, L.R. and Suneson N.H. Geologic map of the Hartshorne Quadrangle, Pittsburg County, Oklahoma (unpublished): Oklahoma Geological Survey, scale 1:24000.

Hendricks, T.A., 1939, The Howe-Wilburton district, Latimer and LeFlore Counties, Oklahoma: U.S.G.S Bulletin 874-D, p. 255-298.

Hess, F. B., 1995, Sedimentology and Depositional Environments of the Lower Atokan Spiro sandstone in the Wilburton, Red Oak, and Kinta fields, Arkoma Basin, Oklahoma: unpublished M.S.thesis, Oklahoma State University, Stillwater, 159 p.

Hooker, E.M., 1988, The Distribution and Depositional Environment of the Spiro sandstone, Arkoma Basin, Haskell, Latimer, and Pittsburg Counties, Oklahoma: unpublished M.S. thesis, Oklahoma State University, Stillwater, 98p.

Houseknecht, D.W., and Kacena, J.A., 1983, Tectonic-Sedimentary Evolution of the Arkoma Basin: Soc. Econ. Paleontologists and Mineralogists, Mid-continent Section, v. 1, 119 p.

Houseknecht, D.W., 1986, Evolution from Passive Margin to Foreland Basin: The Atoka Formation of the Arkoma Basin, south-central USA., in Allen, P.A., and Homewood , P. eds., Foreland Basins: International Association of Sedimentologists Special Publication 8, p. 327-345.

Jamison, W.R. 1994, Triangle Zone Evolution Mechanistic Approaches (Abstract): Western Canadian and International Expertise, Exploration Update; A Joint Convention of CSEG and CSPG, Calgary, Alberta, 1994, p. 217.

Johnson, K.S., 1988, General Geologic Framework of the field-trip area, in Johnson, K.S., ed., Shelf-to Basin Geology and Resources of Pennsylvanian strata in the Arkoma Basin and Frontal Ouachita Mountains of Oklahoma: Oklahoma Geological Survey Guidebook 25, p. 1-5.

Jones, P.B., 1994, Triangle Zone Geometry and Terminology (Abstract): Western Canadian and International Expertise, Exploration Update; A Joint Convention of CSEG and CSPG, Calgary, Alberta, 1994, p. 69-70.

Keller, G.R., and Cebull, S.E., 1973, Plate Tectonics and the Ouachita System in Texas, Oklahoma, and Arkansas: Geol. Soc. America Bull., v. 83, p. 1659-166.

Koinm, D.N., and Dickey, P.A., 1967, Growth Faulting in the McAlester Basin of Oklahoma: AAPG Bull., v. 51, no. 5, p. 710-718.

Lowell, J.D. 1985, Structural Styles in Petroleum Exploration, OGCI Pub. 460 p.

Lumsden, D.N., E.D. Pittman and R.S. Buchanan, 1971, Sedimentation and Petrology of Spiro and Foster sands (Pennsylvanian), McAlester basin, Oklahoma: AAPG Bull. 55, pp. 254-266.

Marshak, S., and Mitra, G., 1988, Basic Methods of Structural Geology, Prentice Hall, 446 p.

Mazengarb, C., 1995, Interpretation of Structure from Surface Geology, Frontal Ouachitas, Southeastern Oklahoma: in Johnson, K.S., ed., Structural Styles in the Southern Midcontinent, 1992 Symposium: Oklahoma Geological Survey Circular 97, p. 26-31.

McClay, K.R , 1992, ed., Glossary of Thrust Tectonic Terms; Thrust Tectonics, Chapman Hall, 447 p.

Milliken, J.V., 1988, Late Paleozoic and Early Mesozoic Geologic Evolution of the Arklatex area: Rice University, Houston, unpublished M.S. thesis, 259 p.

Mitra, S., 1986, Duplex Structures and Imbricate Thrust Systems; Geometry, Structural Position and Hydrocarbon Potential: AAPG Bull, 70, p. 1087-1112.

Morris, R.C., 1974, Sedimentary and Tectonic History of the Ouachita Mountains SEPM Special Publication 22, pp.120-142.

Perry, W.J., Jr., and Suneson, N.H., 1990, Preliminary Interpretation of a Seismic Profile across the Ouachita Frontal Zone near Hartshorne, Oklahoma: Oklahoma Geological Survey Special Publication 90-1, p. 145-148

Perry, W.J., Jr., Agena, W., and Suneson, N.H., 1990, Preliminary reinterpretation of the Ouachita Frontal Zone near Hartshorne, Oklahoma based chiefly on seismic reflection data: U.S. Geological Survey Circular 1060, p. 82.

Price, R.A., 1986, The Southeastern Canadian Cordillera; Thrust Faulting, Tectonic Wedging and Delamination of the Lithosphere: Journal of Structural Geology, v. 8, p. 239-254.

Price, R.A., 1994, "Triangle zones" as Elements in a Temporal and Spatial Spectrum of Tectonic Wedging and Delamination (Abstract); Western Canadian and International Expertise, Exploration Update; A Joint Convention of CSEG and CSPG, Calgary, Alberta, 1994, p. 208.

Reeves, D.L., Schreiner, W.P., and Sheffield, T.M., 1990, Stop 6- New State Mountain (Amoco 1-5 Rosso Unit) Oklahoma Geological Survey Special Publication 90-1, p. 37-40.

Roberts, M.T., 1992, Shelf to Basin Transect, Eastern Oklahoma: Shreveport Geological Society Guidebook, May 27-29, 1992, unnumbered pages.

Sagnak, A., Cemen, I., Al-Shaieb, Z., 1996, Structural Geometry of the Thrust Faulting in the Wilburton Gas Field area, Southeastern Oklahoma (Abstract): Oklahoma Geology Notes, v. 56, no. 1, p. 27.

Sagnak, A., Cemen, I., Al-Shaieb, Z., 1996, Geometry of Late Paleozoic Thrusting in the Wilburton-Hartshorne Area, Arkoma Basin, SE Oklahoma (Abstract): Geological Society of America, South Central Section Meeting 1996, Abstracts with Programs; p.62.

Suneson, N.H. 1988, The Geology of the Ti Valley Fault in the Oklahoma Ouachita Mountains: in Johnson, K.S., ed., Shelf-to Basin Geology and Resources of Pennsylvanian strata in the Arkoma Basin and Frontal Ouachita Mountains of Oklahoma: Oklahoma Geological Survey Guidebook 25, p. 33-47.

Suneson, N.H. and Ferguson A.C., 1989, Geologic map of the Gowen Quadrangle, Latimer County, Oklahoma: Oklahoma Geological Survey, scale 1:24000.

Suneson, N.H. and Ferguson A.C., 1989, Geologic map of the Higgins Quadrangle, Latimer County, Oklahoma: Oklahoma Geological Survey, scale 1:24000.

Suneson, N.H. and Ferguson A.C., 1989, Geologic map of the Damon Quadrangle, Latimer County, Oklahoma: Oklahoma Geological Survey, scale 1:24000.

Suneson, N.H., Campbell, J.A., and Tilford, M.J., 1990,Geologic Setting and Introduction: Geology and Resources of the Frontal Belt of the Western Ouachita Mountains; Oklahoma Geological Survey Special Publication 90-1, p. 1-4.

Suneson, N.H., 1995, Structural Interpretations of the Arkoma Basin-Ouachita mountains Transition Zone, Southeastern Oklahoma; A Review: in Johnson, K.S., ed., Structural Styles in the Southern Midcontinent, 1992 Symposium: Oklahoma Geological Survey Circular 97, p. 259-263.

Sutherland, P.K., 1988, Late Mississippian and Pennsylvanian Depositional History in the Arkoma Basin area, Oklahoma and Arkansas: GSA Bulletin, v. 100, no,. 11, p.1787-1802.

Sykes, M., 1995, Paleokarst Characteristics of the Surface and Subsurface in the Viola Limestone(Ordovician), Arbuckle Mountains, Oklahoma: unpublished M.S. thesis, Oklahoma State University, Stillwater, Oklahoma, 124 p.

Tilford, M.J., 1990, Geological Review of the Ouachita Mountains Thrust Belt Play, Western Arkoma Basin, Oklahoma: Geology and Resources of the Frontal Belt of the Western Ouachita Mountains: Oklahoma Geological Survey Special Publication 90-1, p. 169-196.

Walper, J.L.,1977, Wrench faulting in the Mid-Continent: Shale Shaker, v.21, no. 2, p.32-40.

Vedros, S.G., and Visher, G.S., 1978, The Red Oak sandstone: a Hydrocarbon -producing Submarine Fan Deposit, in Stanley, D.J.; and Kelling, G. eds., Sedimentation in Submarine Canyons, Fans and Trenches: Dowden, Hutchinson, and Ross, Stroudsburg, Pennsylvania, p. 279-308.

Wilkerson, M.S., and Wellman P.C., 1993, Three Dimensional Geometry and Kinematics of the Gale-Buckeye Thrust System, Ouachita Fold and Thr Latimer and Pittsburg Counties, Oklahoma: AAPG Bulletin, v. 77, p 1100.

APPENDICES

APPENDIX I

Photoghraph of the Pan-American Petrleum
Company Reusch #1 ccore

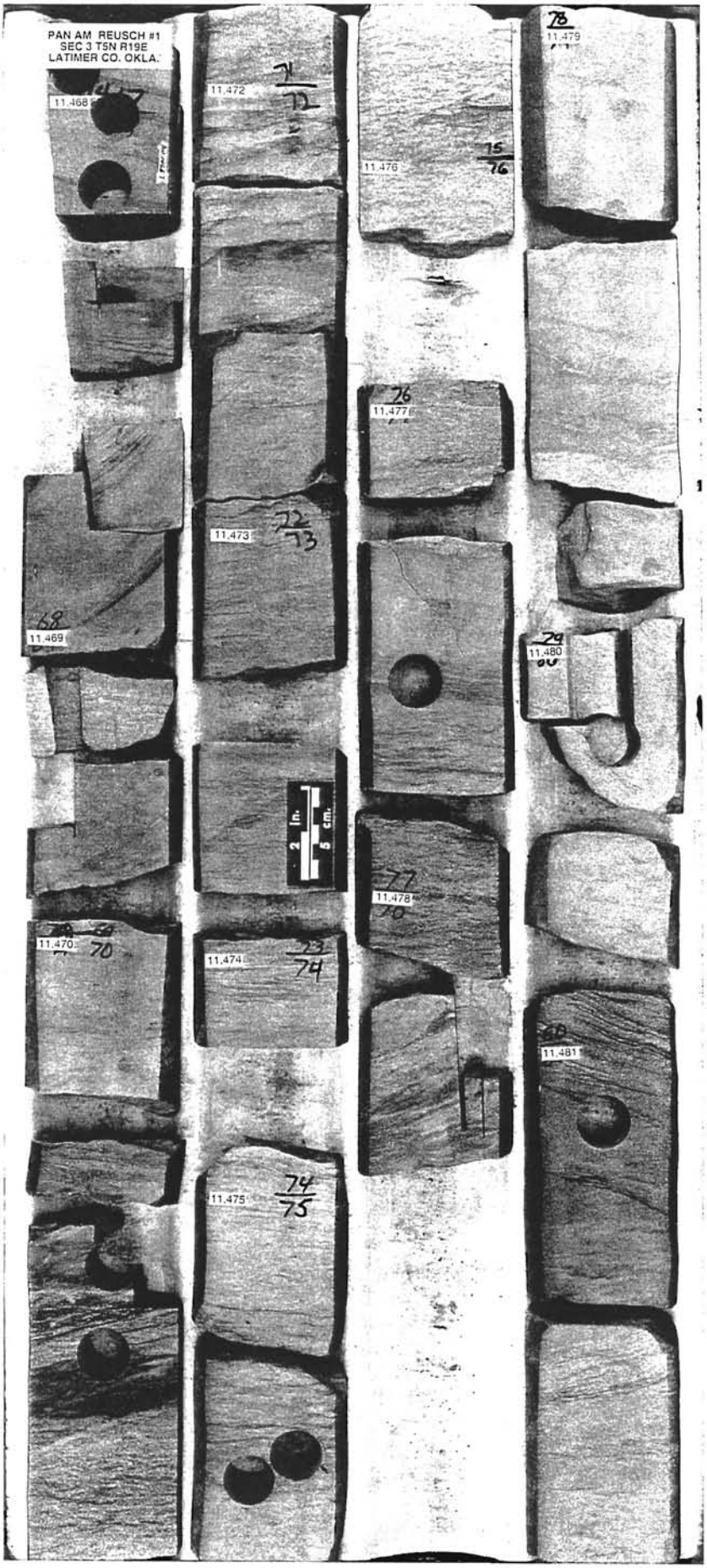
PAN AM REUSCH #1
SEC 3 TSN R19E
LATIMER CO. OKLA.
11,468
11,472
11,476
11,479
11,477
11,473
11,469
11,480
11,478
11,470
11,474
11,481
11,475
2 in.
5 cm.

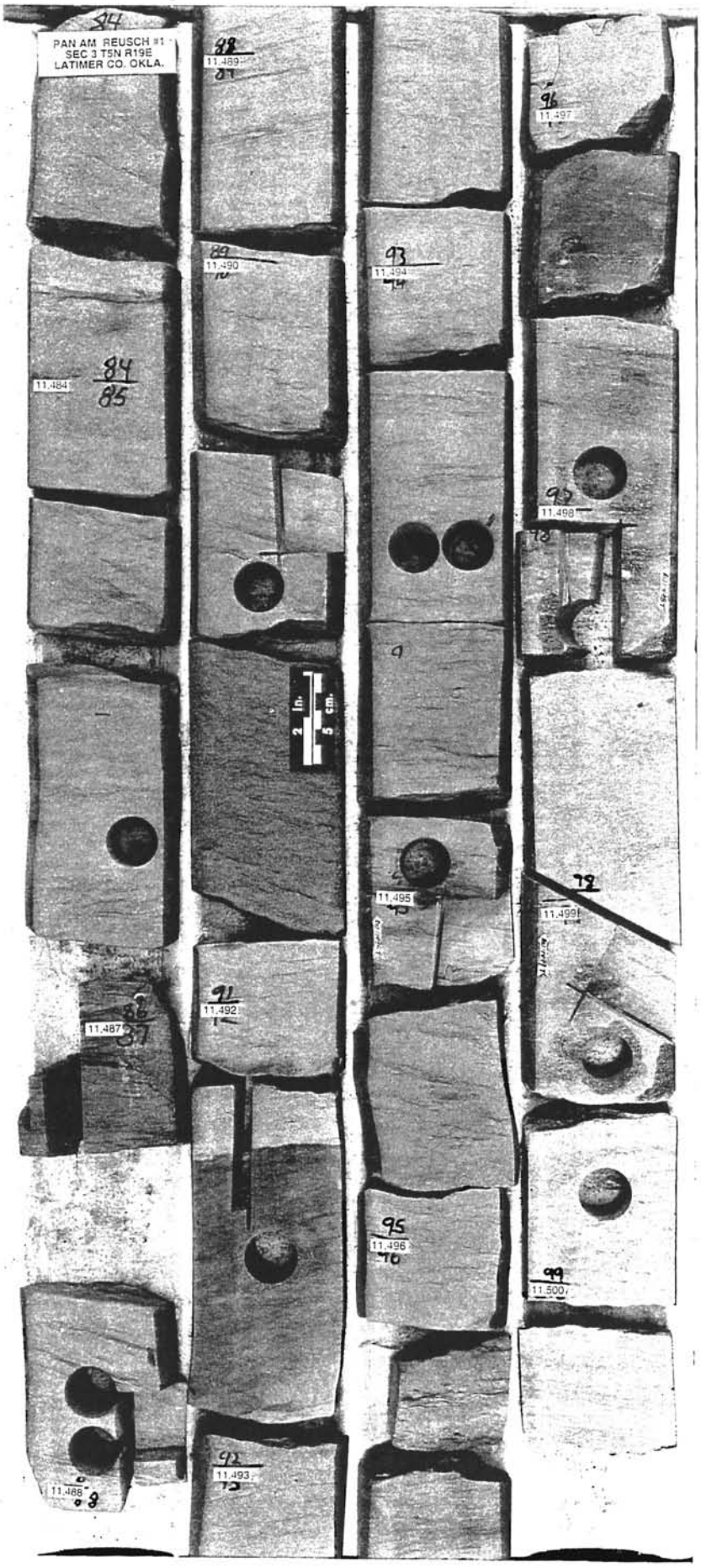
PAN AM REUSCH #1
SEC 3 T5N R19E
LATIMER CO. OKLA.
11,484
11,487
11,488
11,489
11,490
11,492
11,493
11,494
11,495
11,496
11,497
11,498
11,499
11,500
2 in.
5 cm.

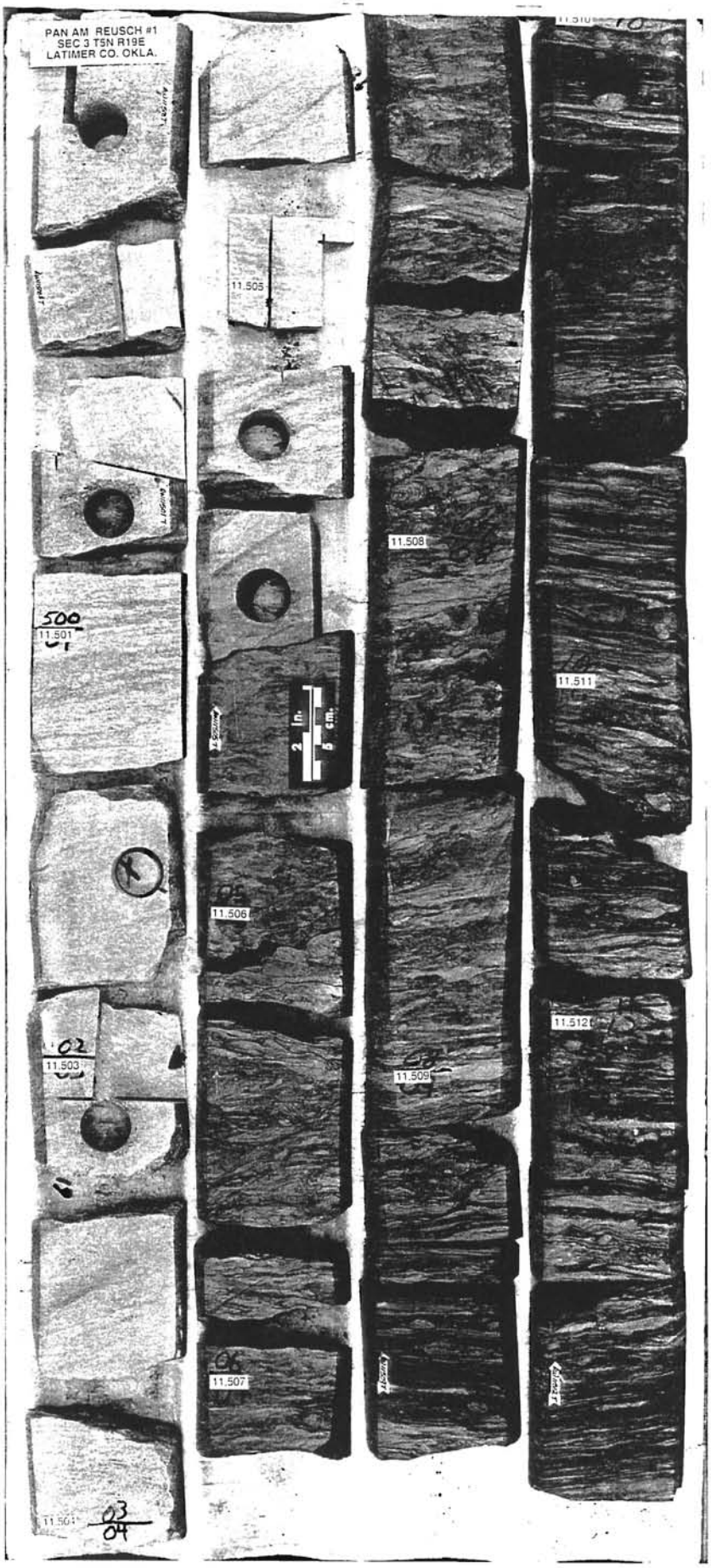
PAN AM REUSCH #1
SEC 3 T5N R19E
LATIMER CO. OKLA.
11.501
11.502
11.503
11.504
11.505
11.506
11.507
11.508
11.509
11.511
11.512
2 In.
5 cm.

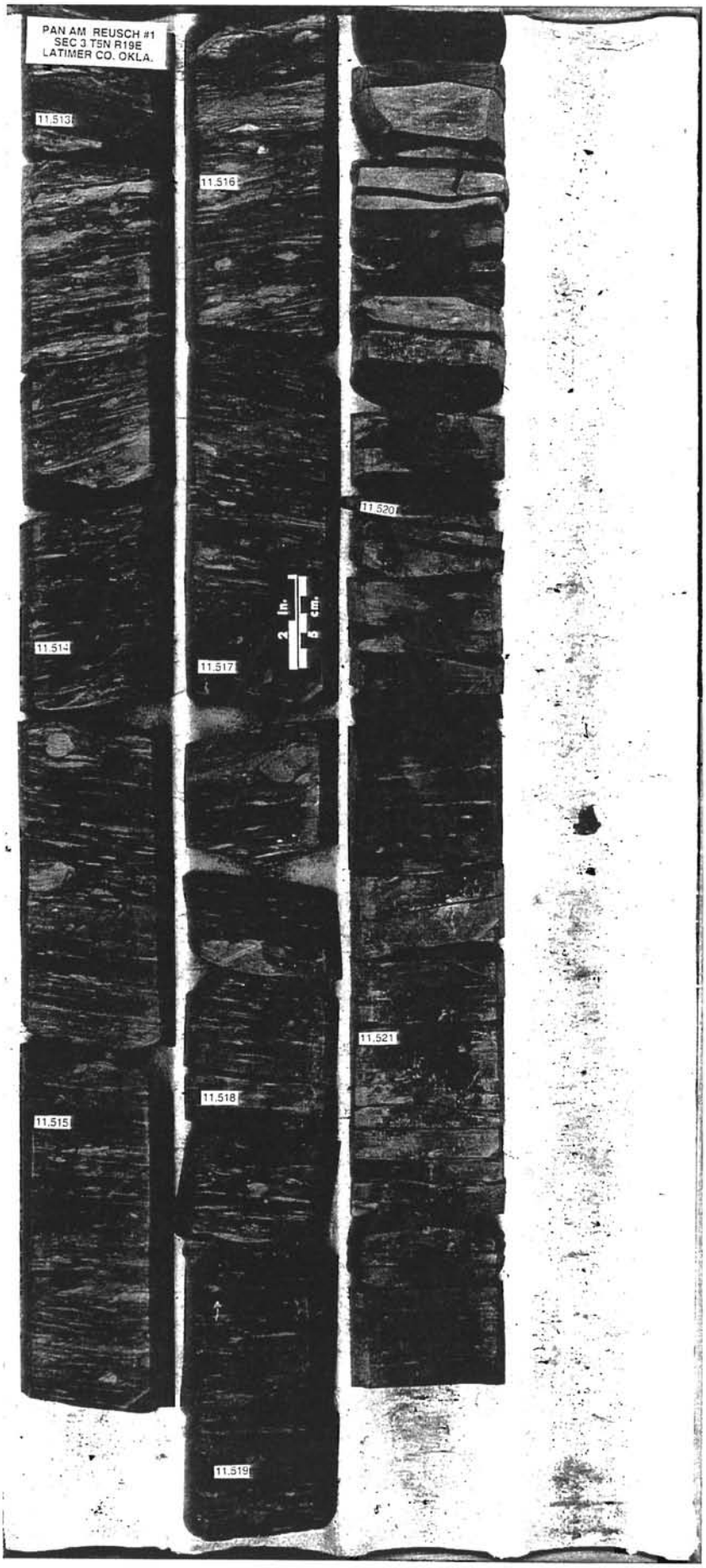
PAN AM REUSCH #1
SEC 3 T5N R19E
LATIMER CO. OKLA.
11,513
11,514
11,515
11,516
11,517
11,518
11,519
11,520
11,521
2 in.
5 cm.

APPENDIX II

Well log data sheets

WELL LOG DATA SHEETS

3N-17E Operator	Well	Location	Sect.	Field	K.B.	Top Spiro	Top Wap
AMOCO	Moses Watts No. 35-1	NE NE SW NW	1	Hartshorne	885	6820	

4N-16E Operator	Well	Location	Sect.	Field	K.B.	Top Spiro	Top Wap
Marathon	Slaughter 1-1	SE SE NE SW	1	Wilburton	806	9835	9905
Marathon	Slaughter Unit #2	SE SW NW	1	Wilburton	758	NDE	
Marathon	Madden #2	2100 FNL 1670 FEL	2	Wilburton	633	10877	10937
Marathon	Madden 1-2	1850 FSL 1330 FEL	2	Wilburton	646	9796	9851
The Headington Co.	Maddox #1	NE SW NE	3	Hartshorne	679	10835	10902
Whitmar Expl.	Smallwood 2-3	SE SE	3	Hartshorne	655	10905	10974
Pan American	Smallwood Unit "B" #1	C SE	3	Haileyville	685	NDE	
Texaco	W.C. Camp 1-4	1785 FNL 1455FEL	4	Wildcat	662	10432	10483
Texaco	W.C. Camp 1-4	1785 FNL 1455FEL	4	Wildcat	662	11356	11406
Amoco	Smallwood #2	SW NE SE	10	Wilburton	680	10025	10086
PanAm	Smallwood #1	SW NE	10	Wildcat	682	10991	11048
Samson	Smallwood # 3	C NE	10	Haileyville	683	NDE	
Marathon	Needham 1-11	2490 FSL 1470 FEL	11	Wilburton	688	10422	10496
Marathon	Needham 2-11	1230 FSL 1420FWL NW	11	Wilburton	672	9969	10043
Marathon	Needham 2-11	1230 FSL 1420 FWL NW	11	Wilburton	672	11411	11481
Marathon	Lewis 1-12	2310 FSL 1520 FWL	12	Wilburton	700	10671	10766
Marathon	Lewis #3	NW SE NW	12	Hartshorne	735	10405	10477

Marathon	Lewis #3	NW SE NW	12	Hartshorne	735	11655	11715
W.P.Lerblance Jr.	Lewis No. 1-12	C NW	12	Wilburton	707	NDE	
Whitmar Expl.	Cope #1	W E NW NW	13	Wilburton	667	11207	11285
Marathon	Needham 1-14	1400 FNL 1400 FWL	14	Wilburton	689	10996	11060
Samson	Tex #1	S NE NE	14	Wilburton	647	11183	11251
Marathon	Lynn 1-15	1520 FNL 2290 FEL	15	Wilburton	689	10831	10887
Donald Slawson	Lynn 1-5	660 FNL 1680 FWL	15	Wilburton	708	10812	10869
Tex-Pek Partnership	BuddySherril #16-1	230 FSL 1520 FWL	16	Pittsburg	696	10550	10622
APexco	Warren Spahn #1	C-NE-SW	22	Wildcat	770	11794	11839
Andover Oil	Gayle Lynn #1-24	C N2	24	Hartshorne	666	NDE	
Texaco	BeltTrust 26-1	2444 FSL 624 FWL NE	26	Haileyville	955	11801	11888
Arkla	Loveless 1-30	1320 FNL 1470 FWL	30	Haileyville	653	12547	12615
Tex Pek	Dromgold 'B' 32-1	320 FSL 2400 FEL	32	Wildcat	990	10880	10960
Exxon	Garrett B-1	SW SE SE	34	Hartshorne	899	11478	11564
Texaco	Dromgold 'D' 35-1	1980 FSL 2310 FWL	35	Wildcat	811	12289	12375
Texaco	Dominic Silva 36-1	NE SW	36	Wilburton	881	13776	13883
4N-17E							
Operator	**Well**	**Location**	**Sect.**	**Field**	**K.B.**	**Top Spiro**	**Top Wap**
King Resources	Pattison 1-1	SE NW NW	1	Wilburton	649	10729	10815
Arkoma	McCaslin #2	SE NW NE	2	Wilburton	744	10545	10616
King Resources	McCaslin 1-2	SE NW NW	2	Wilburton	667	10693	10781
Arkoma	Sparks #1	NE	3	Wilburton	644	10973	
King Resources	Layden 1-3	SE NW NW	3	Wilburton	687	11058	11156
Arkoma Prod. Co.	Stine #2	1500 FNL 1500 FEL	4	Hartshorne	703	10114	10207
Texas International	Stine No. 1-4	NE SW NW	4	Wilburton	714	10176	NDE
Texas International	Rock Is. 5-1	990 FNL 2310 FWL	5	Hartshorne	693	10414	10492
Arkoma	Rock Is 2-5	1320 FNL 1320 FWL	5	Wilburton	676	10586	10662
JMC Expl.	Beluska #1	660 FNL 2148 FEL	6	Wilburton	713	10007	10076
JMC Expl.	Beluska #1	660 FNL 2148 FEL	6	Wilburton	713	11416	11482

Arkoma Prod	Hartshorne #3	1325 FNL 1000 FWL	6	Hartshorne	705	9838	9908
Texas Inter.	Hartshorne 1-6	SW NE NE	6	Wilburton	718	10143	10242
Amoco	Rock Is #1-7	1260 FSL 1320 FEL	7	Wilburton	781.5	10516	10578
Arkoma	Rock Is #2-8	1320 FNL 1320 FEL	8	Hartshorne	776	11250	11335
Arkoma	Alexander #1	660 FNL 1320 FEL	9	Wilburton	660	11545	11630
Whitmar	SilverBullet 1-11	1320 FNL 2640 FWL	11	Hartshorne	689	11637	11736
Exxon	Mabry Trust 1	NE NW SE	12	Wilburton	655	11752	11864
Texaco	Wayne Wallace 15-1	SW SE SE	15	Hartshorne	865	13125	13288
Continental	Wayne Wallace 17#1	SW SE NW	17	Wildcat	741	12011	12099
TXO	Wright E #1	1040 FNL 880 FWL	18	Hartshorne	760	11809	11890
Texaco	Wayne Wallace 21-1	SW NE NW	21	Wildcat	840	12393	12496
Tide West Oil Co.	Wallace 1-6	NW NE NE	21	Pittsburg	803	12589	12707
Shell	Retherford 1-24	S N SE	24	Wildcat	674	12826	12907
Amoco	Reterford 1-A	SW SE SE	25	Wildcat	748	11362	11458
Amoco	Patterson #1	900 FSL 2400 FWL	27	Wildcat	996	11204 O.T.	
Amoco	Patterson #1	900 FSL 2400 FWL	27	Wildcat	996	11287	11397
Texaco	Manuel Rudy	250 FSL 1320 FEL	28	Wilburton	894	11551	11681
Texaco	Manuel Rudy	250 FSL 1320 FEL	28	Wilburton	894	12177	12058
Amoco	Tomlin #1	1175 FNL 1725 FEL	29	Wilburton	1080	11911	12098
Exxon	Ellis Rudy #1	SE SE SE	30	Wilburton	1052	12330	12418
Exxon	Elliot Davis #1	SE SE SE SE	31	Wilburton	929	10924	11010
Exxon	Elliot Davis #1	SE SE SE SE	31	Wilburton	929	12986	12724
Amoco	Zipperer #1	SE SW SE SW	32	Scout	904	10953	11060
Exxon	H&H Cattle Co 'A' 1	SW NW SE	33	Wildcat	742	12188	12313
Amoco	Mose Watts 36-2	SE NE SE	36	Wilburton	888	11294	11384
4N-18E							
Operator	**Well**	**Location**	**Sect.**	**Field**	**K.B.**	**Top Spiro**	**Top Wap**
Shell	Williams Mabry # 1-4	C NW SE	4	Wilburton	788	NDE	
Tennecco	Mabry Trust 1-5	SE NW	5	Wilburton	711	11374	11439

Shell	R.Every # 1-5	785 FSL 2055 FEL	5	Wilburton	796	NDE	
Tex Pex	AJ Mabry	290 FSL 1650 FWL	7	Wilburton	929	12563	12636
Shell	Mabry 1-9	NE SW	9	Wilburton	927	12178	12250
B.T.A.	9001 JVP Glaser #1	700 FSL 2580 FWL	9	Wildcat	884	NDE	
BTA Oil Prod.	1-9001-JVP Mabry	NW NW SE	11	Wildcat	1065	12055	12096
Arco	Dollins 1-13	800 FSL 200 FEL	13	Hartshorne	729	13019	13125
B.T.A.	9001 JVP Johnson #1	2040 FSL 1150 FEL	16	Wilburton	710	NDE	
B.T.A.	9001JVP Workman1	300 FSL 1320 FEL	22	Wildcat	778	13268	13433
Arco	Newell 1-23	200 FSL 1320 FEL	23	Wilburton	917	12640	12720
B.T.A	9001JVP Amason#1	1930 FSL 2250 FWL	24	Wildcat	933	12629	12714
B.T.A.	BTA 9001 JVP Amason1	1930 FSL 2250 FWL	24	Wildcat	933	12631	12782
Anadarko	Robe 'A' 1-25	1550 FSL 2340 FWL	25	Wildcat	826	12774	no spiro or
Exxon	Garrett A-1	330 FSL 2226FWL	26	Wildcat	1037	13716	13817
Exxon	Garrett A-1	SE SE SE	26	Wildcat	1036	13764	13864
Exxon	Moore #1	SW SW SE	28	Wilburton	772	12561	12666
Exxon	Watts 'C' #1	80 FSL 2380 FWL	29	Wilburton	867	12193	12293
Exxon	Watts Bros. A-1	1000 FSL 1360 FWL	30	Wilburton	792	13506	13592
Amoco	Retherford A 30-1	SE SE SW	30	Hartshorne	868	11590	11679
Exxon	Roy Rutherford B-1	SE SW SE	31	Wildcat	962	12144	12259
Amoco	Mose Watts 32-1	250 FSL 840 FEL	32	wilburton	1064	13042	13152
Exxon	Watts Bros 'B'-1	750 FSL 2352 FEL	32	Wilburton	926	12741	12847
Exxon	Garrett C-1	SE SE SW SE	33	Wilburton	1025	13100	13248
Exxon	Garrett D-1	900 FNL 1780 FEL	34	Wilburton	909	12726	12818
Arco	TNT 1-34	1320 FSL 1320 FEL	34	Wilburton	1184	13725	13797
Arco	Ulysses #1	1320 FSL 2300 FEL	35	Wildcat	1032	14486	14608
4N-19E							
Operator	**Well**	**Location**	**Sect.**	**Field**	**K.B.**	**Top Spiro**	**Top Wap**
Mobil	EM Lawless #1	500 FSL 820 FWL	1	Wilburton	952	13446	13548
Helmerich & Payne	Gary 1-5	1320 FSL 2470 FWL NE	5	Wilburton	781	12187	12270

H & P	Burger Trust 1-6	SE SE SE 2500 FSL 1180 FWL	6	Wildcat	797	12260	12347
Williford Energy	Clemons #1	1240 FWL 1320 FNL	8	Wildcat	750	12163	12250
Exxon	Yourman #1	1160 FSL 2417 FWL	9	Wilburton	776	13785	13874
Arco	Holsten #1	250 FNL 1570 FEL	11	Wildct	920	14077	14184
Williford	Clemons #1	1320 FSL 2340 FWL NW	12	Wildcat	748	12166	12256
Arco	James #1-17	896 FSL 40 FEL	17	Wildcat	848	11487	11575
H & H Star	Colony 1-23	2000 FSL 640 FWL	23	Wildcat	913	15757	15867
4N-20E							
Operator	**Well**	**Location**	**Sect.**	**Field**	**K.B.**	**Top Spiro**	**Top Wap**
Exxon	Ellis #1	SW SE SW SE	4	Wildcat	734	15329	15507
H&H Star	Dipping Vat 1-4	1320 FEL 1320 FSL	4	Choctaw Tru	1028	14955	15135
H&H Star	Lucky Strike 1-5	1720 FSL 2380 FWL	5	Choc. Trust	903	13804	13944
Mobil	Kiamichi 1-6	500 FSL 2350 FEL	6	Wilburton	955	13643	13781
5N-16E							
Operator	**Well**	**Location**	**Sect.**	**Field**	**K.B.**	**Top Spiro**	**Top Wap**
Hamilton Bros	Bernardi Jones 1-10	NE	10	Wildcat	661	10449	10549
Midwest	Barnes #1	NW SW NE	13	Wildcat	612	11208	11269
Tenneco	Moss A 1-13	SE SE	13	Wilburton	643	8290	8370
Texas Oil & Gas	Cook K #1	SW SE	14	Hartshorne	615	11145	11216
Hanna Oil & Gas	Martha Cook #1	1470 FSL 1420 FWL	14	Wildcat	675	NDE	
Tenneco	CC & CC 1-15	660 FSL 660 FWL	15	?	695	10455	10523
Sinclair	George B Hall #1	N S SW	17	Wildcat	752	8972	9030
Daniel price	George B Hall	840 FSL 1320 FWL	17	Wildcat	763	8990	9049
Hamilton Broth.	Stansel Welch 1-18	S NE	18	Bache	720	9031	9240
Williford	Armco #1	N N NE	20	Bache	783	10070	10149

Daniel Price	Randel #1	810 FSL 810FWL	22	Pittsburg	671	9799	no spiro
Amaco	Clyde Monroe Unit #1	C SE	22	Wilburton	668	NDE	
Samson	McBee #1	SE SE	23	Wilburton	612	8386	NDE
Sun Oil Co.	Ernest L Cook #1	1980 FSL 860 FWL SE	23	Wilburton	615	9915	no spiro
Amoco	George Peden #2	SW	24	Wilburton	684	8400	8451
Amoco	George Peden #2	SW	24	Wilburton	684	9516	9563
Sun	George Peden #1	NW SE	24	Wilburton	629	8615	8722
ORYX	George Peden #3	245 FSL 2000 FWL	24	Haileyville	642	8356	8401
ORYX	George Peden #3	245 FSL 2000 FWL	24	Haileyville	642	8833	8881
Marathon	Mass #1	1450 FSL 1650 FEL	25	Wilburton	736	9198	9280
Marathon	Mass #2	NW	25	Wilburton	682	9056	9111
Atlantic Pitchford	R A King #1	NW SE SW NE	26	Wilburton	680	8651	8696
Daniel Price	Miller #1	1320 FSL 1980 FWL NE	26	Wilburton	650	8855	8908
Daniel Price	Miller #1	E NE	26	Wilburton	650	8857	8900
Samson	Honea #1	S N NW	27	Wildcat	690	9857	9903
Atlantic Pitchford	US Gov 27-2	2310 FNL 660 FEL	27	Wilburton	630	8780	8830
Atlantic Richfield	US Gov. '27' #1	S SE	27	Wilburton	632	8978	9022
Samson	Monroe #1	720 FSL 1320 FWL	28	Wilburton	803	9979	10049
Mustang	McClean 2-30	400' W of C SE	30	Bache	681	11044	11109
Davis Oil Co	Payne #1	1320 FNL 2300 FEL	33	Hartshorne	663	11093	11148
D-Pex Operating	Aimerito #1	W/2 NE NE	34	Wilburton	645	9750	9819
The Headington & Delta	Mercangeli No.1	730 FSL 1310 FWL	34	Wilburton	633	NDE	
Danel-Price Exp.	Nelson #1	NW SE SE	34	Wilburton	650	NDE	
Daniel Price	Haileyville Townsite	E W SE	35	Wilburton	674	10366	10426
Amoco	USA Unit No.1-35	NE SW NE	35	Wilburton	664	9668	9706
Marathon Oil Co.	Woods Prosp #2	1170 FSL 1170 FEL	36	Wilburton	671	9805	9872
Marathon Oil Co.	Woods Prosp #2	1170 FSL 1170 FEL	36	Wilburton	671	11015	11077
Marathon	Woods Prospect #1	NW SW NE	36	Haileyville	673	10569	10627
5N-17E							
Operator	**Well**	**Location**	**Sect.**	**Field**	**K.B.**	**Top Spiro**	**Top Wap**

Marathon	Fabbro #1						
Arco	Sharp #1	S SW	2	Wildcat	723	10794	10831
Coquina Oil Co.	Tobe #1	W NE	5	Wildcat	897	9403	no spiro
Gulfstream	Adamson Townsite 1-17	SE NE SW NE	7	Hartshorne	622	NDE	
Gulfstream	Randel 1-9	SW NW SE	9	Hartshorne	626	12024	no spiro
Gulfstream	Raspotnik 1-10	SW	12	Hartshorne	643	11536	11577
Gulfstream	Vaughn No.1	C SE NW	12	Hartshorne	665	11685	11896
Sinclair	Dungan 'A' #1	N SE	13	Wilburton	612	7816	7876
Arco	Dunagan #2 'A'	NE SE NW	13	Wilburton	652	9073	9131 mirr
Mobil	#1 Kent Heirs	W W SE	14	Wilburton	625	8119	8183
Samson	Kent #1	E W SW SE	15	Wilburton	616	8305	8354
Samson	Bobo #1	SE SE	16	Wilburton	612	9020	9040
Intex	Emory Estate Unit No.1	330 FSL 990 FEL NE	16	Wildcat	605	NDE	
Samson	Bowman Unit No. 1	C SW SW	17	Adamson	769	NDE	
Dyco Petroleum	Bowman No.1	660 FSL 2140 FEL	17	Wilburton	619	11711	11781
TXO	Beatrice # 1	NE NW SW	17		618	NDE	
NEw Gulf Stream	Duran #1	S N SE	18	Wilburton	645	11355	11395
TXO	Webber 'A' 1	N SW SE	18	Hartshorne	840	8630	8687
Exxon	Anderson K #2	NW SW SE	19	Wilburton	686	8868	8926
Humble	K. Anderson 1	NW SE SE	19	Wilburton	635	8277	8342
Sinclair	Pauline Bowman #1	SW NE	20	Wilburton	803	8461	8525
Arco	Pauline Bowman #3	SE NW SE	20	Wilburton	753	8497	8581
NICOR	Bowman #4	SW NE SW	20	Wildcat	702	8368	8448
NICOR	Bowman #4	SW NE SW	20	Wildcat	702	8788	8878
NICOR	Bowman #4	SW NE SW	20	Wildcat	702	11307	11354
Arco	Pauline Bowman No.5	NW SE NW	20	Pittsburg	782	9040	9125
Sinclair	Pauline Bowman #1	1210 FNL 1320 FWL (SE)	21	Wilburton	787	8835	8915
Mobil	Goldie Sivil #1	NW SW NE	22	Wilburton	682	8488	8557
Samson	Sams 1	SE NW SE	22	Wilburton	756	8764	8827
Mobil	Darby Subdivision	NW NW SE	23	Wilburton	842	9088	9166
Mobil	Darby #2	1320 FNL 1300 FWL	23	Gowen	654	8399	8451
Marathon	Fabbro Unit No.3	365 FSL 1100 FEL	24	Wilburton	940	8776	8849
Marathon	Fabbro Unit No.3	365 FSL 1100 FEL	24	Wilburton	940	10631	10698

Marathon	Fabbro #1	NW SE	24	Wilburton	846	8274	8353
Marathon	Fabbro #2	NE	24	Wilburton	703	8697	8766
Sinclair	JL Henley #1	NE SE NW	25	Wilburton	796	9216	9297
Amoco	Caudron #2	NE SE NW	26	Wilburton	722	8438	8504
Amoco	Caudron #2	NE SE NW	26	Wilburton	722	11314	11428
JMC Exp.	Caudron #5	1450 FNL 800 FWL	26		710	8290	8350
Arco	Parker Alfred #2	W E NW	27	Wilburton	733	8472	8527
Arco	Parker Alfred #2	W E NW	27	Wilburton	733	9486	9545
Sinclair	Alfred Parker Unit #1	NE SW NE	27	Wilburton	708	8377	8452
Sinclair	USA Sect 28 Unit 1	1320 FNL 1170 FWL	28	Wilburton	709	8981	9401
Arco	USA Anderson #2	NW NW SE	28	Wilburton	720	10246	10300
Sinclair	P. D. Bowman #1	SW SW NE	29	Wilburton	676	9869	9942
Arco	P D Bowman #2	SW NE SW	29	Wilburton	665	10059	10125
Barrett Resources	Bowman # 4	660 FSL 1980 FWL SE	29	Wilburton	677	NDE	
JMC Exp.	Bowmann No. 3	W E NW	29	Hartshorne	685	9115	NDE
Arco	Richards Edith #3	N S NW	30	Wilburton	634	8931	8995
Arco	Richards Edith #3	N S NW	30	Wilburton	634	9298	9362
King Resources	Pettit 1-31	SE NW SE	31	Wilburton	662	9680	NDE
Sun	Charles Casteel A #2	990 FSL 810 FWL	32	Wilburton	682	10318	10390
Sunray Dx. Oil	C.W. Casteel Unit #1	C SW SW NE	32	Wilburton	NDE		
Arkoma	Pitichny #2	N N S NW	33	Wilburton	697	9893	9976
King Res & Texas Int.	Potichny No. 1-33	125 FNL NW SE	33	Wilburton	706	10336	10444
Arkla Exp. Inc.	Hare No. 1-33	C NE	33	Wilburton	884	9914	10006
Texas Int. Pet.	B.D. Jordan No.1	NE Sw NW	33	Wilburton	699	NDE	
Arkoma	Potichney No. 3	C SW	33	Hartshorne	781	9881	9974
Texas International	B.D. Jordan No.1	NE SW NW	33	Wilburton	699	NDE	
Arkoma	Whitney #2	1120 FSL 970 FWL	34	Wilburton	914.8	10538	10603
Arkoma	Whitney #3	2000 FSL 1320 FWL	34	Wilburton	712	9988	10051
Atlantic Richfield	Andrew Kurilko	SW NE SW	35	Wilburton	691	10383	10482
Arco	Kucilke Andrew #2	NW SE NW	35	Wilburton	684	10294	10361
JMC Exp.	Delia Holt #1	SW SW NE	35	Wilburton	704	10052	10122
Arco	Lerblance #2	NE SW NE	36	Wilburton	734	9577	9648
Arco	Lerblance #2	NE SW NE	36	Wilburton	734	10320	10391

5N-18E Operator	Well	Location	Sect.	Field	K.B.	Top Spiro	Top Wap
Sinclair Oil & Gas	USA Anderson #1	SW SW NE	1	Wilburton	675	10725	NDE
Ambassador Oil Corp	Davis #1	SW	2	Wilburton	701	10977	11032
Ambassador Oil	Kinnikin Pate #1	SW NE SW	3	Wildcat	693	10966	11022
Ambassador	Woods #1	SE	4	Wilburton	699	10958	11011
Ambassador	Sawyer #1	NW SE NE	5	Wilburton	659	10981	11041
Ambassador	Chaudoin #1	NW NE SE	6	Wilburton	661	11276	11329
Sinclair	Gardner #1	NW	7	Wilburton	642	11358	11408
Petroleum Inc.	Ferguson Unit No.1	SE SW	7	Wilburton	650	NDE	
Ambassador	Raunikar #1	NW NE	8	Wilburton	663	10985	11041
Jones Pellow	McClain #1	SE SE	8	Wilburton	664	10721	10784
Ambassador	Topping State #1	NE	9	Wilburton	683	11028	0
JMC Explor	Topping State #2	1150 FEL 660' FSL	9	Wilburton	666	10153	10215
JMC Explor	edit for lower	overturned beds	9	Wilburton	666	11014 bas	10860
Ambassador	McAlester A #1	SW NE NE	10	Wilburton	684	11069	11131
Ambassador	Davis A #1	SW NW NE	11	Wilburton	693	11215	11275
Arco	Davis A #2	NE NW SE	11	Wilburton	690	11402	11458
Samson	Junior #1	660 FSL 990 FWL	12	Wilburton	675	11591	11653
Ambassador	Robinson #1	NW	12	Wilburton	727	11235	11338
Arco	Wayne Austin #2	1720 FSL 2440 FEL	13	Wilburton	688	8886	8987
Arco	Wayne Austin #2	1720 FSL 2440 FEL	13	Wilburton	688	10342	10388
Samson	Costilow #4	660 FSL 1630 FWL	14	Wilburton	674	7854	7926
Samson	Costilow #5	900 FSL 1200 FEL	14	Wilburton	682	8110	8186
Ambassador	Costilow #1	E NW SE	14	Wilburton	683	7875	7947
Arco	Yourman #3	1470 FNL 1320 FWL	15	Wilburton	676	7813	7877
Arco	Yourman #3	1470 FNL 1320 FWL	15	Wilburton	676	9625	9684
Arco	Kilpatrick 2-16	1896 FNL 1600 FEL	16	Wilburton	667	7936	8003
Arco	Kilpatrick 2-16	1896 FNL 1600 FEL	16	Wilburton	667	9503	9565

Arco	Kilpatrick #3	2296 FNL 2000 FEL	16	Wilburton	662	8031	8094
Arco	Kilpatrick #3	2296 FNL 2000 FEL	16	Wilburton	662	9567	9626
Ambassador	Kilpatrik #1	SW NE SE	16	Wilburton	660	7910	7971
Arco	Steve Fazekas #2	SE NW SE	17	Wilburton	659	7892	7962
Arco	Steve Fazekas #2	SE NW SE	17	Wilburton	659	9615	9668
Vastar Resources	Fazekas #3	660 FSL 2326 FWL	17	Wilburton	645	7835	7908
Vastar Resources	Fazekas #3	660 FSL 2326 FWL	17	Wilburton	645	9716	9773
Ambassador	Fazekas #1	E SW	17	Wilburton	658	8124	8203
Arco	Bud Hampton #2	830 FSL 660 FEL	18	Wilburton	655	8420	8503
Arco	Bud Hampton #2	830 FSL 660 FEL	18	Wilburton	655	10826	10876
Ambassador	Hampton #1	E SW	18	Wilburton	647	8383	8461
Ambassador	Hampton Unit #1	C E SW	18	Wilburton	647	8383	8458
Arco	Bennett State #2	1500 FNL 1500 FEL	19	Wilburton	646	7843	7905
Arco	Bennett State #2	1500 FNL 1500 FEL	19	Wilburton	646	10086	10143
Arco	Smith MA #2	1838 FWL 1336 FSL	20	Wilburton	632	7364	7419
Arco	Smith MA #2	1838 FWL 1336 FSL	20	Wilburton	632	8444	8518
Arco	Smith MA #2	1838 FWL 1336 FSL	20	Wilburton	632	10019	10069
Arco	Paschall #2	1960 FNL 1640 FWL	21	Wilburton	667	8244	8322
Arco	Paschall #2	1960 FNL 1640 FWL	21	Wilburton	667	9755	9808
Arco	Paschall #3	2040 FWL 1580 FNL	21	Wilburton	662	8308	8383
Arco	Paschall #3	2040 FWL 1580 FNL	21	Wilburton	662	9793	9845
Arco	RF McAlester #3	1600 FEL 2000 FSL	22	Wilburton	677	7945	7977
Arco	RF McAlester #3	1600 FEL 2000 FSL	22	Wilburton	677	8247	8311
Arco	RF MCAlester #3	1600 FEL 2000 FSL	22	Wilburton	677	10791	10853
Ambassador	McAlester #2	N SW NW	22	Wildcat	678	7604	7679
Anadarko Petro	Williams A #3	2465 FNL 1890 FWL	23	Wilburton	690	8310	8388
Anadarko Petro	Williams A #3	2465 FNL 1890 FWL	23	Wilburton	690	10812	missing
Ambassador	Williams #1	NW	23	Wildcat	691	8102	8179
Arco	James Unit #2	1600 FNL 1500 FWL	24	Wilburton	707	8312	8389
Arco	James Unit #2	1600 FNL 1500 FWL	24	Wilburton	707	10753	10818
Ambassador	James 'A' #1	NE SW NW	24	Wildcat	686	8322	8389
Donald Slawson	Malitz 1-25	S NE NE	25	Wilburton	964	9750	9868
Skelly	Guy Vernum #1	1285 FSL 1355 FWL	25	Wilburton	782	9658	9753

Arco	Watts Jones #2	200 FSL 990 FEL	26	Wilburton	770	9873	9950
Arco	Watts Jones #2	200 FSL 990 FEL	26	Wilburton	770	12260	12325
Arco	EV Enis #2	1600 FNL 1600 FWL	27	Wilburton	730	9194	9276
Arco	State 'C' #2	1500 FNL 2000 FWL	28	Wilburton	703	8398	8473
Arco	State 'C' #2	1500 FNL 2000 FWL	28	Wilburton	703	10843	10900
Arco	Dobbs State #2	1600 FNL 2200 FWL	29	Wilburton	664	9108	9179
Arco	Dobbs State #2	1600 FNL 2200 FWL	29	Wilburton	664	10772	10823
Ambassador	Dobbs State #1	1320 FSL 1470 FWL	29	Wilburton	642	8066	8138
Arco	Dobbs State #2	NE SE NW	29	Wilburton	664	8133	8181
Arco	Dobbs State #2	NE SE NW	29	Wilburton	664	9110	9179
Arco	Dobbs State #2	NE SE NW	29	Wilburton	664	10772	10824
Arco	Jesse Bennett #2	1825 FNL 1900 FWL	30	Wilburton	663	9117	9188
Arco	Jesse Bennett #2	1825 FNL 1900 FWL	30	Wilburton	663	10288	10347
Arco	Jessie Bennet # 2	NW SE NW	30	Wilburton	663	9117	9187
Arkoma	Hunter Tucker #3	1320 FWL 1000 FNL	31	Wilburton	649	9163	9236
Arkoma	Hunter Tucker #3	1320 FWL 1000 FNL	31	Wilburton	649	9959	10031
Arkoma	Hunter Tucker #2	NE	31	Wilburton	646	9823	9895
Trigg Drilling Co.	Hunter Tucker No. 1-31	C NW	31	Wilburton	634	9451	NDE
Arkoma	Kennedy B-2	1143 FSL 1497 FWL NW	32	Wilburton	660	10257	10331
Sinclair	Mc Watts #1	C NE	33	Wilburton	753	10608	10678
Coquina Oil Co.	Watts #1	NE	34	Wilburton	730	10760	10873
Samson	Mose #1	1320 FNL 660 FWL	35	Wilburton	881	10679	10761

5N-19E

Operator	Well	Location	Sect.	Field	K.B.	Top Spiro	Top Wap
Shell	Williams #32-27		27	Wilburton	1073	14339	14383
Chapparal	VFW 1-29	SW	29	Wilburton	886	11022	11099
Daniel Price	Church Lake #1	2180 FSL 1120 FWL	29	Wilburton	805	12165	12242
Sun Expl.	Diamond #2	SW	30	Wilburton	847	10433	10524
Amoco	A J Mabry #1	NW SE	31	Wilburton	1344	11427	11517

Amoco	Virginia Walker #1	NW NW SE SW	32	Wilburton	898	11657	11726
6N-16E							
Operator	**Well**	**Location**	**Sect.**	**Field**	**K.B.**	**Top Spiro**	**Top Wap**
Snee & Eberly	No.1 Baldwin A	SE SE SW NE	14	S. Quinton	675	NDE	
Bonanza Petroleum	Baldwin # 1-14	C W W NE	14	S. Blocker	642	NDE	
Sunray Dx Oil	Mary White Unit #1	NW SW NE	15	Wildcat	641	NDE	
Oxley Petroleum	Davis Kemp #1	1882 FSL 1540 FWL	16	Wildcat	672	9153	8179
Oxley Petroleum	Kieth #1	990 FSL 2300 FWL NW	19	Wildcat	795	8699	8735
Oxley Petroleum	Opal #1	660 FNL 660 FWL	20		774	8666	8698
Oxlet Petroleum	Lucy Mary Smith #1	E E NW	22		673	NDE	
Tom Hutchinson	EC McKinzie #1	1951 FSL 539 FWL	23	Wildcat	631	8369	8404
Snee & Eberly	Oneth No.1	C NE	25	Wildcat	916		

Plates 1, 2, 4, 5, 6, 7, 8, 9, 9a, and 10.

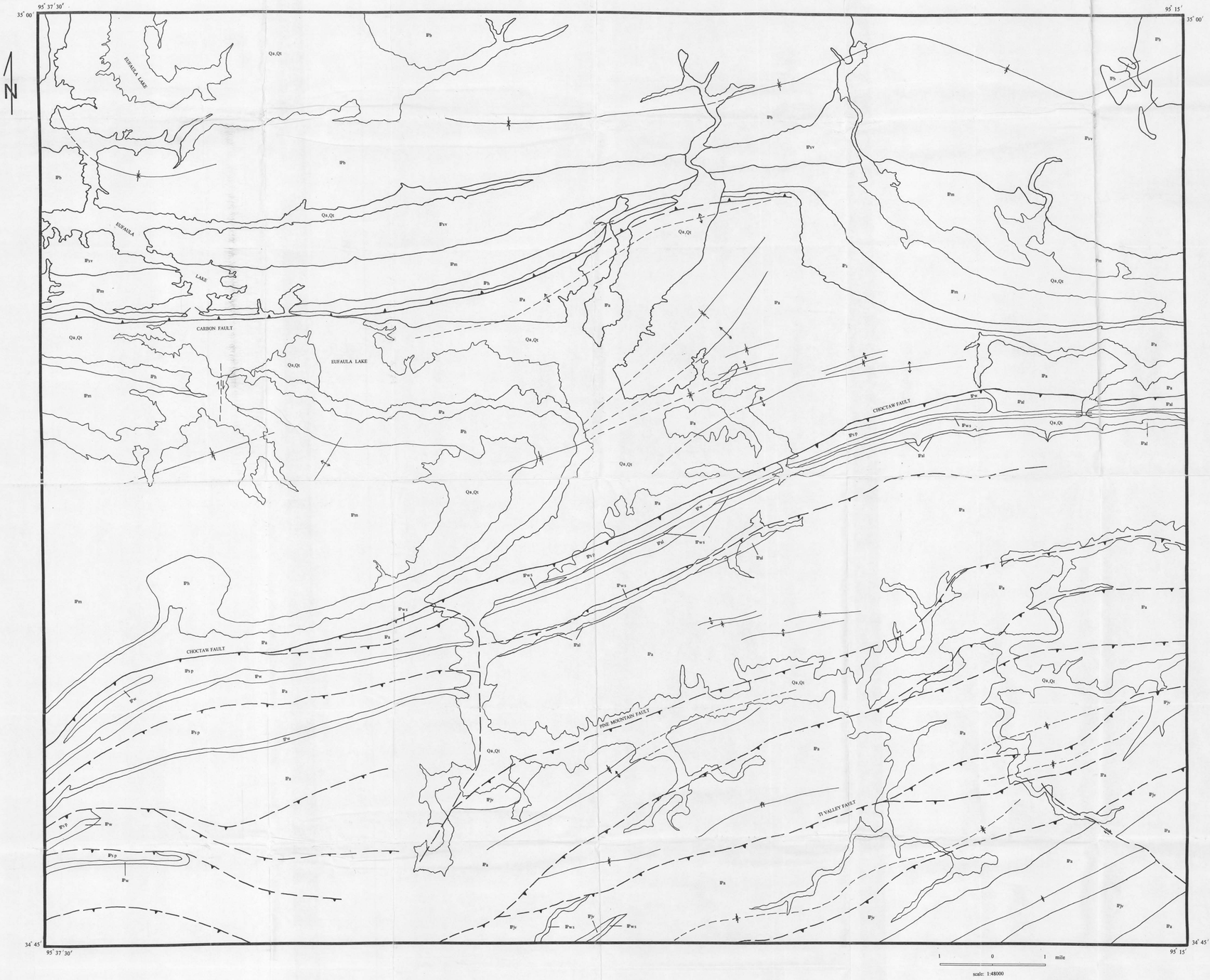

EXPLANATION

- Qa,Qt — QUATERNARY
- IPb — BOGGY FORMATION (PENNSYLVANIAN)
- IPsv — SAVANNA FORMATION (PENNSYLVANIAN)
- IPm — Mc ALESTER FORMATION (PENNSYLVANIAN)
- IPh — HARTSHORNE FORMATION (PENNSYLVANIAN)
- IPa — ATOKA FORMATION (PENNSYLVANIAN)
- IPal — LOWER ATOKA SHALE (PENNSYLVANIAN)
- IPws — SPIRO SANDSTONE MEMBER (informal) of Wapanucka Formation (PENNSYLVANIAN)
- IPw — WAPANUCKA FORMATION (PENNSYLVANIAN)
- IPjv — JOHNS VALLEY SHALE of Wapanucka Formation (PENNSYLVANIAN)
- IPsp — SPRINGER FORMATION (PENNSYLVANIAN)

SIMPLIFIED GEOLOGICAL MAP OF THE STUDY AREA

ATA SAGNAK — PLATE I

SIMPLIFIED GEOLOGICAL MAP OF THE WILBURTON GAS FIELD AREA

(From Suneson and Ferguson , 1989 ; Hemish , 1992 ; Hemish , Suneson and Ferguson , 1990 ; Hemish and Suneson , in press)

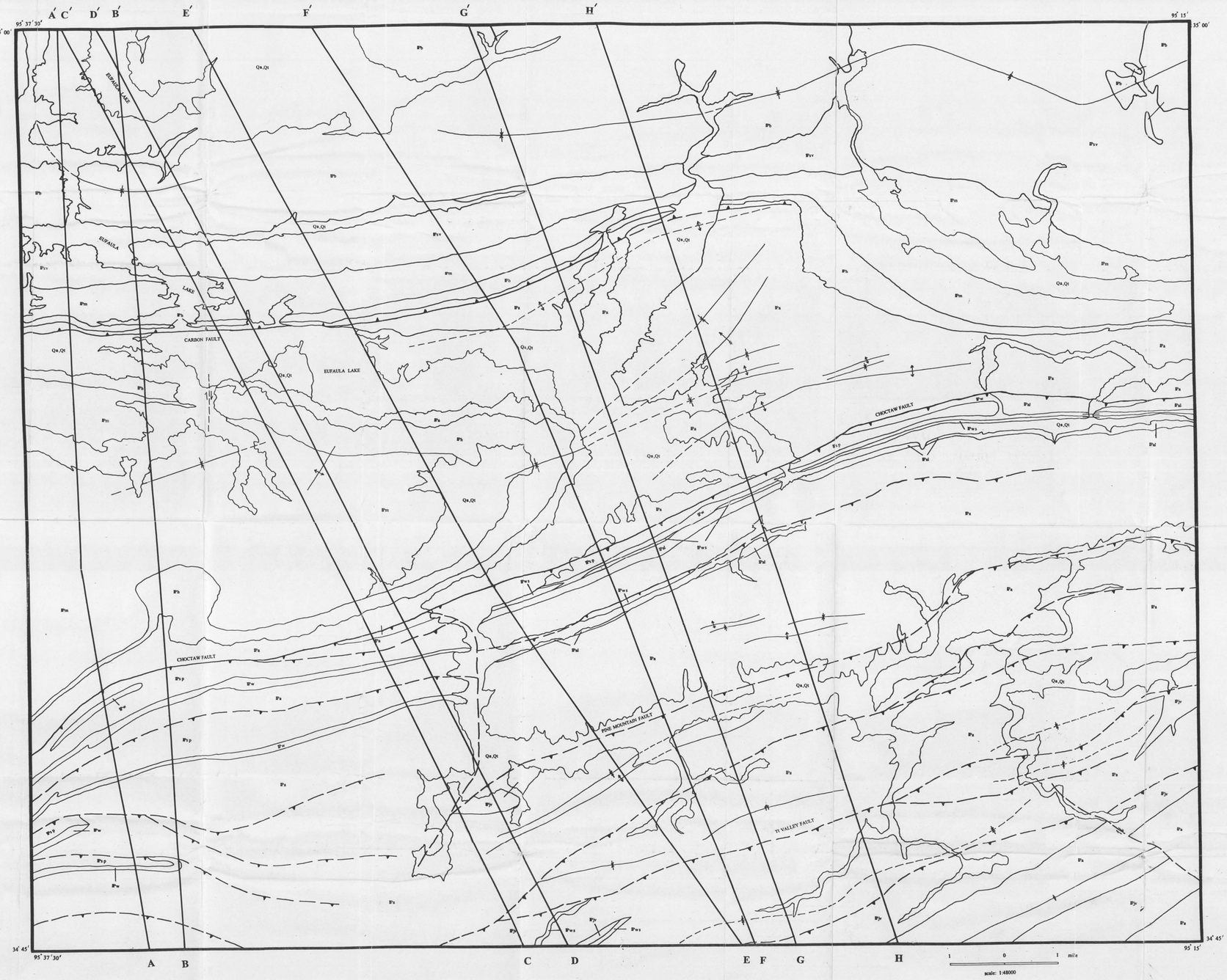

EXPLANATION

Qa,Qt	QUATERNARY
IPb	BOGGY FORMATION (PENNSYLVANIAN)
IPsv	SAVANNA FORMATION (PENNSYLVANIAN)
IPm	Mc ALESTER FORMATION (PENNSYLVANIAN)
IPh	HARTSHORNE FORMATION (PENNSYLVANIAN)
IPa	ATOKA FORMATION (PENNSYLVANIAN)
IPal	LOWER ATOKA SHALE (PENNSYLVANIAN)
IPws	SPIRO SANDSTONE MEMBER (Informal) of Wapanucka Formation (PENNSYLVANIAN)
IPw	WAPANUCKA FORMATION (PENNSYLVANIAN)
IPjv	JOHNS VALLEY SHALE of Wapanucka Formation (PENNSYLVANIAN)
IPsp	SPRINGER FORMATION (PENNSYLVANIAN)

SIMPLIFIED GEOLOGICAL MAP OF THE STUDY AREA
SHOWING THE LINES OF CROSS SECTIONS

ATA SAGNAK PLATE II

SIMPLIFIED GEOLOGICAL MAP OF THE WILBURTON GAS FIELD AREA

(From Suneson and Ferguson , 1989 ; Hemish , 1992 ; Hemish , Suneson and Ferguson , 1990 ; Hemish and Suneson , in press)

B

B´

TEXACO
Dominic Silva No. 36-1
36-4N-16E

WHITMAR & GEODYNE
Cope No.1
13-4N-16E (~500W)

W.P.LARSLANCE Jr.
Lewis No. 2-12
12-4N-16E (~400E)

MARATHON
Slaughter Unit # 2
1-4N-16E

AMOCO
USA Unit No. 1-35
35-5N-16E (~750W)

ATLA-ATIC RICHFIELD
R.A.-KING Unit No.1
26-6-N-16E (~700W)

SUN OIL
Ernst L. Cook No. 1
23-5N-16E

HANNA OIL
Martha Cook # 1
14-5N-16E (~2500W)

ANDOVER
Goyle Lynch # 1-24
24-4N-16E (~1000E)

MARATHON
Lewis No. 1-12
12-4N-16E (~700E)

MARATHON
Slaughter Unit No.1-1
1-4N-16E (~1000E)

DANIEL PRICE
Miller #1
26-5N-16E (~700E)

SAMSON
Mc. Bee Unit 1
23-5N-16E (~1200E)

TEXAS OIL & GAS
Cook "K" No. 1
14-5N-16E (~1000E)

TOM HUTCHINSON
E. C.Mc.Kinzie No.1
23-5N-16E (~500E)

BONANZA
Baldwin # 1-14
14-6N-16E (~1000E)

SNEE & EBERLY
No.1 Baldwin "A"
14-6N-16E (~2000E)

elevation (feet)

SEA LEVEL

-1000
-2000
-3000
-4000
-5000
-6000
-7000
-8000
-9000
-10000
-11000
-12000
-13000
-14000
-15000
-16000

QaQt

IPm

IPh

IPa

TOP OF RED OAK

SPIRO

CHOCTAW FAULT

LOOSE LINE

WOODFORD DETACHMENT

SPRINGER DETACHMENT

PEK LINE

IPb

IPsv

CARRON FAULT

EXPLANATION

QaQt	QUATERNARY
IPb	BOGGY FORMATION (PENN.)
IPsv	SAVANNA FORMATION (PENN.)
IPm	Mc ALESTER FORMATION (PENN.)
IPh	HARTSHORNE FORMATION (PENN.)
IPa	ATOKA FORMATION (PENN.)

scale
(feet)
2000
1000
0 1 (mile)

Lf = 68.90 cm = 27.13 in = 10.27 mi

Lo = 167.10 cm = 65.79 in = 24.92 mi

dL = Lf - Lo = 98.20 cm = 38.66 in = 14.64 mi

e = - dL / Lo = 0.5876

e = 58.76 % shortening

scale
0 1 (mile)

BALANCED AND RESTORED CROSS-SECTION

B - B´

ATA SAGNAK PLATE IV

C

C´

AMOCO
Mcnair-Wolfe No.35-1
1-2N-17E (~500W)

TEXACO
Wayne Wallace #15-1
15-4N-17E (~100E)

ARKOMA
Alexander #1
9-4N-17E (~500W)

TEXAS INT.
Stine No.1-14
4-4N17E (~1500W)

ARKOMA
Stine # 2
4-4N- 17E (~100W)

SUNRAY DX.
C.W. Cavitt Unit #1
32-5N-17E (~1200W)

ARCO
P.D. Bowman #2
29-5N-17E (~800W)

BARRET RES.
Bowman #4
29-5N-17E (~500W)

JMC EXP.
P.I. Bowman No.3
29-5N-17E

EXXON
K. Anderson No.2
19-5N-17E (~1400W)

ARCO
Pauline Bowman No.5
20-5N-17E (~2000E)

TXO
Weldon A # 1
18-5N-17E

ARKOMA
Pulchney No.3
33-5N-17E (~1400E)

ARKOMA
Pulchney No.2
33-5N-17E (~1200E)

TEXAS INT.
B.D. Jordan No.1
33-5N-17E (~2500W)

SINCLAIR
P.D. Bowman Unit 1
29-5N-17E (~900E)

NICOR EXP.
Bowman No.4
20-5N-17E (~1400E)

HUMBLE
K. Anderson No.1
19-5N-17E (~1500W)

GULFSTREAM
Duran No.1-18
18-5N-17E (~800E)

elevation (feet)

SEA LEVEL

- 1000
- 2000
- 3000
- 4000
- 5000
- 6000
- 7000
- 8000
- 9000
- 10000
- 11000
- 12000
- 13000
- 14000
- 15000
- 16000

QaQt

IPm

IPh

IPa

IPb

IPsv

TUVALLEY FAULT

PINE MOUNTAIN FAULT

CHOCTAW FAULT

CARBON FAULT

SPIRO

TOP OF RED OAK

TOP OF MARKER X

LOOSE LINE

PIN LINE

SPRINGER DETACHMENT

WOODFORD DETACHMENT

EXPLANATION

QaQt	QUATERNARY
IPb	BOGGY FORMATION (PENN.)
IPsv	SAVANNA FORMATION (PENN.)
IPm	Mc ALESTER FORMATION (PENN.)
IPh	HARTSHORNE FORMATION (PENN.)
IPa	ATOKA FORMATION (PENN.)

scale

(feet)

2000

1000

0 1 (mile)

Lf = 75.60 cm = 29.76 in = 11.27 mi

Lo = 193.90 cm = 76.34 in = 28.92 mi

dL = Lf - Lo = 118.30 cm = 46.57 in = 17.64 mi

e = - dL / Lo = 0.6101

e = 61.01 % shortening

scale

0 1 (mile)

BALANCED AND RESTORED CROSS-SECTION

C - C´

ATA SAGNAK PLATE V

D

D´

elevation (feet)

SEA LEVEL

-1000
-2000
-3000
-4000
-5000
-6000
-7000
-8000
-9000
-10000
-11000
-12000
-13000
-14000
-15000
-16000

AMOCO
Moss Watts # 35-2
36-4N-17E (~1055E)

AMOCO
Retherford No. 1-A
25-4N-17E (~1550E)

KING RESOURCE
Layden No. 1-3
3-4N-17E

KING RESOURCE
Pottchey No. 1-33
33- 5N- 17E (~300E)

TEXAS INT.
B.D. Jordan No.1
33-5N-17E (~600W)

NICOR
Bowman No. 4
20-5N-17E (~1402W)

ARCO
P. Bowman No. 8
20-5N-17E (~700W)

SAMSON
Bowman Unit # 1
17-5N-17E (~603W)

HUTCHINSON & KING RES.
E.G. Mc. Kinzie No. 1
23-6N-16E (~1402W)

ARKOMA
Sparks No. 1
3-4N-17E (~2300E)

ARKLA
Hare No. 1-33
33-5N-17E (~1300E)

ARCO
USA Sec. 28 # 2
28-5N-17E (~2050E)

SINCLAIR
USA Sec. 20 Unit # 1
28-5N-17E (~1502E)

ARCO
Pauline Bowman No. 3
20-5N-17E (~304E)

SINCLAIR
Pauline Bowman #1
20-5N-17E (~606E)

DYCO
Bowman No. 1
17-5N-17E (~1402E)

TXO
Beatrice # 1
17-5N-17E (~203E)

GULFSTREAM
Arbuckle Township No. 1-7
7- 5N-17E (~205E)

SNEE & EBERLY
Dueth No. 1
25-6N-16E (~2300E)

SNEE & EBERLY
No. 1 Bashore A
14-6N-16E (~1702E)

QaQt

IPb

IPsv

IPm

IPh

IPa

TOP OF RED OAK

TOP OF MARKER X

TVALLEY FAULT

PINE MOUNTAIN FAULT

CHOCTAW FAULT

CARBON FAULT

SPIRO

LOOSE LINE

PEN LINE

SPRINGER DETACHMENT

WOODFORD DETACHMENT

EXPLANATION

QaQt	QUATERNARY
IPb	BOGGY FORMATION (PENN.)
IPsv	SAVANNA FORMATION (PENN.)
IPm	Mc ALESTER FORMATION (PENN.)
IPh	HARTSHORNE FORMATION (PENN.)
IPa	ATOKA FORMATION (PENN.)

scale

(feet)
2000
1000
0
1 (mile)

Lf = 77.8 cm = 30.63 in = 11.60 mi

Lo = 197.8 cm = 77.87 in = 29.50 mi

dL = Lf -Lo = 120 cm = 47.24 in = 17.90 mi

e = - dL / Lo = 0.6067

e = 60.67 % shortening

scale
0 1 (mile)

BALANCED AND RESTORED CROSS-SECTION

D - D´

ATA SAGNAK PLATE VI

E

E´

EXXON
Garret No.C-1
33-4N-16E (~1020W)

EXXON
Moore No.1
28-4N-16E (~700E)

TEX-PEK
A.J. Maley # 1-7
7-4N-16E (~100W)

KING RESOURCES
Pattison No. 1-1
1-4N-17E (~200E)

ATLANTIC RICHFIELD
Andrew Kuriliko # 1
35-5N-17E (~700W)

ARCO
Andrew Kuriliko # 2
35-5N-17E

JMC EXP.
Della Holt # 1
35-5N-17E (~600E)

SINCLAIR
Alfred Parker Unit # 1
27-5N-17E (~600W)

JMC EXP.
Cauldron # 5
26- 5N-17E (~1500E)

SAMSON
Bobo No.1
16-5N-17E (~1300W)

SAMSON
Sanna # 1
22-5N-17E (~600E)

MOBIL
Bobbie Sivil Unit 1
22-5N-17E (~1200E)

INTEX
Emory Estate Unit No.1
16-5N-17E (~700W)

GULFSTREAM
Randel No.1-9
9-5N-17E

COQUINA
Tobe No.1
9-5N-17E (~1000W)

EBERLY & MEADE
Angie Vaughn No.1
18-6N-17E

EBERLY & MEADE
Vaughn # 2-13
13-6N-16E (~700W)

EBERLY & MEADE
Vaughn # 3-13
13-6N-16E (~1500W)

OXLEY
Angie Vaughn No.1
18-6N-17E

elevation (feet)

1000
SEA LEVEL
-1000
-2000
-3000
-4000
-5000
-6000
-7000
-8000
-9000
-10000
-11000
-12000
-13000
-14000
-15000
-16000

QaQt
IPm
IPh
IPb
IPsv
IPa

TOP OF RED OAK
TOP OF MARKER X

TYVALLEY FAULT
PINE MOUNTAIN FAULT
CHOCTAW FAULT
CARBON FAULT

SPIRO
LOOSE LINE
SPRINGER DETACHMENT
WOODFORD DETACHMENT
PATS KNOB

EXPLANATION

QaQt	QUATERNARY
IPb	BOGGY FORMATION (PENN.)
IPsv	SAVANNA FORMATION (PENN.)
IPm	Mc ALESTER FORMATION (PENN.)
IPh	HARTSHORNE FORMATION (PENN.)
IPa	ATOKA FORMATION (PENN.)

scale
(feet)
2000
1000
0 1 (mile)

scale
0 1 (mile)

Lf = 82.80 cm = 32.60 in = 12.35 mi

Lo = 223.50 cm = 88.00 in = 33.33 mi

dL = Lf - Lo = 140.70 cm = 55.39 in = 20.98 mi

e = - dL / Lo = 0.6295

e = 62.95 % shortening

BALANCED AND RESTORED CROSS-SECTION

E - E´

ATA SAGNAK PLATE VII

F

F´

elevation (feet)

1000
SEA LEVEL
-1000
-2000
-3000
-4000
-5000
-6000
-7000
-8000
-9000
-10000
-11000
-12000
-13000
-14000
-15000
-16000

ARCO
TNT No. 1-34
31-4N-18E (~ 10000E)

EXXON
Garnet No. D-1
34-4N-18 (~1700E)

SHELL
Maloy # 1-9
9-4N-18E (~3400E)

TENECO
Maloy Trust No.1-5
5-4N-18E (~500W)

BTA
9001 JV-P Johnson #1
16-4N-18E (~2100E)

BTA
9001 JV-P Glasar #1
16-4N-18E (~ 2200E)

SHELL
R. Every # 1-5
8-4N-18E

TRIGGY
Hunter Tucker No.1-31
31-5N-18E (~1500W)

ARKOMA
Hunter Tucker No.2
31-5N-18E (~1000E)

MARATHON
Fallbrs Unit 3
24-5N-17E (~1000W)

ARCO
Jessie Bonnet #2
36-5N-18E (~900E)

MARATHON
Fallbrs Unit #1
24-5N-17E (~1300E)

MARATHON
Fallbrs #2
24-5N-17E

SINCLAIR
Dunagan Unit # A-1
13-5N-17E (~1500W)

ARCO
Dunagan #A2
13-5N-17E (~400E)

GULFSTREAM
Vaughn No.1
12-5N-17E (~1900E)

ARCO
Sharp #1
2-5N17E (~2000E)

SNEE & EBERLY
Ollbrott No.1-21
21-4N-17E (~600W)

OXLEY
Daly Hartshorne No.1
16-4N-17E

IPh

IPa

IPb

IPsv

IPm

IPh

TOP OF RED OAK

TOP OF MARKER X

?

TIVALLEY FAULT

PINE MOUNTAIN FAULT

CHOCTAW FAULT

CARBON FAULT

SPIRO

LOOSE LINE

PEN LINE

SPRINGER DETACHMENT

WOODFORD DETACHMENT

EXPLANATION

QaQt	QUATERNARY
IPb	BOGGY FORMATION (PENN.)
IPsv	SAVANNA FORMATION (PENN.)
IPm	Mc ALESTER FORMATION (PENN.)
IPh	HARTSHORNE FORMATION (PENN.)
IPa	ATOKA FORMATION (PENN.)

scale
(feet)
2000
1000
0
1 (mile)

scale
0
1 (mile)

Lf = 81.50 cm = 32.09 in = 12.15 mi

Lo = 219.20 cm = 86.30 in =32.69 mi

dL = Lf -Lo = 137.7 cm = 54.21 in = 20.54 mi

e = - dL / Lo = 0.6282

e = 62.82 % shortening

BALANCED AND RESTORED CROSS-SECTION

F - F´

ATA SAGNAK

PLATE VIII

Lf = 91.80 cm = 36.14 in = 13.69 mi

Lo = 252.30 cm = 99.33 in = 37.63 mi

dL = Lf - Lo = 160.50 cm = 63.19 in = 23.94 mi

e = - dl / Lo = 0.6361

e = 63.61 % shortening

BALANCED AND RESTORED CROSS-SECTION

G - G´

ATA SAGNAK PLATE IX

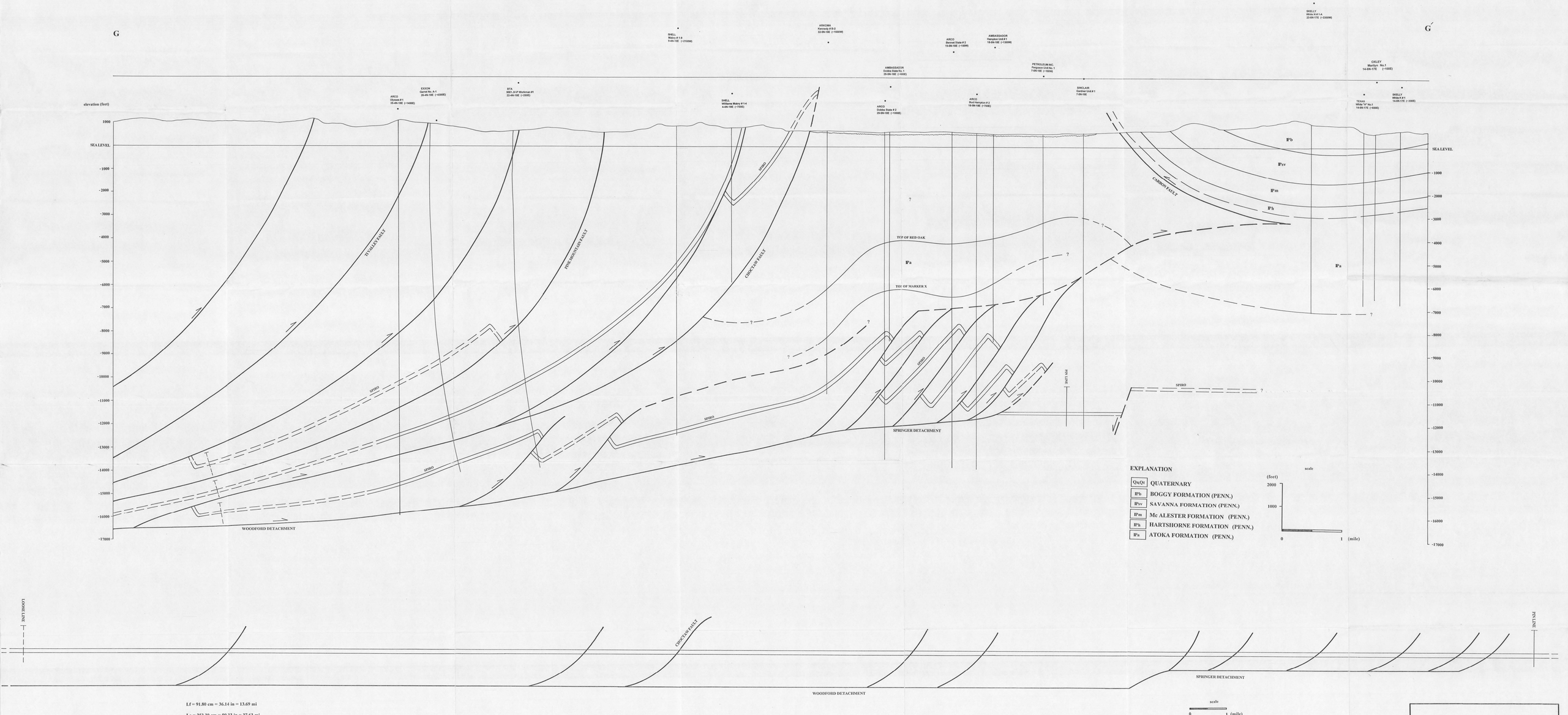

Lf = 91.80 cm = 36.14 in = 13.69 mi

Lo = 252.30 cm = 99.33 in = 37.63 mi

dL = Lf - Lo = 160.50 cm = 63.19 in = 23.94 mi

e = - dl / Lo = 0.6361

e = 63.61 % shortening

BALANCED AND RESTORED CROSS-SECTION

G - G´

ATA SAGNAK PLATE IX

Lf = 82.1 cm = 32.32 in = 12.24 mi

Lo = 216.20 cm = 85.12 in = 32.24 mi

dL = Lf - Lo = 134.1 cm = 52.80 in = 20.00 mi

e = - dL / Lo = 0.6203

e = 62.03 % shortening

BALANCED AND RESTORED CROSS-SECTION

H - H´

ATA SAGNAK — PLATE X

VITA

Ata Sagnak

Candidate for the Degree of

Master of Science

Thesis: GEOMETRY OF LATE PALEOZOIC THRUSTING BETWEEN WILBURTON-HARTSHORNE AREA, ARKOMA BASIN, SOUTHEAST OKLAHOMA

Major Field: Geology

Biographical:

Personal Data: Born in Ankara, Turkey, the son of Ahmet Orhan and Sulin Sagnak

Education: Graduate of T. E. D. Ankara College, Ankara, Turkey in June 1987; received Bachelor of Science degree in Geological Engineering from Middle East Technical University, Ankara, Turkey in July 1992. Completed the requirements for the Master of Science degree with a major of Geology at Oklahoma State University in May 1996.

Professional Experience: Teaching and Research Assistant: Department of Geology, Oklahoma State University